Investigating the Environmental and Anthropogenic Impact on Insect Gene Expression and Physiology Using *Drosophila* as a Model

By

CHRISTINE A. TABULOC
DISSERTATION

Submitted in partial satisfaction of the requirements for the degree of

DOCTOR OF PHILOSOPHY

in

ENTOMOLOGY

in the

OFFICE OF GRADUATE STUDIES

of the

UNIVERSITY OF CALIFORNIA

DAVIS

Approved:

_____
Joanna Chiu, Chair

_____
Stacey Harmer

_____
Susan Lott

Committee in Charge

2023

Table of Contents

Acknowledgements

First and foremost, I would like to thank my mentor, Dr. Joanna Chiu. Words cannot express how grateful I am for you. When you welcomed me into your lab in 2012, I would have never guessed that I could have as much knowledge and lab skills as I have today. Thank you for taking a chance on me. Thank you for years of mentorship, patience, generosity, kindness, and encouragement. You believed in me when I didn't even believe in myself. I attribute everything I am as a scientist to your mentorship and guidance. I am grateful for everything I have learned from you: from laboratory skills to life lessons. Thank you for always putting your students first and for always helping us improve as scientists and researchers. Thank you for always pushing us and preparing us for our future career endeavors. I am incredibly lucky to have you as my mentor. I truly could not have made it this far without you.

I would also like to my thesis committee, Drs. Stacey Harmer and Susan Lott, for their encouragement and support throughout graduate school. It was an honor to have you both on my Qualifying Exam and Dissertation committees. Your questions and suggestions have been incredibly helpful, and I am very grateful for your guidance, time, and expertise.

I would also like to thank all my lab mates throughout the years, especially Anna, Vu, Nitrol, Yao, and Kyle. Thank you for all the help and scientific discussions, but thank you especially for all the years of friendship and life-long memories. I also express my gratitude to my mentees over the years. I appreciate your help and everything I have learned from being your mentor. You each taught me more than you probably know. I would like to express a special thank you to my partner, Sergio. Thank you for always listening to my ideas and helping me along the way. Thank you for reading every draft of my dissertation and for encouraging me and celebrating all of my achievements, big and small alike.

Finally, I would like to thank my family for their never-ending support and understanding throughout my academic career. My parents (Salvador, Juanita, and Rosario) and siblings (Mark, Andrea,

Christian, and Clarissa) have been instrumental in giving me the strength to push forward on my lowest and most difficult days. Thank you for always believing in me and cheering me on. Thank you for showing interest in my science, and most of all, thank you for being the greatest support system anyone could ever ask for.

I am truly blessed to have all you amazing people in my life, and I am grateful that you have been a part of my journey.

Abstract

Natural environmental factors and anthropogenic disturbances can modulate gene expression, resulting in alteration of organismal phenotype. In the first part of my thesis project, I used *Drosophila melanogaster* as a model to understand the mechanisms by which 24-hour light-dark cycles can regulate rhythmic changes in the chromatin to generate circadian rhythms of gene expression and orchestrate daily biological rhythms in insects. I observed that two circadian clock proteins, CLOCK and TIMELESS, regulate daily rhythmicity in the binding of BRAHMA, a chromatin remodeler, to DNA spanning clock-controlled genes to facilitate their rhythmic gene expression cycles. Moreover, because TIMELESS degrades in the presence of light, my results provide new insights into how light affects DNA structure and gene expression. In the second part of my thesis project, I investigated the molecular mechanisms by which the fruit pest *Drosophila suzukii* adapt to insecticide applications and develop resistance. Specifically, I performed RNA sequencing analysis on *D. suzukii* flies that are either susceptible or resistant to common insecticides to determine genetic mechanisms underlying insecticide resistance in this agricultural pest. My results revealed that enhanced metabolic detoxification confers pyrethroid resistance while spinosad resistance is the result of both metabolic and penetration resistance. Finally, we identified alternative splicing as a potential mechanism of resistance. My results will facilitate the development of efficient molecular diagnostics to monitor insecticide resistance development in the field and enable growers to develop more informed *D. suzukii* spray programs to control this devastating pest more effectively.

Introduction

Gene expression, the process of turning on a gene to produce mRNA and eventually a protein, is the most fundamental way of converting genetic information into a phenotypical output [reviewed in (Nachtomy et al., 2007)]. It is known that both natural environmental and anthropogenic factors can alter gene expression, and these alterations enable organisms to adapt to their external environment (Gibson, 2008). Environmental stimuli include predictable or "pre-programmed" events as well as transient or "random" events. Some examples of pre-programmed events include the daily light-dark cycle, temperature cycles, as well as resource availability. These are factors that occur regularly and in a predictable manner, allowing organisms to anticipate these environmental changes and therefore react and adapt accordingly. For example, sunflower heads track the sun's movement throughout the day, from east to west, and in the evening, the flower orients itself to face east again, in anticipation of sunrise (Atamian et al., 2016). The final eastward orientation of mature plants is beneficial to the flower because it promotes pollinator visitation, increasing the plant's reproductive fitness. Random events, on the other hand, are non-predictable changes in the environment such as human intervention events, like the application of chemicals and drugs, and exposure to parasites and pathogens. In such cases, organisms cannot anticipate these changes and thus need to react to them upon exposure. The focus of this thesis is to understand how pre-programmed factors, specifically the day-night cycle, and random environmental factors, namely insecticide exposure, influence gene expression and physiology in insects.

In Chapter 1 (Tabuloc et al., 2023), I explored how predictable changes in the day-night cycle influence gene expression regulation by the BRAHMA chromatin remodeling complex using *Drosophila melanogaster* as a model. Earth's rotation about its axis and around the sun, produces predictable changes in the environment, including cycles of daylight and darkness. Organisms have developed an

internal time-keeping mechanism, termed the circadian clock, to anticipate these changes [reviewed in (Cox & Takahashi, 2019; Dubowy & Sehgal, 2017; Dunlap & Loros, 2017; Patke et al., 2020)]. The circadian clock is composed of three parts: the input, the oscillator, and the output (Eskin, 1979). The input is comprised of environmental stimuli, such as light, temperature, and nutrition [reviewed in (Cox & Takahashi, 2019; Dubowy & Sehgal, 2017; Dunlap & Loros, 2017; Patke et al., 2020)]. These time cues get interpreted by the oscillator, a biochemical timer that maintains the pace of the circadian clock. The oscillator then produces rhythmic expression of clock-controlled genes that results in rhythmic behaviors and physiology such as sleep-wake cycles and feeding-fasting cycles; they represent clock output.

In *D. melanogaster,* the oscillator is a transcriptional translational feedback loop in which transcriptional activators, CLOCK (CLK) and CYCLE (CYC), bind to the promoters of clock-regulated genes, including *period* (*per*) and *timeless* (*tim*), which encode transcriptional repressors (Darlington et al., 2000; Hao et al., 1997; Hardin et al., 1990; Zhou et al., 2016). Next, *per* and *tim* are transcribed and translated mid-day (Darlington et al., 2000; Hao et al., 1997; Zhou et al., 2016). However, because TIM is a light-sensitive protein and degrades in the presence of light (Hunter-Ensor et al., 1996; Myers et al., 1996; Zeng et al., 1996), PER-TIM heterodimers do not accumulate until the evening (Jang et al., 2015; Lam et al., 2018; Top et al., 2016), which is when they translocate into the nucleus and interact with CLK-CYC heterodimers to repress transcription of clock genes, including their own transcription (Chiu et al., 2008; Grima et al., 2002; Ko et al., 2002; Szabó et al., 2018). Thus, it is evident that the interaction of these transcription factors with the DNA is important in ensuring proper functioning of the circadian clock.

In eukaryotes, DNA is wrapped around histones, forming a compacted structure termed chromatin. It has been shown that the chromatin landscape at clock genes is also rhythmic—opening and closing at certain times of the day to regulate access of transcription factors and transcription

machinery to the DNA (reviewed in (Koike et al., 2012; Kwok et al., 2016; Zhu & Belden, 2020). The BRAHMA (BRM) chromatin-remodeling complex is known to be critical for proper timekeeping (Kwok et al., 2015, 2016). When BRM is knocked down in *D. melanogaster* with RNA interference, these flies possess a slower clock, running at 25 hours as opposed to a wild type fly that has a 24-hour clock (Kwok et al., 2015). BRM decreases CLK-activated gene expression by condensing the chromatin and potentially by recruiting histone deacetylases (Kwok et al., 2015, 2016). BRM regulates approximately 80% of the genes in the *D. melanogaster* genome (Jordán-Pla et al., 2018), and only a small subset of those genes is rhythmically expressed, thus prompting the question as to how a general chromatin remodeler can target only some loci in a rhythmic manner. I hypothesized that clock proteins are involved in regulating this specificity given that clock proteins are present in the nucleus at certain times of the day, and two core clock transcription factors, CLK and TIM, have been shown to interact with BRM (Kwok et al., 2015).

Leveraging a newly generated polyclonal antibody against BRM, I performed chromatin immunoprecipitation to assess whether CLK and TIM play a role in enabling BRM to target clock genes in a rhythmic manner. I observed that despite its constitutive protein expression throughout the day, BRM binds rhythmically to clock gene promoters. Using the *per* promoter as a prototypical clock gene, I observed reduced BRM occupancy in a *clk* null mutant, suggesting that CLK promotes BRM binding to the DNA. Similarly, overexpressing TIM also results in decreased BRM occupancy, suggesting that TIM plays a role in promoting BRM removal from the DNA. Furthermore, I assessed Histone H3 occupancy as a proxy for nucleosome density (Kwok et al., 2015; Lee et al., 2004) given that BRM condenses the chromatin. We observed that these perturbations in BRM occupancy result in a disruption of the chromatin landscape at the same locus. Finally, I demonstrated that constant light, which results in low levels of TIM (Abrieux et al., 2020; Kwok et al., 2016), results in increased BRM occupancy at night, consequently resulting in a more condensed chromatin landscape. My results reveal that CLK and TIM are necessary for regulating rhythmic BRM occupancy at the *per* promoter, showing reciprocal

regulation between a chromatin remodeler and the circadian clock. These results illuminate how a general chromatin remodeler can target specific loci in a rhythmic manner. These results also shed light on how disruption of the circadian clock can influence genome structure and ultimately gene expression. The involvement of light-sensitive TIM provides insight as to how light can influence the chromatin landscape and therefore gene expression.

In Chapter 2, I explored how human activities, specifically the application of insecticides in agriculture, influences gene expression and adaptation in the fruit pest *D. suzukii*. Originally from southeast Asia, this pest arrived in the continental United States in 2008 (Bolda et al., 2010). *D. suzukii* is also known as spotted wing *Drosophila* (SWD), due to the characteristic black spots located on the wings of the male. The females, on the other hand, have a serrated ovipositor that enables them to lay eggs into soft-skinned, ripening fruits, as opposed to laying eggs in rotting fruits, like many other *Drosophila* species (Walsh et al., 2011; Walton et al., 2016). As a result, *D. suzukii* control programs rely heavily on calendar spray programs, increasing the likelihood of these pests of developing resistance to commonly used commercial insecticides, such as pyrethroids and spinosads (Bruck et al., 2011; Van Timmeren & Isaacs, 2013). To date, three studies have documented insecticide resistance in field populations of *D. suzukii* in California (Ganjisaffar, Demkovich, et al., 2022; Ganjisaffar, Gress, et al., 2022; Gress & Zalom, 2019). However, the molecular mechanisms underlying insecticide resistance in *D. suzukii* has yet to be described. Therefore, the aim of Chapter 2 is to identify the molecular mechanisms conferring resistance in *D. suzukii*. Understanding these mechanisms will enable the development of molecular diagnostics that can be used to monitor insecticide resistance and can provide insights into how to improve *D. suzukii* management practices.

To identify the molecular mechanisms underlying insecticide resistance, I used both short-read and long-read sequencing to analyze the transcriptomes of fly lines resistant to either pyrethroid or spinosad insecticides, as well as control fly lines derived from the same field-collected populations but

susceptible to the insecticides. Utilizing short-read sequencing data (Illumina platform), I identified that *D. suzukii* resistant to pyrethroids expressed increased basal levels of metabolic enzymes and decreased levels of the pyrethroid target gene, *para*. *Drosophila suzukii* resistant to spinosad, on the other hand, showed increased basal expression of metabolic enzymes and increased expression of genes in the insect cuticle. Additionally, my long-read sequencing data (PacBio platform) revealed transcriptome-wide changes in splicing between the resistant and susceptible fly lines derived from the same geographical population, suggesting that alternative splicing can potentially be an additional mechanism conferring insecticide resistance.

Chapter 2 is the first description of the mechanisms of insecticide resistance in *D. suzukii*. In addition to identifying mechanisms of insecticide resistance previously characterized in other insect species, I also identified transcriptome-wide alterations in splicing as a new mechanism that has not been previously described. Furthermore, we selected biomarkers of resistance from our transcriptome dataset to design and validate quantitative PCR-based molecular diagnostics to identify insecticide resistance and monitor resistance development in the field. Finally, these results can inform growers how to improve *D. suzukii* management strategies to effectively control *D. suzukii* infestations, including insecticide-resistant populations.

In summary, this thesis contributes to our knowledge of how environmental stimuli influence gene expression and organismal physiology. Specifically, pre-programmed changes in the environment, such as the 24-hour day-night cycle, produce rhythmic circadian gene expression, which is in part regulated by the chromatin remodeler, BRM. Additionally, human activities, such as the application of insecticides, provides adaptive pressure that results in changes in gene expression, resulting in the development of insecticide resistance over time.

REFERENCES

Abrieux, A., Xue, Y., Cai, Y., Lewald, K. M., Nguyen, H. N., Zhang, Y., & Chiu, J. C. (2020). EYES ABSENT and TIMELESS integrate photoperiodic and temperature cues to regulate seasonal physiology in *Drosophila*. *Proceedings of the National Academy of Sciences*, *117*(26), 15293–15304. https://doi.org/10.1073/pnas.2004262117

Atamian, H. S., Creux, N. M., Brown, E. A., Garner, A. G., Blackman, B. K., & Harmer, S. L. (2016). Circadian regulation of sunflower heliotropism, floral orientation, and pollinator visits. *Science*, *353*(6299), 587–590. https://doi.org/10.1126/science.aaf9793

Bolda, M. P., Goodhue, R. E., & Zalom, F. G. (2010). Spotted Wing *Drosophila*: Potential Economic Impact of a Newly Established Pest. *Agricultural and Resource Economics Update*, *13*(3), 5–8.

Bruck, D. J., Bolda, M., Tanigoshi, L., Klick, J., Kleiber, J., DeFrancesco, J., Gerdeman, B., & Spitler, H. (2011). Laboratory and field comparisons of insecticides to reduce infestation of *Drosophila suzukii* in berry crops. *Pest Management Science*, *67*(11), 1375–1385. https://doi.org/10.1002/ps.2242

Chiu, J. C., Vanselow, J. T., Kramer, A., & Edery, I. (2008). The phospho-occupancy of an atypical SLIMB-binding site on PERIOD that is phosphorylated by DOUBLETIME controls the pace of the clock. *Genes & Development*, *22*(13), 1758–1772. https://doi.org/10.1101/gad.1682708

Cox, K. H., & Takahashi, J. S. (2019). Circadian clock genes and the transcriptional architecture of the clock mechanism. *Journal of Molecular Endocrinology*, *63*(4), R93–R102. https://doi.org/10.1530/JME-19-0153

Darlington, T. K., Lyons, L. C., Hardin, P. E., & Kay, S. A. (2000). The *period* E-box Is Sufficient to Drive Circadian Oscillation of Transcription *In Vivo*. *Journal of Biological Rhythms*, *15*(6), 462–470. https://doi.org/10.1177/074873040001500603

Dubowy, C., & Sehgal, A. (2017). Circadian Rhythms and Sleep in *Drosophila melanogaster*. *Genetics*, *205*(4), 1373–1397. https://doi.org/10.1534/genetics.115.185157

Dunlap, J. C., & Loros, J. J. (2017). Making time: Conservation of biological clocks from fungi to animals. *Microbiology Spectrum*, *5*(3), 10.1128/microbiolspec.FUNK-0039–2016. https://doi.org/10.1128/microbiolspec.FUNK-0039-2016

Eskin, A. (1979). Identification and physiology of circadian pacemakers. Introduction. *Federation Proceedings*, *38*(12), 2570–2572.

Ganjisaffar, F., Demkovich, M. R., Chiu, J. C., & Zalom, F. G. (2022). Characterization of Field-Derived *Drosophila suzukii* (Diptera: Drosophilidae) Resistance to Pyrethroids in California Berry Production. *Journal of Economic Entomology*, *115*(5), 1676–1684. https://doi.org/10.1093/jee/toac118

Ganjisaffar, F., Gress, B. E., Demkovich, M. R., Nicola, N. L., Chiu, J. C., & Zalom, F. G. (2022). Spatio-temporal Variation of Spinosad Susceptibility in *Drosophila suzukii* (Diptera: Drosophilidae), a Three-year Study in California's Monterey Bay Region. *Journal of Economic Entomology*, *115*(4), 972–980. https://doi.org/10.1093/jee/toac011

Gibson, G. (2008). The environmental contribution to gene expression profiles. *Nature Reviews Genetics*, *9*(8), Article 8. https://doi.org/10.1038/nrg2383

Gress, B. E., & Zalom, F. G. (2019). Identification and risk assessment of spinosad resistance in a California population of *Drosophila* suzukii. *Pest Management Science*, *75*(5), 1270–1276. https://doi.org/10.1002/ps.5240

Grima, B., Lamouroux, A., Chélot, E., Papin, C., Limbourg-Bouchon, B., & Rouyer, F. (2002). The F-box protein slimb controls the levels of clock proteins period and timeless. *Nature*, *420*(6912), 178–182. https://doi.org/10.1038/nature01122

Hao, H., Allen, D. L., & Hardin, P. E. (1997). A circadian enhancer mediates PER-dependent mRNA cycling in *Drosophila melanogaster*. *Molecular and Cellular Biology*, *17*(7), 3687–3693. https://doi.org/10.1128/MCB.17.7.3687

Hardin, P. E., Hall, J. C., & Rosbash, M. (1990). Feedback of the *Drosophila period* gene product on circadian cycling of its messenger RNA levels. *Nature*, *343*(6258), Article 6258. https://doi.org/10.1038/343536a0

Hunter-Ensor, M., Ousley, A., & Sehgal, A. (1996). Regulation of the *Drosophila* Protein Timeless Suggests a Mechanism for Resetting the Circadian Clock by Light. *Cell*, *84*(5), 677–685. https://doi.org/10.1016/S0092-8674(00)81046-6

Jang, A. R., Moravcevic, K., Saez, L., Young, M. W., & Sehgal, A. (2015). *Drosophila* TIM Binds Importin α1, and Acts as an Adapter to Transport PER to the Nucleus. *PLOS Genetics*, *11*(2), e1004974. https://doi.org/10.1371/journal.pgen.1004974

Jordán-Pla, A., Yu, S., Waldholm, J., Källman, T., Östlund Farrants, A.-K., & Visa, N. (2018). SWI/SNF regulates half of its targets without the need of ATP-driven nucleosome remodeling by Brahma. *BMC Genomics*, *19*(1), 367. https://doi.org/10.1186/s12864-018-4746-2

Ko, H. W., Jiang, J., & Edery, I. (2002). Role for Slimb in the degradation of *Drosophila* Period protein phosphorylated by Doubletime. *Nature*, *420*(6916), 673–678. https://doi.org/10.1038/nature01272

Koike, N., Yoo, S.-H., Huang, H.-C., Kumar, V., Lee, C., Kim, T.-K., & Takahashi, J. S. (2012). Transcriptional Architecture and Chromatin Landscape of the Core Circadian Clock in Mammals. *Science*, *338*(6105), 349–354. https://doi.org/10.1126/science.1226339

Kwok, R. S., Lam, V. H., & Chiu, J. C. (2016). Understanding the role of chromatin remodeling in the regulation of circadian transcription in *Drosophila*. *Fly*, *9*(4), 145–154. https://doi.org/10.1080/19336934.2016.1143993

Kwok, R. S., Li, Y. H., Lei, A. J., Edery, I., & Chiu, J. C. (2015). The Catalytic and Non-catalytic Functions of the Brahma Chromatin-Remodeling Protein Collaborate to Fine-Tune Circadian Transcription in *Drosophila*. *PLOS Genetics*, *11*(7), e1005307. https://doi.org/10.1371/journal.pgen.1005307

Lam, V. H., Li, Y. H., Liu, X., Murphy, K. A., Diehl, J. S., Kwok, R. S., & Chiu, J. C. (2018). CK1α Collaborates with DOUBLETIME to Regulate PERIOD Function in the *Drosophila* Circadian Clock. *Journal of Neuroscience*, *38*(50), 10631–10643. https://doi.org/10.1523/JNEUROSCI.0871-18.2018

Lee, C.-K., Shibata, Y., Rao, B., Strahl, B. D., & Lieb, J. D. (2004). Evidence for nucleosome depletion at active regulatory regions genome-wide. *Nature Genetics*, *36*(8), Article 8. https://doi.org/10.1038/ng1400

Myers, M. P., Wager-Smith, K., Rothenfluh-Hilfiker, A., & Young, M. W. (1996). Light-induced degradation of TIMELESS and entrainment of the *Drosophila* circadian clock. *Science (New York, N.Y.)*, *271*(5256), 1736–1740. https://doi.org/10.1126/science.271.5256.1736

Nachtomy, O., Shavit, A., & Yakhini, Z. (2007). Gene expression and the concept of the phenotype. *Studies in History and Philosophy of Science Part C: Studies in History and Philosophy of Biological and Biomedical Sciences*, *38*(1), 238–254. https://doi.org/10.1016/j.shpsc.2006.12.014

Patke, A., Young, M. W., & Axelrod, S. (2020). Molecular mechanisms and physiological importance of circadian rhythms. *Nature Reviews Molecular Cell Biology*, *21*(2), Article 2. https://doi.org/10.1038/s41580-019-0179-2

Szabó, Á., Papin, C., Cornu, D., Chélot, E., Lipinszki, Z., Udvardy, A., Redeker, V., Mayor, U., & Rouyer, F. (2018). Ubiquitylation Dynamics of the Clock Cell Proteome and TIMELESS during a Circadian Cycle. *Cell Reports*, *23*(8), 2273–2282. https://doi.org/10.1016/j.celrep.2018.04.064

Tabuloc, C. A., Cai, Y. D., Kwok, R. S., Chan, E. C., Hidalgo, S., & Chiu, J. C. (2023). CLOCK and TIMELESS regulate rhythmic occupancy of the BRAHMA chromatin-remodeling protein at clock gene promoters. *PLOS Genetics*, *19*(2), e1010649. https://doi.org/10.1371/journal.pgen.1010649

Top, D., Harms, E., Syed, S., Adams, E. L., & Saez, L. (2016). GSK-3 and CK2 Kinases Converge on Timeless to Regulate the Master Clock. *Cell Reports*, *16*(2), 357–367. https://doi.org/10.1016/j.celrep.2016.06.005

Van Timmeren, S., & Isaacs, R. (2013). Control of spotted wing *Drosophila*, *Drosophila suzukii*, by specific insecticides and by conventional and organic crop protection programs. *Crop Protection*, *54*, 126–133. https://doi.org/10.1016/j.cropro.2013.08.003

Walsh, D. B., Bolda, M. P., Goodhue, R. E., Dreves, A. J., Lee, J., Bruck, D. J., Walton, V. M., O'Neal, S. D., & Zalom, F. G. (2011). *Drosophila suzukii* (Diptera: Drosophilidae): Invasive Pest of Ripening Soft Fruit Expanding its Geographic Range and Damage Potential. *Journal of Integrated Pest Management*, *2*(1), G1–G7. https://doi.org/10.1603/IPM10010

Walton, V. M., Burrack, H. J., Dalton, D. T., Isaacs, R., Wiman, N., & Ioriatti, C. (2016). Past, present and future of *Drosophila suzukii:* distribution, impact and management in United States berry fruits. *Acta Horticulturae*, *1117*, 87–94. https://doi.org/10.17660/ActaHortic.2016.1117.16

Zeng, H., Qian, Z., Myers, M. P., & Rosbash, M. (1996). A light-entrainment mechanism for the *Drosophila* circadian clock. *Nature*, *380*(6570), Article 6570. https://doi.org/10.1038/380129a0

Zhou, J., Yu, W., & Hardin, P. E. (2016). CLOCKWORK ORANGE Enhances PERIOD Mediated Rhythms in Transcriptional Repression by Antagonizing E-box Binding by CLOCK-CYCLE. *PLoS Genetics*, *12*(11), e1006430. https://doi.org/10.1371/journal.pgen.1006430

Zhu, Q., & Belden, W. J. (2020). Molecular Regulation of Circadian Chromatin. *Journal of Molecular Biology*, *432*(12), 3466–3482. https://doi.org/10.1016/j.jmb.2020.01.009

Chapter 1: CLOCK and TIMLESS regulate rhythmic occupancy of the BRAHMA chromatin-remodeling protein at clock gene promoters

Christine A. Tabuloc, Yao D. Cai, Rosanna S. Kwok, Elizabeth C. Chan, Sergio Hidalgo, and Joanna C. Chiu*

Department of Entomology and Nematology, College of Agricultural and Environmental Sciences, University of California Davis, CA, USA

Published in PLOS Genetics (2023), 19(2): e1010649. doi: 10.1371/journal.pgen.1010649

Author contributions: C.A.T., R.S.K., Y.D.C., and J.C.C. designed research; C.A.T. and R.S.K performed research and analyzed data; C.A.T., R.S.K., and E.C.C generated reagents; C.A.T., Y.D.C., R.S.K., and J.C.C. contributed to critical interpretation of the data; C.A.T. wrote the paper with the input of J.C.C., S.H., and Y.D.C.

PLOS GENETICS

RESEARCH ARTICLE

CLOCK and TIMELESS regulate rhythmic occupancy of the BRAHMA chromatin-remodeling protein at clock gene promoters

Christine A. Tabuloc, Yao D. Cai, Rosanna S. Kwok, Elizabeth C. Chan, Sergio Hidalgo, Joanna C. Chiu*

Department of Entomology and Nematology, College of Agricultural and Environmental Sciences, University of California Davis, Davis, California, United States of America

* jcchiu@ucdavis.edu

Citation: Tabuloc CA, Cai YD, Kwok RS, Chan EC, Hidalgo S, Chiu JC (2023) CLOCK and TIMELESS regulate rhythmic occupancy of the BRAHMA chromatin-remodeling protein at clock gene promoters. PLoS Genet 19(2): e1010649. https://doi.org/10.1371/journal.pgen.1010649

Editor: Gaiti Hasan, National Centre for Biological Sciences, TIFR, INDIA

Received: October 17, 2022

Accepted: February 2, 2023

Published: February 21, 2023

Data Availability Statement: All data discussed in the paper have been made available to readers in the manuscript or in Supporting information files.

Funding: This project is supported by NIH R01 GM102225, NSF IOS 1456297, and UCSCCC/EHSC pilot award from NIH P30 ES023513 to JCC. Research in the laboratory of JCC is supported by NIH R01 DK124068. The funders had no role in study design, data collection and analysis, decision to publish, or preparation of the manuscript.

Abstract

Circadian clock and chromatin-remodeling complexes are tightly intertwined systems that regulate rhythmic gene expression. The circadian clock promotes rhythmic expression, timely recruitment, and/or activation of chromatin remodelers, while chromatin remodelers regulate accessibility of clock transcription factors to the DNA to influence expression of clock genes. We previously reported that the BRAHMA (BRM) chromatin-remodeling complex promotes the repression of circadian gene expression in *Drosophila*. In this study, we investigated the mechanisms by which the circadian clock feeds back to modulate daily BRM activity. Using chromatin immunoprecipitation, we observed rhythmic BRM binding to clock gene promoters despite constitutive BRM protein expression, suggesting that factors other than protein abundance are responsible for rhythmic BRM occupancy at clock-controlled loci. Since we previously reported that BRM interacts with two key clock proteins, CLOCK (CLK) and TIMELESS (TIM), we examined their effect on BRM occupancy to the *period* (*per*) promoter. We observed reduced BRM binding to the DNA in *clk* null flies, suggesting that CLK is involved in enhancing BRM occupancy to initiate transcriptional repression at the conclusion of the activation phase. Additionally, we observed reduced BRM binding to the *per* promoter in flies overexpressing TIM, suggesting that TIM promotes BRM removal from DNA. These conclusions are further supported by elevated BRM binding to the *per* promoter in flies subjected to constant light and experiments in *Drosophila* tissue culture in which the levels of CLK and TIM are manipulated. In summary, this study provides new insights into the reciprocal regulation between the circadian clock and the BRM chromatin-remodeling complex.

Author summary

Circadian clocks are endogenous time-keeping mechanisms that allow organisms to anticipate and adapt to daily changes in their external environment. These clocks are driven by a molecular oscillator that generates rhythms in the expression of many genes, termed clock-controlled genes. The genomic DNA containing these clock-controlled genes are

Competing interests: The authors have declared that no competing interests exist.

also modified in a rhythmic manner throughout the day. DNA is more tightly packaged with histone proteins when transcription of clock-controlled genes is repressed while the interaction between DNA and histone proteins is more relaxed during transcriptional activation. We found that two key clock proteins, CLOCK and TIMELESS, regulate daily rhythmicity in the binding of BRAHMA, a chromatin remodeler, to DNA spanning clock-controlled genes to facilitate their rhythmic gene expression cycles. Moreover, because TIMELESS is sensitive to light, our study provides new insights into how light can affect DNA structure and gene expression.

Introduction

The circadian clock is an endogenous time-keeping mechanism that enables organisms to synchronize their behavioral and physiological processes to their external environment [1–4]. Cellular clocks are driven by molecular oscillators, each of which is composed of a negative transcriptional translational feedback loop (TTFL) [5]. In *Drosophila melanogaster* (herein referred to as *Drosophila)*, transcription factors CLOCK (CLK) and CYCLE (CYC) heterodimerize and bind to the Enhancer box (E-box) sequences located in the promoters of clock-controlled genes, including *period* (*per*) and *timeless* (*tim*), thereby activating their transcription in early to midday [6–8]. Delay in the accumulation of PER and TIM proteins contributes to the extension of the TTFL to 24 hours (reviewed in [1,4]). This delay is mediated by post-transcriptional mechanisms including RNA splicing [9], translation [10,11], control of subcellular localization [12], and protein degradation [13–15]. Around midnight, when PER and TIM levels accumulate to sufficient levels, they heterodimerize and translocate into the nucleus [16–18], where they interact with the CLK-CYC complex to repress their own transcription and the transcription of other CLK-activated genes [8,19,20]. Finally, proteasome dependent degradation of PER and TIM [13,15,21,22] and modulation of CLK activity by post-translational modifications [23–28] terminates the circadian repression phase in late day to early morning, initiating the next circadian cycle.

The chromatin at clock-controlled genes undergoes rhythmic modifications mediated by the activities of histone modifiers and chromatin-remodeling proteins, thus facilitating rhythmic gene expression over the 24-hour cycle [29–31]. There is accumulating evidence showing that these proteins interact with core clock components to impose temporal control of their activities at clock gene loci. For instance, the mammalian homolog of *Drosophila* CLK, CLOCK, interacts with histone acetyltransferases [32] and ubiquitin ligases [33] to modulate histone density at clock gene loci. In *Drosophila*, CLK interacts with NIPPED-A, a component of both the SAGA and TIP60 chromatin-remodeling complexes to promote circadian transcription [34,35]. And finally, the transcriptional activator of the *Neurospora* clock, White Collar 1, interacts with the Switch/Sucrose Non-Fermentable (SWI/SNF) chromatin-remodeling complex to activate clock gene expression [36]. These interactions suggest that core clock proteins closely coordinate with chromatin remodelers and histone modifiers to shape chromatin landscape and rhythmic gene expression.

We previously characterized the BRAHMA (BRM) complex, a member of the SWI/SNF chromatin-remodeling family, as a regulator of circadian transcription in *Drosophila* [30,37]. Specifically, we found that BRM condenses the chromatin and possibly serves as a scaffold for repressive complexes at the promoters of *per* and *tim*. We also observed that BRM interacts with core clock proteins, CLK and TIM, in fly tissues at specific times of the day-night cycle [37], prompting the question of whether clock proteins might reciprocally regulate BRM

activity to shape rhythmic nucleosome density and gene expression. In addition to clock-controlled genes, BRM regulates genes involved in cell cycle [38–41], DNA damage response [42–44], development [45,46], and stem cell renewal and differentiation [47–50]. In fact, BRM is estimated to regulate the expression of approximately 80% of the *Drosophila* genome [51]. This further begs the question of how BRM regulates certain loci in a rhythmic manner while majority of its targets are not rhythmically regulated. Given the precedents of interactions between core clock transcription factors and histone modifiers/chromatin remodelers, we hypothesize that core clock proteins regulate BRM occupancy at circadian loci to ensure rhythmic BRM activity at these sites.

Here, we investigated the mechanisms that promote rhythmic BRM activity, specifically at CLK-activated loci. We observed that BRM rhythmically binds to the promoters of clock-controlled genes despite its constitutive protein expression in fly heads. Using the *per* gene as a prototypical CLK-activated gene, we revealed that core clock components, CLK and TIM, play key roles in regulating rhythmic BRM occupancy at clock gene promoters. In particular, we found that CLK promotes the recruitment of BRM to these promoters and paves the way for the initiation of circadian repression by stabilizing BRM protein, which functions to increase nucleosome density. TIM, on the other hand, promotes the removal of BRM from the DNA to reset the chromatin landscape following transcriptional repression to prepare for the next transcriptional cycle. Our study provides new insights into how general chromatin remodelers collaborate with clock proteins to facilitate expression of the circadian transcriptome.

Results

BRM exhibits rhythmic occupancy at clock gene promoters despite constitutive protein expression

We first sought to determine whether BRM occupancy at CLK target loci is rhythmic. Although we previously showed that BRM localizes at the E-boxes of *per* and *tim* promoters, specifically the *per* circadian regulatory sequence (CRS) and *tim* E-box 1 (E1) [37], those experiments were performed in flies expressing epitope tagged BRM expressed under the control of the *tim* promoter. We therefore generated a polyclonal antibody against BRM to more accurately detect endogenous BRM occupancy. We validated the antibody in *Drosophila* Schneider (S2) cells and fly head tissue. The new antibody was able to detect endogenous BRM expression in both preparations (Fig 1A). In S2 cells, a sharp band is observed around 250 kDa, consistent with the predicted size of BRM. Higher protein levels are observed when overexpressing BRM by transient transfection as compared to untransfected control S2 cells ($t = 4.683$, $df = 2$, $p = 0.0427$) (Fig 1B). We generated flies overexpressing BRM with a 3XFLAG-HIS (FH) epitope tag in *tim*-expressing cells by crossing a *tim-UAS-Gal4* (*TUG*) driver line with a responder line expressing *UAS-brm-FH*. We observed higher BRM signal in head extracts of flies overexpressing BRM as compared to the *TUG* parental control ($t = 4.941$, $df = 2$, $p = 0.0386$) (Fig 1B). Furthermore, the specificity of the signal was confirmed with pre-adsorption of the antibody with a dilution series of the BRM antigen (S1 Fig). As increasing amounts of the BRM antigen were incubated with the BRM polyclonal antibody prior to addition to western blots, the BRM signal became progressively weaker (0.1ul antigen at 1ul/ug: $q = 23.90$, $df = 8$, $p<0.0001$; 1ul antigen: $q = 31.92$, $df = 8$, $p<0.0001$; 10ul antigen: $q = 31.21$, $df = 8$, $p<0.0001$). BRM signal was normalized to a non-specific band on the same blot.

Leveraging the new BRM polyclonal antibody, we assayed daily BRM occupancy at a number of clock gene promoters in whole head extracts collected from wild type (WT, w^{1118}) flies entrained in 12:12 light:dark (LD) conditions (Fig 1C-F). We observed robust rhythmicity of BRM occupancy at each of the tested promoters, including *per*, *tim*, *vrille* (*vri*), and *clockwork*

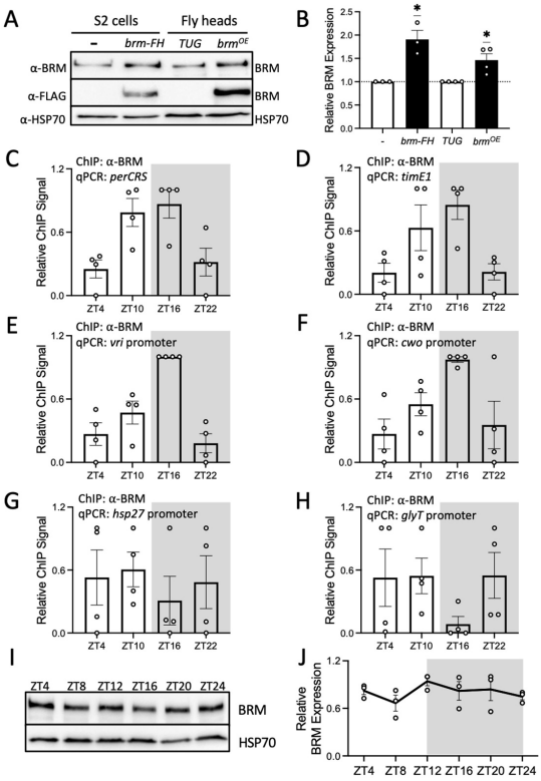

Fig 1. BRM binding to clock gene promoters in fly heads is rhythmic despite constitutive BRM protein expression. (A) Western blot validation of the BRM antibody detecting proteins extracted from *Drosophila* S2 cells and heads of flies collected at ZT16 on LD3 (light-dark cycle day 3) subsequent to 2-day entrainment at 12h:12h LD. S2 cells were either untransfected or transfected with *pAc-brm-3XFLAG-His*. The two fly lines used for validation are flies expressing either endogenous levels of BRM (*w; tim(UAS)-Gal4* parental driver line referred to as *TUG*) or flies expressing FLAG-His-tagged BRM (referred to as brm^{OE}) (top panel). FLAG epitope was simultaneously detected to confirm expression of FLAG-tagged BRM (middle panel). HSP70 was used as a loading control (bottom panel). (B) Quantification of BRM signal shown in Fig 1A. Each data point represents a biological replicate. Error bars represent ±SEM (S2 cells: n = 3; Fly heads: n = 4). Asterisks denote significant p-values: $^{*}p<0.05$. (C-H) BRM occupancy at the promoters of (C) *period* (*per*), (D) *timeless* (*tim*), (E) *vrille (vri)*, (F) *clockwork orange (cwo)*, (G) *heat shock protein 27* (*hsp27)*, and (H) *glycine transporter* (*glyT*) was detected in heads of w^{1118} (WT) flies collected at the indicated time points on LD3 subsequent to 2-day entrainment at 12h:12h LD. The grey background denotes the dark phase of the LD cycle. Each data point represents a biological replicate (n = 4), and each biological replicate is an average of 2 technical replicates of qPCR. RAIN: (C) p = 0.0053; peak: ZT16, (D) p = 0.0487; peak: ZT16, (E) p = 0.0124; peak: ZT16, (F) p = 0.0005; peak: ZT16, (G) p = 0.9543, and (H) p = 0.3140 (I) Western blot showing BRM expression in heads of w^{1118} flies (top panel) collected at the indicated time points on LD3. HSP70 was used as a loading control (bottom panel). (J) Quantification of BRM signal normalized to HSP70 as shown in Fig 1I (n = 3, RAIN p = 0.5811).

https://doi.org/10.1371/journal.pgen.1010649.g001

orange (*cwo*) (Fig 1C RAIN p = 0.0053; peak: ZT16, Fig 1D RAIN p = 0.0487; peak: ZT16, Fig 1E RAIN p = 0.0124; peak: ZT16, and Fig 1F RAIN p = 0.0005; peak: ZT16; ZT is defined as Zeitgeber Time, and ZT0 denotes lights on time in the LD cycle). To assess the specificity of rhythmic BRM occupancy, we also assessed BRM binding at the promoters of two non-clock

gene promoters, *heat shock protein* 27 (*hsp27*) and *glycine transporter* (*glyT*), (Fig 1G and 1H). Neither of these genes exhibit rhythmic BRM occupancy over the 24-hour LD cycle (Fig 1G RAIN p = 0.9543; Fig 1H RAIN: p = 0.3140). To determine whether rhythmic BRM occupancy is a result of rhythmic BRM protein abundance, we analyzed BRM protein levels in WT fly head extracts over a LD cycle. We observed that BRM protein expression is constitutive throughout the 24-hour cycle (Fig 1I and 1J) (Fig 1J RAIN p = 0.5811), indicating that the daily oscillation in BRM occupancy at clock gene promoters is not dependent on rhythmic BRM abundance.

CLK promotes BRM occupancy at the *per* promoter

We have previously observed that BRM binds to CLK in fly head extracts between ZT12 to ZT20 while BRM-TIM interactions were observed at and after ZT20 [37]. We therefore hypothesized that CLK promotes BRM occupancy to CLK target loci since BRM occupancy at clock genes starts to increase around ZT10 (Fig 1C–1F). We reasoned that if CLK promotes BRM occupancy to clock gene promoters, BRM binding to the DNA would be lower in the absence of CLK. To test this hypothesis, we performed chromatin immunoprecipitation in combination with quantitative real-time PCR (ChIP-qPCR) to compare BRM occupancy in WT (w^{1118}) and *clk* null (w^{1118};clk^{out}) flies. Because BRM binds rhythmically to the promoters of *per*, *tim*, *vri*, and *cwo* with the same phase (Fig 1C–1F), we opted to use the *perCRS* as a representative CLK-activated promoter in subsequent experiments. We observed that BRM occupancy was not rhythmic (RAIN: WT p = 0.0056, peak: ZT16; clk^{out} p = 0.7915) and significantly lower in the clk^{out} mutant at ZT16 (t = 4.877, df = 24, p = 0.0002) (Fig 2A), the

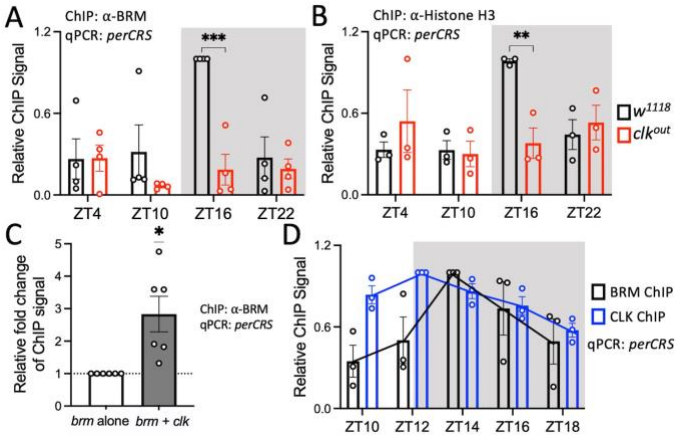

Fig 2. CLK promotes BRM occupancy at the *per* promoter. (A) BRM and (B) Histone H3 occupancy at the *perCRS* in head tissues of w^{1118} (black) and clk^{out} (red) flies (A: n = 4; w^{1118} RAIN p = 0.0056, clk^{out} RAIN p = 0.7915; B: n = 3; w^{1118} RAIN p = 0.0488, clk^{out} RAIN p = 0.2080). Each data point represents a biological replicate, and each biological is an average of at least 2 technical replicates of qPCR. Asterisks denote significant p-values: *p<0.05, ***p<0.001. Error bars represent ±SEM. The grey background denotes the dark phase of the LD cycle. (C) BRM binding at the *perCRS* in S2 cell nuclear extracts expressing either *brm* alone (white) or *brm* co-expressed with *clk* (grey). Relative fold change of ChIP signal is calculated with amount of BRM binding in the *brm* alone condition equal to 1(n = 6). (D) BRM (black) and CLK (blue) occupancy at the *perCRS* in heads of w^{1118} flies collected at the indicated time points on LD3 (n = 3; BRM ChIP: RAIN p = 0.0016, phase = ZT14; CLK ChIP: RAIN p = 6.17e-6, phase = ZT12; DODR p = 0.0033). Trendlines connect the mean relative ChIP signal of each time point.

https://doi.org/10.1371/journal.pgen.1010649.g002

time point at which BRM occupancy normally peaks in WT flies at the time points we sampled (Fig 1C).

Because BRM condenses the chromatin by increasing nucleosome density at clock loci [37], we expect rhythms of nucleosome density to match BRM occupancy. Therefore, we assayed Histone H3 occupancy in WT and clk^{out} flies to assess whether the decrease and loss of rhythmicity in BRM binding to the *per* promoter results in reduced Histone H3 density and rhythmicity at the same locus. H3 occupancy is often used to reflect nucleosome density [37,52]. As predicted, we observed a significant reduction in Histone H3 occupancy at ZT16 ($t = 3.629$, $df = 16$, $p = 0.0090$) as well as a loss of rhythmicity (RAIN: WT $p = 0.0488$, peak: ZT16; clk^{out} $p = 0.2080$) in the clk^{out} mutant as compared to WT flies (Fig 2B).

We next assayed BRM occupancy in *Drosophila* S2 cells to further support the function of CLK on BRM occupancy. S2 cells do not possess a functional molecular clock, so it is a simplified and valuable system to investigate functions of key clock proteins in the molecular oscillator without the complication of TTFL. We observed elevated BRM binding to the *perCRS* when *brm* is co-expressed with *clk* when compared to cells expressing *brm* alone ($t = 3.340$, $df = 5$, $p = 0.0205$) (Fig 2C), suggesting that CLK plays a role in promoting BRM occupancy to the *per* promoter.

We reasoned that CLK should bind to the promoter prior to BRM if CLK recruits BRM to this locus. Therefore, we assayed BRM and CLK occupancy every 2 hours from ZT10 to ZT18 to obtain a higher resolution view of the occupancy of these proteins at the *perCRS*. We observed that BRM binding peaks at ZT14 while CLK occupancy peaks at ZT12 (BRM RAIN $p = 0.0016$; CLK RAIN p = 6.17e-6; DODR: 0.0033) (Fig 2D), confirming that CLK binding to the *per* promoter precedes BRM binding. All together, these results suggest that CLK plays a role in promoting BRM occupancy, potentially via recruitment of BRM to the *per* promoter or stabilizing BRM once it has been recruited to the promoter.

CLK expression stabilizes BRM

In addition to recruiting BRM to the *per* promoter, it is possible that CLK can increase BRM binding to DNA through other mechanisms such as promoting BRM protein levels. To determine if CLK influences BRM expression, we compared daily BRM protein abundance in WT (w^{1118}) and clk^{out} flies (Fig 3A and 3B). We observed significantly lower BRM abundance in clk^{out} flies at ZT16 ($t = 3.111$, $df = 16$, $p = 0.0266$) (Fig 3B), revealing that lower BRM protein levels may contribute to decreased BRM occupancy (Fig 2A). Lower BRM levels in clk^{out} flies also suggests that *brm* could be a CLK-activated gene, and a CLK ChIP-chip dataset showed that CLK binds to the *brm* promoter [53]. We therefore assessed daily rhythms in *brm* mRNA expression in WT and clk^{out} flies (Fig 3C). We found no difference in *brm* mRNA levels between the clk^{out} mutant and the WT control. Thus, rather than regulating *brm* mRNA expression, it is possible that CLK stabilizes BRM protein. We tested this possibility by performing a cycloheximide (CHX) chase experiment in *Drosophila* S2 cells. BRM protein degrades significantly slower when co-expressed with *clk* ($t = 7.316$, $df = 5$, $p<0.0001$) (Fig 3D and 3E). Furthermore, we observed that BRM migrates slower when co-expressed with CLK, suggesting BRM is post-translationally modified in the presence of CLK (S2A Fig). When lysate extracted from S2 cells expressing both BRM and CLK was treated with lambda phosphatase, this shift in migration is no longer present, suggesting that CLK is promoting BRM stability through phosphorylation (S2B Fig).

TIM reduces BRM occupancy at the *per* promoter

We next explored the mechanism by which BRM is removed from clock gene promoters. Since BRM interacts with TIM in fly head tissues at ZT20, which is subsequent to CLK-BRM

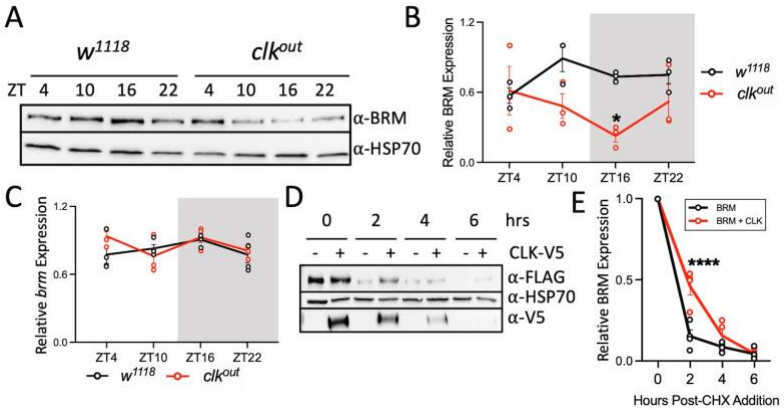

Fig 3. CLK stabilizes BRM protein. (A-B) BRM protein and (C) *brm* mRNA levels in the heads of w^{1118} (black) and clk^{out} (red) flies collected at the indicated time points on LD3. (B) BRM signal (A: top panel) was quantified and normalized to HSP70 (A: bottom panel) (n = 3). The grey background denotes the dark phase of the LD cycle. Each data point represents a biological replicate. Error bars represent ±SEM. Asterisks denote significant p-values: $^{*}p<0.05$. (C) Steady state *brm* mRNA was normalized to *cbp20* mRNA expression. Each biological replicate (n = 4) is an average of 2 technical replicates of qPCR. (D) Western blot detecting FLAG-tagged BRM (top panel) every 2 hours (hrs) post-cycloheximide (CHX) addition to S2 cells expressing *brm* alone or *brm* co-expressed with *clk*. HSP70 was used as a loading control (middle panel). V5 was detected to confirm CLK-V5 expression (bottom panel). (E) BRM expression was normalized to HSP70 (n = 3). Asterisks denote significant p-values: $^{****}p<0.0001$.

https://doi.org/10.1371/journal.pgen.1010649.g003

interaction [37], we hypothesized that TIM facilitates BRM removal from the *per* promoter. We therefore examined whether increased TIM expression would result in decreased BRM occupancy by comparing BRM binding to the *perCRS* in WT (w^{1118}) flies and in flies overexpressing *tim* (w^{1118};*ptim(WT)*) (herein referred to as tim^{OE} flies) [54]. We observed reduced BRM binding at ZT16 in tim^{OE} flies (t = 2.843, df = 16, p = 0.0462) (Fig 4A) and confirmed that this reduction is not a result of lower BRM levels in tim^{OE} flies as compared to WT control (S3A and S3C Fig). TIM overexpression in tim^{OE} flies was validated by western blot detection (ZT16: t = 5.661, df = 16, p = 0.0001; ZT22: t = 5.976, df = 16, p<0.0001) (S3A and S3B Fig). We examined the effect of reduced BRM binding to nucleosome density by measuring Histone H3 occupancy in WT and tim^{OE} flies, and we observed a significant decrease in H3 occupancy at the *per* promoter at ZT22 in the mutant (t = 2.963, df = 16, p = 0.0361) (Fig 4B).

We further investigated the effect of TIM on BRM by analyzing BRM occupancy in WT flies entrained in LD cycles and subsequently released into constant light (LL). Because TIM undergoes light-dependent degradation [55–57], its expression is drastically reduced in LL [30,54]. As expected, we observed an increase in BRM binding at CT22 in flies maintained in LL as compared to flies in LD (t = 11.17, df = 16, p<0.0001; CT is defined as Circadian Time) (Fig 4C). Because LL can affect the levels of proteins in addition to TIM, e.g. CLK, we sought to determine the direct effect of TIM on BRM by assaying BRM occupancy at the *perCRS* in *Drosophila* S2 cells by expressing either *brm* alone or *brm* co-expressed with *tim*. In the presence of *tim*, BRM occupancy is lower (t = 4.654, df = 3, p = 0.0187) (Fig 4D), supporting the model that TIM promotes the removal of BRM from the DNA.

Furthermore, we leveraged a *brm* gain-of-function (brm^{GOF}) mutant fly to confirm our findings on the effect of TIM on BRM function. This mutant expresses a non-phosphorylatable

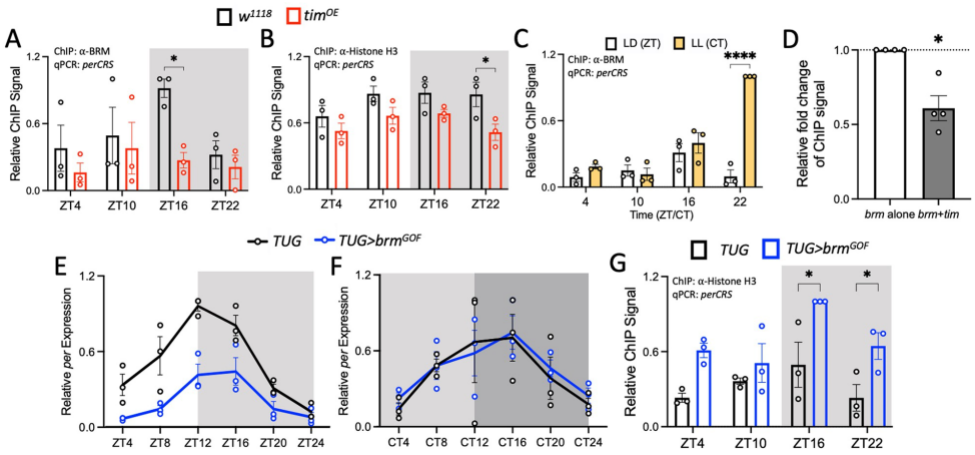

Fig 4. TIM promotes the reduction of BRM occupancy at the *per* promoter. (A) BRM and (B) Histone H3 occupancy at the *perCRS* in head nuclear extracts of w^{1118} (black) and w^{1118};*ptim(WT)* (referred to as tim^{OE}) (red) flies collected at the indicated time points on LD3. Each data point represents a biological replicate (n = 3), and each biological replicate is an average of at least 2 technical replicates of qPCR. Error bars represent ±SEM. The grey background denotes the dark phase of the LD cycle. Asterisks denote significant p-values: *p<0.05. (C) BRM occupancy at the *perCRS* in head extracts of *TUG* flies entrained for 3 days in 12:12LD and collected on LD4 (white) or LL1 (yellow) (n = 3). (D) BRM binding at the *perCRS* in S2 cell nuclear extracts expressing either *brm* alone (white) or *brm* co-expressed with *tim* (grey) (n = 4). ChIP signal is relative to the amount of BRM binding in the *brm* alone condition. (E-F) Steady state mRNA expression of *per* in the heads of *TUG* (black) and *TUG>brm*^{GOF} (blue) flies entrained in LD for 3 days and collected on (E) LD4 and (F) DD1. Steady state *cbp20* mRNA levels were used for normalization. Each biological replicate (n = 3) is an average of at least 2 technical replicates of qPCR. The light grey background denotes subjective day, and the dark grey background denotes subjective night in complete darkness (DD) conditions. CircaCompare: (E) MESOR: 9.997e-8, amplitude: 0.0026 and (F) MESOR: 0.688, amplitude: 0.597. (G) Histone H3 occupancy at the *perCRS* in *TUG* and *TUG>brm*^{GOF} flies (n = 3). Asterisks denote significant p-values: *p<0.05 and ****p<0.0001.

https://doi.org/10.1371/journal.pgen.1010649.g004

mutant of *brm* at specific cyclin dependent kinase (CDK) sites [58]. *brm*^{GOF} was expressed in *tim*-expressing cells using the *TUG* driver (*TUG>brm*^{GOF}), and *per* mRNA expression was assayed in LD and in constant darkness (DD). We expect that increased levels of TIM protein in DD would diminish the effect of the gain-of-function *brm* mutation if TIM indeed removes BRM from the *per* promoter. We observed dampening of *per* mRNA rhythms in the mutant when compared to the *TUG* parental control in LD conditions (CircaCompare: MESOR p = 9.997e-8, amplitude p = 0.0026) (Fig 4E). This can be explained by elevation of *per* repression mediated by increased BRM activity in *TUG>brm*^{GOF} flies. As expected, no differences in *per* mRNA expression and rhythm were found between *TUG* control and *TUG>brm*^{GOF} flies in DD, given more TIM is available to remove BRM^{GOF} (CircaCompare: MESOR p = 0.688, amplitude p = 0.597) (Fig 4F).

Finally, we examined whether lower clock gene expression in LD (Fig 4E) correlates with higher nucleosome density by measuring Histone H3 occupancy in *TUG* and *TUG>brm*^{GOF} flies. Consistent with *per* mRNA rhythms, we observed an increase in Histone H3 occupancy in the mutant, specifically at ZT16 (t = 3.476, df = 16, p = 0.0124) and ZT22 (t = 2.849, df = 16, p = 0.0124) (Fig 4G). Our results indicate that the *brm*^{GOF} mutation enhances the ability of BRM to condense the chromatin at the *per* promoter, resulting in lower clock gene expression. This is in agreement with our previous finding that BRM promotes repression of clock genes [37]. Taken together the results from our four independent approaches, we conclude that TIM reduces BRM function by reducing its occupancy at the *per* promoter.

Discussion

In this study, we provide evidence that key clock transcription factors facilitate rhythmic BRM activity at clock gene promoters by mediating rhythmic BRM binding to these loci (Fig 5). Our findings reveal that following peak CLK-CYC binding, CLK interacts with BRM and increases BRM occupancy at clock gene loci partly by stabilizing BRM protein. Once bound, BRM modifies the chromatin to produce a more repressive chromatin landscape by condensing the chromatin catalytically and possibly serving as a scaffold for other repressors [37]. At the end of the activation phase of the circadian transcription cycle, TIM interacts with BRM and promotes its

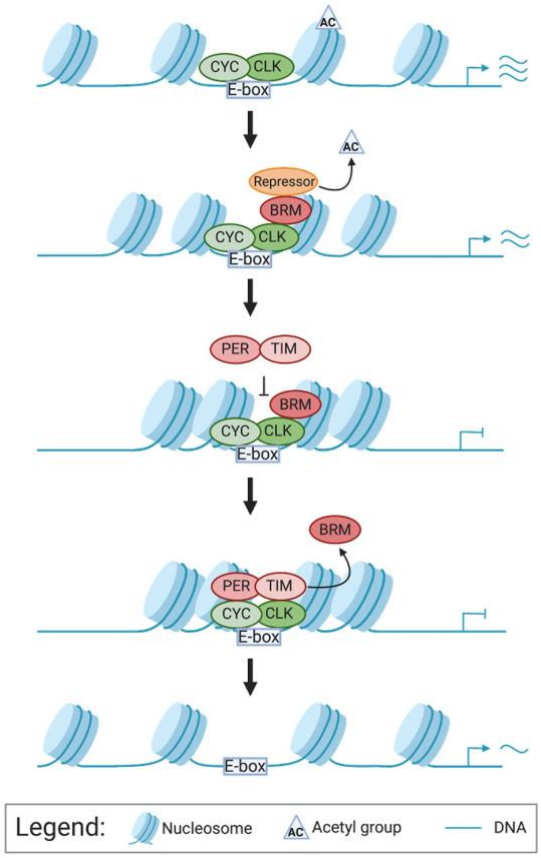

Fig 5. Model depicting the impact of CLK and TIM on BRM occupancy at the *per* promoter. CLK-CYC heterodimers bind to the E-box of *per* to activate transcription. At the peak of transcription, CLK promotes BRM binding to the chromatin. While bound, BRM condenses the chromatin and recruits repressors to reduce gene transcription levels. When PER-TIM complexes are in the nucleus to repress CLK-CYC activated transcription, TIM promotes the removal of BRM from the DNA to reset the chromatin for the next cycle of transcription. This figure was created with BioRender.com (license to lab of JCC).

https://doi.org/10.1371/journal.pgen.1010649.g005

removal from DNA, thus resetting the chromatin state for the next daily transcription cycle. Based on available data, we cannot determine whether BRM is removed from the DNA together with clock proteins at the conclusion of the transcriptional activation phase or whether BRM is removed from the DNA prior to the departure of clock proteins from DNA.

It is now known that rhythmic activity of histone modifiers and chromatin-remodeling complexes are responsible for creating a dynamic chromatin landscape at clock gene loci (reviewed in [31,59,60]). Studies have shown that the clock promotes rhythmic activity of chromatin remodelers [34–36,61], consistent with our results. Our study expands on this body of work by illuminating on the activity of clock proteins to shape rhythmic recruitment and removal of the chromatin remodeler BRM at clock-regulated loci, providing an additional layer of regulation to facilitate robust rhythmic gene expression. Our results also provide new insights into reciprocal regulation between circadian clock proteins and chromatin remodelers. This has significant implication to the maintenance of robust circadian gene expression, suggesting that any environmental, nutritional, or genetic factors that impact expression of clock genes, e.g. the aging process [62–64], could disrupt the robustness of rhythmic chromatin landscape and further dampen rhythmic clock output.

Using our newly produced polyclonal BRM antibody, we found that endogenous BRM binds rhythmically to clock gene loci (Fig 1). This result is different than our previous study showing that BRM occupancy is constitutive at the promoters of *per* and *tim* [37]. This discrepancy is likely due to the fact that our previous study was performed in flies overexpressing an epitope tagged BRM, while the current study examined BRM occupancy with a polyclonal antibody in wild type flies. Notably, the rhythmic BRM occupancy we observed here is consistent with a previous study showing that Brahma Regulated Gene 1 (BRG1), the mammalian homolog of BRM, binds rhythmically to the promoters of *Per1* and *Per2* [65]. Although BRM binding is rhythmic, BRM protein expression is not (Fig 1). This is consistent with its role in regulating the transcription of constitutively expressed genes including *heat shock protein (hsp) 26*, *hsp67Bc*, and *hsp70A* [51]. Constitutive BRM protein expression indicates that other factors are involved in regulating rhythmic BRM occupancy at clock gene promoters. We should point out that we cannot rule out the possibility that BRM expression in non-clock cells may mask BRM rhythmic expression in clock cells, given BRM expression was measured in whole head extracts. However, because many cells within the fly head are clock cells, including photoreceptors, neurons, and glia [66–69], and that we were able to detect rhythmic BRM occupancy on clock gene promoters (Fig 1C-F) and reduced expression of BRM in clk^{out} flies (Fig 3A and 3B) using whole head extracts, it is reasonable to assume we would be able to detect rhythmic BRM expression even if only a portion of BRM-expressing cells have clocks.

Previously, we have shown that BRM interacts with CLK in S2 cells and fly heads [30,37]. Therefore, we investigated the effect of CLK on BRM occupancy. Although our results indicate that CLK promotes rhythmic BRM occupancy at the *per* promoter and likely at other clock gene promoters (Fig 2), the exact mechanism by which CLK promotes BRM occupancy to the DNA is unclear. We speculate that CLK indirectly promotes BRM binding to the DNA given that CLK occupancy peaks at ZT12 and BRM occupancy peaks 2 hours after (ZT14) (Fig 2D). One possibility is that CLK brings in kinases that phosphorylate BRM, increasing its stability at night, resulting in its increased binding to clock gene promoters. We show that CLK promotes BRM stability when both proteins are co-expressed in S2 cells, and this stability may be a result of CLK promoting the phosphorylation of BRM (Fig 3 and S2 Fig). We speculate that CK2, a kinase that regulates PER-TIM nuclear accumulation [18,24,70–73] and phosphorylates CLK [28], may phosphorylate BRM to promote its stability given that CK2α phosphorylates BRG1 in mice [74,75]. Thus, phosphorylation of BRM by CLK-recruited CK2 could stabilize BRM protein levels, promoting its activity at clock loci.

Other mechanisms for CLK to increase BRM occupancy could also be at play apart from BRM phosphorylation. For instance, it is possible that CLK facilitates a hyperacetylated chromatin landscape which BRM recognizes via its bromodomain [76–79]. Mammalian CLOCK has histone acetyl transferase (HAT) activity [80,81] while *Drosophila* CLK interacts with the HAT, NEJIRE [82,83]. Finally, it is possible that BRM binding to clock gene promoters is directed by other proteins, such as OSA and Histone H2Av. The BAP complex, one of the two BRM complexes in flies, is directed to its target binding sites by OSA [84]. OSA was shown to be a rhythmic target of CLK in a ChIP-chip analysis [53], suggesting that it may be rhythmically expressed in flies. Alternatively, BRM may be recognizing Histone H2Av at CLK-regulated loci. It has been shown that H2Av localizes at the promoters of *per* and *tim* in flies [85]. Similarly in *Arabidopsis*, BRM interacts with H2Az, a H2Av homolog, to coordinate transcription [86]. Therefore, rhythmic BRM recruitment could be mediated by daily rhythms of OSA or H2Av present at clock loci. Future studies will need to be conducted to explore these possibilities.

We then investigated the mechanism by which BRM is removed from the DNA. We hypothesized that TIM plays a role in promoting the removal of BRM from the promoter because peak BRM binding to the DNA (~ZT14, Fig 2D) precedes peak TIM and BRM interaction (~ZT20) [37]. We therefore investigated the effect of TIM on BRM occupancy. We showed that reduction of BRM occupancy at the *per* promoter and possibly other clock gene promoters is mediated by TIM. Given that TIM levels affect PER levels [87–90], it is possible that rather than TIM, PER is acting on BRM occupancy, however, we reason that this is not the case because our previous study revealed that BRM binds to TIM and not to PER in fly tissue extracts [37]. However, it is unclear how exactly TIM influences BRM occupancy. Similar to the effect of CLK on BRM occupancy, we propose that the effect of TIM on BRM occupancy is indirect. It is possible that TIM recruits phosphatases or deacetylases that affect BRM stability and binding to the chromatin respectively. Some phosphatases that the PER-TIM complex interacts with include *Protein Phosphatase 2A*, *Protein Phosphatase I*, and *Phosphatase of Regenerating Liver-1* [91–93]. Alternatively, TIM may be serving as a scaffold for deacetylases to promote BRM removal since mammalian SWI/SNF ATPase bromodomains stabilize interactions between BRM and the DNA [94]. The deacetylase Sirtuin 1 interacts with the PER-CRY complex [81,95] and interacts with BRG1 in mice [96]. Future studies can assess BRM binding to clock gene promoters when co-expressed with these phosphatases and deacetylases to determine if they are involved in promoting the removal of BRM from clock gene promoters.

The involvement of TIM in regulating rhythmic BRM occupancy prompts interesting questions, such as how light and temperature may affect the chromatin landscape. Because TIM protein abundance is regulated by light [55–57], future work can investigate how artificial light at night (ALAN) can disrupt the chromatin landscape at clock genes and therefore the clock itself as well as its output. This could be useful in understanding the impact of ALAN on health and disease. Additionally, future experiments can explore whether BRM occupancy and the chromatin landscape change at different temperatures given that *tim* mRNA is spliced in a temperature-dependent manner to produce different TIM isoforms that vary in structure and function [54,97,98].

Finally, given that transcription can be damaging to the DNA (reviewed in [99,100]) and BRG1 is implicated in DNA damage response [42–44], it is possible that BRM serves as a scaffold for DNA repair proteins. Therefore, CLK may be mediating rhythmic DNA repair at clock-controlled genes by promoting rhythmic BRM occupancy at these loci. It is also possible that BRM is not only condensing the chromatin following transcription but also facilitating chromatin remodeling to enable successful DNA repair. It is known that some DNA lesions

result in chromatin mobilization to the periphery of the nucleus [101], and a recent study has shown that CLK and PER are involved in regulating the spatial organization of clock gene loci near the periphery of the nucleus during the transcriptional repression phase [102]. However, the mechanism driving this spatiotemporal phenomenon has yet to be fully uncovered. Given the role of BRG1 in DNA repair, it is possible that BRM is involved in driving this spatiotemporal phenomenon.

In summary, our study reveals that core clock proteins are involved in regulating rhythmic binding of a general chromatin remodeler at clock gene loci to facilitate rhythmic circadian gene expression. Our work provides additional evidence that the circadian clock creates a dynamic chromatin landscape at clock genes and provides new insights into how external stimuli, such as light, affects chromatin structure.

Materials and methods

Fly strains and genetic crosses

Targeted expression of wild type *brm* tagged with 3XFLAG or the *brm* gain-of-function mutation (brm^{GOF}) in *tim*-expressing neurons was achieved using the UAS-GAL4 system [103]. Virgin females of w^{1118}; *tim(UAS)-Gal4* driver line [104] (referred to as *TUG*) were crossed to male flies of the following responder lines: w^{1118}; *UAS*-FLAG-*brm* (strain M21) [37] and w^{1118}; *UAS-*brm^{GOF} (Bloomington *Drosophila* Stock Center stock no. 59048) [58]. The resulting progenies of the crosses are referred to as brm^{OE} and *TUG>*brm^{GOF} respectively. Both male and female progenies of the crosses were used in protein, mRNA, and chromatin immunoprecipitation assays. Other fly strains used in this study include *w*; clk^{out}, referred to as clk^{out} [27] (Bloomington *Drosophila* Stock Center stock no. 56754) and *w; ptim (WT)*, referred to as tim^{OE} [54].

Generating BRM polyclonal antibody

A 558 bp region of the *brm* CDS (Flybase: FBpp0075278) encoding amino acids 1321–1506 was cloned into pET28a-6XHis (Sigma, St. Louis, MO). The construct was transformed into BL21-DE3 *E. coli* competent cells and expression was induced with 0.5M IPTG. Total protein was extracted from cells using His lysis buffer (50mM sodium phosphate pH 8.0, 300mM NaCl, 10% glycerol, and 0.1% Triton X-100). The BRM antigen was affinity-purified by IMAC using the NGC Medium-Pressure Liquid Chromatography System (Bio-Rad, Hercules, CA) and eluted in elution buffer (50mM sodium phosphate pH 8.0, 300mM NaCl, and 10mM imidazole). The purified antigen was dialyzed in dialysis buffer (50mM sodium phosphate pH 8.0, 300mM NaCl, and 10% glycerol) using a Slide-A-Lyzer Dialysis Casette 10K MWCO (Thermo Fisher Scientific, Waltham, MA) prior to being sent to Labcorp Drug Development (Princeton, New Jersey) for injection into rats. The serum from final bleed was tested for use in western blot detection of BRM in *Drosophila* Schneider (S2) cells and fly head protein extracts (Fig 1A and 1B, and S1 Fig).

Protein extraction from *Drosophila* S2 cells and fly heads

Drosophila S2 cells were seeded at 3 X 10^6 cells in 3ml of Schneider's *Drosophila* Medium (Life Technologies, Waltham, MA) supplemented with 10% fetal bovine serum (VWR, Radnor, PA) and 0.5% penicillin-streptomycin (Sigma). To test the BRM antibody, S2 cells were transiently transfected with pAc-*brm*-FLAG-6xHIS using Effectene (Qiagen, Valencia, CA). Cells were harvested 48 hours after transfection and proteins were extracted using EB2 buffer (20mM HEPES pH 7.5, 100mM KCl, 5% glycerol, 5 mM EDTA, 1mM DTT, 0.1% Triton X-100,

25mM NaF, 0.5mM PMSF) supplemented with EDTA-free protease inhibitor cocktail (Sigma) as described in [105]. To assess protein expression profiles, flies were entrained for 2 days at 25˚C in 12hr light: 12hr dark (LD) conditions. On LD3, flies were flash frozen on dry ice at the indicated time points (ZT). For experiments conducted in constant conditions, flies were entrained for 3 days in 12:12 LD conditions, and the treatment groups were then moved into constant light (LL) or constant dark (DD). Flies were flash frozen on dry ice and collected at the indicated time points on LD4, LL1, and DD1. Heads were separated from bodies using frozen metal sieves (Newark Wire Cloth Company, Clifton, New Jersey). Protein lysate was extracted in RBS buffer (20mM HEPES pH 7.5, 50mM KCl, 10% glycerol, 2mM EDTA, 1% Triton X-100, 0.4% NP-40, 1mM DTT, 0.5mM PMSF, 0.01 mg/ml aprotinin, 0.005 mg/ml leupeptin, and 0.001 mg/ml pepstatin A) as described in [17]. Extracts were sonicated for 5 s with 10 s pauses between sonication cycles for a total of 5 cycles. Protein concentration was measured using Pierce Coomassie Plus Assay Reagents (Thermo Fisher Scientific). 2X SDS sample buffer was added to the protein lysate, and the mixture was boiled at 95˚C for 5 minutes before running on an SDS-PAGE gel.

Western blotting of protein extracts, detection, and quantification

Equal amounts of protein lysate were resolved on SDS-PAGE gels and transferred to nitrocellulose membranes (Bio-Rad) using the Semi-Dry Transfer Cell (Bio-Rad). Protein-containing membranes were incubated in 5% blocking reagent (Bio-Rad) dissolved in 1X TBST (99.95% Tris buffered saline and 0.05% Tween-20) supplemented with primary antibodies at the appropriate dilutions for 16–24 hours. The primary antibodies and corresponding dilutions used in this study are rat α-BRM (RRID: AB_2827509) at 1:5000, mouse α-HSP70 (Sigma) at 1:10000, mouse α-FLAG (Sigma) at 1:7000, mouse α-V5 (Invitrogen, Waltham, MA) at 1:5000, and rat α-TIM (R5839, RRID: AB_2782953) [54] at 1:1000. Blots were washed every 10 minutes with 1X TBST for a total of one hour to remove non-specific antibody binding. The blots were then incubated in 5% blocking solution containing the appropriate secondary antibodies at their corresponding dilutions for 1 hour. The secondary antibodies used in this study are α-rat-IgG-HRP (Cytiva, Marlborough, MA) at 1:2000 if detecting BRM and 1:1000 if detecting TIM and α-mouse-IgG-HRP (Cytiva) at 1:10000 if detecting HSP70 and 1:2000 if detecting FLAG or V5. Blots were washed for another hour with 1X TBST. Finally, blots were treated with Clarity Western ECL Substrate (Bio-Rad) according to the manufacturer's instructions prior to being imaged on the ChemiDoc MP Imaging System (Bio-Rad). Image analyses were performed using Image Lab Software (Bio-Rad). Protein signal was normalized to HSP70. Values were scaled such that the highest value of all samples was set to 1.

For the pre-adsorption assay used to validate the BRM antibody, SDS-PAGE and western blotting were all carried out as described above with the following modification. The BRM antibody was first incubated with either 0ul, 0.1ul, 1ul, or 10ul of purified BRM antigen (concentration 1ug/ul) in 5% blocking solution for 1 hour at room temperature. The blocking solution containing the antigen and antibody was then added to a protein-containing membrane. The blot was then washed, probed with secondary antibody, and imaged as described above. BRM signal was normalized to a non-specific band detected on the same blot.

Chromatin Immunoprecipitation-qPCR (ChIP-qPCR) in *Drosophila* S2 cells and flies

ChIP in flies was performed as described in [37] with the following modifications. 5.25 μl of α-BRM (this study), 1.5 μl of α-Histone H3 (Abcam, Cambridge, MA), or 5.63 μl α-CLK (Santa Cruz Biotechnology, Dallas, TX) were incubated with 25ul of DynaBeads Protein G

(Invitrogen) per IP. 1.5 μl of α-V5 (Invitrogen) was used for negative IP which was utilized for background deduction in Fig 1C–1H, and negative ChIP values were replaced with zeroes as described in [106]. For ChIP using S2 cell extracts, cells were transiently transfected with pAc-*brm*-FLAG-6xHIS in combination with pAc-*clk*-V5-HIS, pAc-*tim*-HA, pAc-V5-HIS empty plasmid, or pAc-HA empty plasmid using Effectene (Qiagen). Cells were harvested 48 hours after transfection for processing. An intergenic region on the X chromosome proximal to FBgn0003638 was used for background deduction. The primer sets used during quantitative RT-PCR (qPCR) to amplify specific gene regions subsequent to ChIP, either designed in this study or in [37], can be found in S1 Table, and a schematic for the location of the primers designed in this study can be found in S4 Fig. At least 3 biological ChIP replicates were performed per experiment, and each biological replicate is an average of at least 2 qPCR technical replicates. ChIP signal for the target and background was calculated as a percentage of the input samples. Background signal was subtracted from the target signal. In experiments comparing 2 conditions at multiple time points, values were scaled such that the highest value of all samples was set to 1. When only one comparison is being made, the value of the control is set to 1 and the values of the other condition are relative to that value.

Steady state mRNA analysis

Total RNA extraction was performed as described in [24], and cDNA synthesis and quantitative RT-PCR analysis was performed as described in [54]. The primer sets used to detect *brm*, *cbp20*, and *per* are described in [37,107] and are listed in S1 Table. Each experiment consists of at least 3 biological replicates, and at least 2 technical replicates were performed for each biological replicate.

Cycloheximide (CHX) chase and lambda phosphatase (λ_{pp}) experiments

Drosophila S2 cells were transiently transfected with pAc-*brm*-FLAG-6xHIS in combination with either pAc-*clk*-V5-HIS or pAc-V5-HIS empty plasmid using Effectene (Qiagen). For cycloheximide experiments, protein was extracted with EB2 (recipe is listed in "Protein extraction from *Drosophila* S2 cells and fly heads" section), and CHX was added to a final concentration of 10μg/ml 48 hours post-transfection. Cells were harvested every 2 hours over a 6-hour period after CHX addition. SDS-PAGE and Western blotting and detection were performed as described in the "Western blotting of protein extracts, detection, and quantification" section. For λ_{pp} experiments, protein was extracted with EB2 supplemented with PhosStop (Roche, Indianapolis, IN) and were subjected to IP with 15 μl of settled α-FLAG beads (Sigma) per reaction for 4 hours at 4˚C. Beads were washed 2 times with EB2 without NaF or PhosStop and one time with λ_{pp} buffer (New England Biolabs, Ipswich, MA) before resuspension in 40 μl of λ_{pp} buffer. Experimental reactions were treated with 0.6ul λ_{pp} (New England Biolabs), and both experimental and control reactions were then incubated in a 30˚C water bath for 30 mins. 45 μl of 2X SDS sample buffer was added to the beads for protein elution. Eluted protein was subjected to SDS-PAGE and Western blotting and detection. CHX and λ_{pp} experiments were each performed 3 times.

Statistical analysis

Rhythmicity Analysis Incorporating Non-parametric methods (RAIN) [108] was used to determine rhythmicity and phase of protein occupancy in ChIP assays, protein expression, and mRNA expression. Differences in daily rhythmicity were assessed using Detection of Differential Rhythmicity (DODR) [109] and differences in overall expression of rhythmic data (MESOR and amplitude) was measured using CircaCompare [110]. RAIN, DODR, and

CircaCompare were performed using R version 4.0.3. To analyze the differences between treatments at each time point, two-way ANOVA followed by Sidak's multiple comparisons test was used. Comparisons between only two conditions was determined using One sample t and Wilcoxon test to a hypothetical mean value corresponding to the normalization condition. One-way ANOVA followed by Dunnett's multiple comparison tests was performed to analyze the comparisons of a control and experimental conditions, e.g. in S1B Fig. Two-way ANOVA, One sample t, and one-way ANOVA were performed using GraphPad Prism Version 9.3.1 (GraphPad Software, La Jolla, California, USA).

Supporting information

S1 Fig. Pre-adsorption of BRM polyclonal antibody with BRM antigen supports the specificity of the BRM antibody signal. (A) The BRM antibody was incubated with a dilution series of the BRM antigen (0.1ul, 1ul, and 10ul at 1ug/ul) prior to detecting BRM in protein lysate extracted from w^{1118} flies collected at ZT16. The non-specific band is denoted as NS. (B) BRM signal was normalized to the NS signal (n = 3). Each data point represents a biological replicate. Error bars represent ±SEM. Asterisks denote significant p-values: $^{****}p<0.0001$.
(TIFF)

S2 Fig. Lambda phosphatase treatment reveals BRM is phosphorylated when expressed with CLK. (A) BRM (top panel) and CLK (bottom panel) expression prior to lambda phosphatase (λpp) treatment in protein lysate from S2 cells expressing either BRM alone or BRM co-expressed with CLK. (B) BRM protein after treatment with λpp.
(TIFF)

S3 Fig. Protein expression in tim^{OE} flies. (A) TIM (top panel) and BRM (middle panel) protein in w^{1118} and w^{1118};*ptim(WT)* fly heads collected at the indicated time points on LD3. w^{1118};*ptim(WT)* flies are denoted as tim^{OE} flies. HSP70 (bottom panel) was used as a loading control. (B-C) Normalized (B) TIM and (C) BRM expression in w^{1118} (black) and tim^{OE} (red) flies (n = 3). Each data point represents a biological replicate. Error bars represent ±SEM. The grey background denotes the dark phase of the LD cycle.
(TIFF)

S4 Fig. Primer locations. Schematic of region amplified by primers (grey) used in ChIP to assess BRM occupancy at the promoters of *vrille (vri)*, *clockwork orange* (*cwo*), *heat shock protein 27* (*hsp27)*, and *glycine transporter (glyT*). Positions are relative to the transcription start site (TSS). Locations of other ChIP primers are shown in [37].
(TIFF)

S1 Table. Sequences for primers used for generation of BRM antigen, Chromatin Immunoprecipitation-qPCR, and steady-state mRNA analysis.
(DOCX)

S2 Table. Raw Data Excel File.
(XLSX)

Acknowledgments

We thank the Bloomington *Drosophila* Stock Center for providing fly stocks. We also thank Xianhui Liu for providing valuable feedback on the manuscript and Qi Wei for intellectual discussion.

Author Contributions

Conceptualization: Christine A. Tabuloc, Yao D. Cai, Rosanna S. Kwok, Joanna C. Chiu.

Data curation: Christine A. Tabuloc, Rosanna S. Kwok, Elizabeth C. Chan.

Formal analysis: Christine A. Tabuloc, Rosanna S. Kwok, Elizabeth C. Chan.

Funding acquisition: Joanna C. Chiu.

Investigation: Christine A. Tabuloc, Rosanna S. Kwok, Elizabeth C. Chan.

Methodology: Christine A. Tabuloc, Rosanna S. Kwok, Joanna C. Chiu.

Project administration: Joanna C. Chiu.

Resources: Christine A. Tabuloc, Rosanna S. Kwok, Elizabeth C. Chan.

Supervision: Joanna C. Chiu.

Writing – original draft: Christine A. Tabuloc, Yao D. Cai, Sergio Hidalgo, Joanna C. Chiu.

Writing – review & editing: Christine A. Tabuloc, Yao D. Cai, Rosanna S. Kwok, Sergio Hidalgo, Joanna C. Chiu.

References

1. Dubowy C, Sehgal A. Circadian Rhythms and Sleep in *Drosophila melanogaster*. Genetics. 2017; 205: 1373–1397. https://doi.org/10.1534/genetics.115.185157 PMID: 28360128
2. Dunlap JC, Loros JJ. Making time: conservation of biological clocks from fungi to animals. Microbiol Spectr. 2017; 5: https://doi.org/10.1128/microbiolspec.FUNK-0039-2016 PMID: 28527179
3. Cox KH, Takahashi JS. Circadian clock genes and the transcriptional architecture of the clock mechanism. J Mol Endocrinol. 2019; 63: R93–R102. https://doi.org/10.1530/JME-19-0153 PMID: 31557726
4. Patke A, Young MW, Axelrod S. Molecular mechanisms and physiological importance of circadian rhythms. Nat Rev Mol Cell Biol. 2020; 21: 67–84. https://doi.org/10.1038/s41580-019-0179-2 PMID: 31768006
5. Hardin PE, Hall JC, Rosbash M. Feedback of the *Drosophila period* gene product on circadian cycling of its messenger RNA levels. Nature. 1990; 343: 536–540. https://doi.org/10.1038/343536a0 PMID: 2105471
6. Darlington TK, Lyons LC, Hardin PE, Kay SA. The *period* E-box Is Sufficient to Drive Circadian Oscillation of Transcription In Vivo. J Biol Rhythms. 2000; 15: 462–470. https://doi.org/10.1177/074873040001500603 PMID: 11106063
7. Hao H, Allen DL, Hardin PE. A circadian enhancer mediates PER-dependent mRNA cycling in *Drosophila melanogaster*. Mol Cell Biol. 1997; 17: 3687–3693. https://doi.org/10.1128/MCB.17.7.3687 PMID: 9199302
8. Zhou J, Yu W, Hardin PE. CLOCKWORK ORANGE Enhances PERIOD Mediated Rhythms in Transcriptional Repression by Antagonizing E-box Binding by CLOCK-CYCLE. PLoS Genet. 2016; 12: e1006430. https://doi.org/10.1371/journal.pgen.1006430 PMID: 27814361
9. Shakhmantsir I, Nayak S, Grant GR, Sehgal A. Spliceosome factors target *timeless* (*tim*) mRNA to control clock protein accumulation and circadian behavior in *Drosophila*. Takahashi JS, VijayRaghavan K, Ewer J, editors. eLife. 2018; 7: e39821. https://doi.org/10.7554/eLife.39821 PMID: 30516472
10. Lim C, Lee J, Choi C, Kilman VL, Kim J, Park SM, et al. The novel gene *twenty-four* defines a critical translational step in the *Drosophila* clock. Nature. 2011; 470: 399–403. https://doi.org/10.1038/nature09728 PMID: 21331043
11. Zhang Y, Ling J, Yuan C, Dubruille R, Emery P. A role for *Drosophila* ATX2 in activation of PER translation and circadian behavior. Science. 2013; 340: 879–882. https://doi.org/10.1126/science.1234746 PMID: 23687048
12. Price JL, Blau J, Rothenfluh A, Abodeely M, Kloss B, Young MW. *double-time* is a novel *Drosophila* clock gene that regulates PERIOD protein accumulation. Cell. 1998; 94: 83–95. https://doi.org/10.1016/s0092-8674(00)81224-6 PMID: 9674430

13. Grima B, Lamouroux A, Chélot E, Papin C, Limbourg-Bouchon B, Rouyer F. The F-box protein Slimb controls the levels of clock proteins Period and Timeless. Nature. 2002; 420: 178–182. https://doi.org/10.1038/nature01122 PMID: 12432393

14. Grima B, Dognon A, Lamouroux A, Chélot E, Rouyer F. CULLIN-3 Controls TIMELESS Oscillations in the *Drosophila* Circadian Clock. Schibler U, editor. PLoS Biol. 2012; 10: e1001367. https://doi.org/10.1371/journal.pbio.1001367 PMID: 22879814

15. Ko HW, Jiang J, Edery I. Role for Slimb in the degradation of *Drosophila* Period protein phosphorylated by Doubletime. Nature. 2002; 420: 673–678. https://doi.org/10.1038/nature01272 PMID: 12442174

16. Jang AR, Moravcevic K, Saez L, Young MW, Sehgal A. *Drosophila* TIM Binds Importin α1, and Acts as an Adapter to Transport PER to the Nucleus. PLOS Genet. 2015; 11: e1004974. https://doi.org/10.1371/journal.pgen.1004974 PMID: 25674790

17. Lam VH, Li YH, Liu X, Murphy KA, Diehl JS, Kwok RS, et al. CK1α Collaborates with DOUBLETIME to Regulate PERIOD Function in the *Drosophila* Circadian Clock. J Neurosci. 2018; 38: 10631–10643. https://doi.org/10.1523/JNEUROSCI.0871-18.2018 PMID: 30373768

18. Top D, Harms E, Syed S, Adams EL, Saez L. GSK-3 and CK2 Kinases Converge on Timeless to Regulate the Master Clock. Cell Rep. 2016; 16: 357–367. https://doi.org/10.1016/j.celrep.2016.06.005 PMID: 27346344

19. Menet JS, Abruzzi KC, Desrochers J, Rodriguez J, Rosbash M. Dynamic PER repression mechanisms in the *Drosophila* circadian clock: from on-DNA to off-DNA. Genes Dev. 2010; 24: 358–367. https://doi.org/10.1101/gad.1883910 PMID: 20159956

20. Yu W, Zheng H, Houl JH, Dauwalder B, Hardin PE. PER-dependent rhythms in CLK phosphorylation and E-box binding regulate circadian transcription. Genes Dev. 2006; 20: 723–733. https://doi.org/10.1101/gad.1404406 PMID: 16543224

21. Chiu JC, Vanselow JT, Kramer A, Edery I. The phospho-occupancy of an atypical SLIMB-binding site on PERIOD that is phosphorylated by DOUBLETIME controls the pace of the clock. Genes Dev. 2008; 22: 1758–1772. https://doi.org/10.1101/gad.1682708 PMID: 18593878

22. Szabó Á, Papin C, Cornu D, Chélot E, Lipinszki Z, Udvardy A, et al. Ubiquitylation Dynamics of the Clock Cell Proteome and TIMELESS during a Circadian Cycle. Cell Rep. 2018; 23: 2273–2282. https://doi.org/10.1016/j.celrep.2018.04.064 PMID: 29791839

23. Andreazza S, Bouleau S, Martin B, Lamouroux A, Ponien P, Papin C, et al. Daytime CLOCK Dephosphorylation Is Controlled by STRIPAK Complexes in *Drosophila*. Cell Rep. 2015; 11: 1266–1279. https://doi.org/10.1016/j.celrep.2015.04.033 PMID: 25981041

24. Cai YD, Xue Y, Truong CC, Del Carmen-Li J, Ochoa C, Vanselow JT, et al. CK2 Inhibits TIMELESS Nuclear Export and Modulates CLOCK Transcriptional Activity to Regulate Circadian Rhythms. Curr Biol. 2021; 31: 502–514.e7. https://doi.org/10.1016/j.cub.2020.10.061 PMID: 33217322

25. Lamaze A, Lamouroux A, Vias C, Hung H-C, Weber F, Rouyer F. The E3 ubiquitin ligase CTRIP controls CLOCK levels and PERIOD oscillations in *Drosophila*. EMBO Rep. 2011; 12: 549–557. https://doi.org/10.1038/embor.2011.64 PMID: 21525955

26. Luo W, Li Y, Tang C-HA, Abruzzi KC, Rodriguez J, Pescatore S, et al. CLOCK deubiquitylation by USP8 inhibits CLK/CYC transcription in *Drosophila*. Genes Dev. 2012; 26: 2536–2549. https://doi.org/10.1101/gad.200584.112 PMID: 23154984

27. Mahesh G, Jeong E, Ng FS, Liu Y, Gunawardhana K, Houl JH, et al. Phosphorylation of the transcription activator CLOCK regulates progression through a ~ 24-h feedback loop to influence the circadian period in *Drosophila*. J Biol Chem. 2014; 289: 19681–19693. https://doi.org/10.1074/jbc.M114.568493 PMID: 24872414

28. Szabó A, Papin C, Zorn D, Ponien P, Weber F, Raabe T, et al. The CK2 kinase stabilizes CLOCK and represses its activity in the *Drosophila* circadian oscillator. PLoS Biol. 2013; 11: e1001645. https://doi.org/10.1371/journal.pbio.1001645 PMID: 24013921

29. Koike N, Yoo S-H, Huang H-C, Kumar V, Lee C, Kim T-K, et al. Transcriptional Architecture and Chromatin Landscape of the Core Circadian Clock in Mammals. Science. 2012; 338: 349–354. https://doi.org/10.1126/science.1226339 PMID: 22936566

30. Kwok RS, Lam VH, Chiu JC. Understanding the role of chromatin remodeling in the regulation of circadian transcription in *Drosophila*. Fly (Austin). 2016; 9: 145–154. https://doi.org/10.1080/19336934.2016.1143993 PMID: 26926115

31. Zhu Q, Belden WJ. Molecular Regulation of Circadian Chromatin. J Mol Biol. 2020; 432: 3466–3482. https://doi.org/10.1016/j.jmb.2020.01.009 PMID: 31954735

32. Etchegaray J-P, Lee C, Wade PA, Reppert SM. Rhythmic histone acetylation underlies transcription in the mammalian circadian clock. Nature. 2003; 421: 177–182. https://doi.org/10.1038/nature01314 PMID: 12483227

33. Tamayo AG, Duong HA, Robles MS, Mann M, Weitz CJ. Histone monoubiquitination by Clock-Bmal1 complex marks *Per1* and *Per2* genes for circadian feedback. Nat Struct Mol Biol. 2015; 22: 759–766. https://doi.org/10.1038/nsmb.3076 PMID: 26323038

34. Bu B, Chen L, Zheng L, He W, Zhang L. Nipped-A regulates the *Drosophila* circadian clock via histone deubiquitination. EMBO J. 2020; 39: e101259. https://doi.org/10.15252/embj.2018101259 PMID: 31538360

35. Mahesh G, Rivas GBS, Caster C, Ost EB, Amunugama R, Jones R, et al. Proteomic analysis of *Drosophila* CLOCK complexes identifies rhythmic interactions with SAGA and Tip60 complex component NIPPED-A. Sci Rep. 2020; 10: 17951. https://doi.org/10.1038/s41598-020-75009-5 PMID: 33087840

36. Wang B, Kettenbach AN, Gerber SA, Loros JJ, Dunlap JC. *Neurospora* WC-1 recruits SWI/SNF to remodel frequency and initiate a circadian cycle. PLoS Genet. 2014; 10: e1004599. https://doi.org/10.1371/journal.pgen.1004599 PMID: 25254987

37. Kwok RS, Li YH, Lei AJ, Edery I, Chiu JC. The Catalytic and Non-catalytic Functions of the Brahma Chromatin-Remodeling Protein Collaborate to Fine-Tune Circadian Transcription in *Drosophila*. Emery P, editor. PLOS Genet. 2015; 11: e1005307. https://doi.org/10.1371/journal.pgen.1005307 PMID: 26132408

38. Coisy-Quivy M, Disson O, Roure V, Muchardt C, Blanchard J-M, Dantonel J-C. Role for Brm in cell growth control. Cancer Res. 2006; 66: 5069–5076. https://doi.org/10.1158/0008-5472.CAN-05-0596 PMID: 16707429

39. Helming KC, Wang X, Roberts CWM. Vulnerabilities of mutant SWI/SNF complexes in cancer. Cancer Cell. 2014; 26: 309–317. https://doi.org/10.1016/j.ccr.2014.07.018 PMID: 25203320

40. Masliah-Planchon J, Bièche I, Guinebretière J-M, Bourdeaut F, Delattre O. SWI/SNF chromatin remodeling and human malignancies. Annu Rev Pathol. 2015; 10: 145–171. https://doi.org/10.1146/annurev-pathol-012414-040445 PMID: 25387058

41. Muchardt C, Yaniv M. When the SWI/SNF complex remodels . . . the cell cycle. Oncogene. 2001; 20: 3067–3075. https://doi.org/10.1038/sj.onc.1204331 PMID: 11420722

42. Hara R, Sancar A. Effect of Damage Type on Stimulation of Human Excision Nuclease by SWI/SNF Chromatin Remodeling Factor. Mol Cell Biol. 2003; 23: 4121–4125. https://doi.org/10.1128/MCB.23.12.4121-4125.2003 PMID: 12773556

43. Smith-Roe SL, Nakamura J, Holley D, Chastain PD, Rosson GB, Simpson DA, et al. SWI/SNF complexes are required for full activation of the DNA-damage response. Oncotarget. 2015; 6: 732–745. https://doi.org/10.18632/oncotarget.2715 PMID: 25544751

44. Zhang L, Zhang Q, Jones K, Patel M, Gong F. The chromatin remodeling factor BRG1 stimulates nucleotide excision repair by facilitating recruitment of XPC to sites of DNA damage. Cell Cycle Georget Tex. 2009; 8: 3953–3959. https://doi.org/10.4161/cc.8.23.10115 PMID: 19901545

45. Curtis BJ, Zraly CB, Marenda DR, Dingwall AK. Histone lysine demethylases function as co-repressors of SWI/SNF remodeling activities during *Drosophila* wing development. Dev Biol. 2011; 350: 534–547. https://doi.org/10.1016/j.ydbio.2010.12.001 PMID: 21146519

46. Shi J, Zheng M, Ye Y, Li M, Chen X, Hu X, et al. *Drosophila* Brahma complex remodels nucleosome organizations in multiple aspects. Nucleic Acids Res. 2014; 42: 9730–9739. https://doi.org/10.1093/nar/gku717 PMID: 25081211

47. He L, Liu H, Tang L. SWI/SNF Chromatin Remodeling Complex: A New Cofactor in Reprogramming. Stem Cell Rev Rep. 2012; 8: 128–136. https://doi.org/10.1007/s12015-011-9285-z PMID: 21655945

48. Ruijtenberg S, van den Heuvel S. G1/S Inhibitors and the SWI/SNF Complex Control Cell-Cycle Exit during Muscle Differentiation. Cell. 2015; 162: 300–313. https://doi.org/10.1016/j.cell.2015.06.013 PMID: 26144318

49. Singhal N, Graumann J, Wu G, Araúzo-Bravo MJ, Han DW, Greber B, et al. Chromatin-Remodeling Components of the BAF Complex Facilitate Reprogramming. Cell. 2010; 141: 943–955. https://doi.org/10.1016/j.cell.2010.04.037 PMID: 20550931

50. Toto PC, Puri PL, Albini S. SWI/SNF-directed stem cell lineage specification: dynamic composition regulates specific stages of skeletal myogenesis. Cell Mol Life Sci CMLS. 2016; 73: 3887–3896. https://doi.org/10.1007/s00018-016-2273-3 PMID: 27207468

51. Jordán-Pla A, Yu S, Waldholm J, Källman T, Östlund Farrants A-K, Visa N. SWI/SNF regulates half of its targets without the need of ATP-driven nucleosome remodeling by Brahma. BMC Genomics. 2018; 19: 367. https://doi.org/10.1186/s12864-018-4746-2 PMID: 29776334

52. Lee C-K, Shibata Y, Rao B, Strahl BD, Lieb JD. Evidence for nucleosome depletion at active regulatory regions genome-wide. Nat Genet. 2004; 36: 900–905. https://doi.org/10.1038/ng1400 PMID: 15247917

53. Abruzzi KC, Rodriguez J, Menet JS, Desrochers J, Zadina A, Luo W, et al. *Drosophila* CLOCK target gene characterization: implications for circadian tissue-specific gene expression. Genes Dev. 2011; 25: 2374–2386. https://doi.org/10.1101/gad.178079.111 PMID: 22085964

54. Abrieux A, Xue Y, Cai Y, Lewald KM, Nguyen HN, Zhang Y, et al. EYES ABSENT and TIMELESS integrate photoperiodic and temperature cues to regulate seasonal physiology in *Drosophila*. Proc Natl Acad Sci. 2020; 117: 15293–15304. https://doi.org/10.1073/pnas.2004262117 PMID: 32541062

55. Hunter-Ensor M, Ousley A, Sehgal A. Regulation of the *Drosophila* Protein Timeless Suggests a Mechanism for Resetting the Circadian Clock by Light. Cell. 1996; 84: 677–685. https://doi.org/10.1016/S0092-8674(00)81046-6 PMID: 8625406

56. Myers MP, Wager-Smith K, Rothenfluh-Hilfiker A, Young MW. Light-induced degradation of TIMELESS and entrainment of the *Drosophila* circadian clock. Science. 1996; 271: 1736–1740. https://doi.org/10.1126/science.271.5256.1736 PMID: 8596937

57. Zeng H, Qian Z, Myers MP, Rosbash M. A light-entrainment mechanism for the *Drosophila* circadian clock. Nature. 1996; 380: 129–135. https://doi.org/10.1038/380129a0 PMID: 8600384

58. Roesley SNA, La Marca JE, Deans AJ, Mckenzie L, Suryadinata R, Burke P, et al. Phosphorylation of *Drosophila* Brahma on CDK-phosphorylation sites is important for cell cycle regulation and differentiation. Cell Cycle. 2018; 17: 1559–1578. https://doi.org/10.1080/15384101.2018.1493414 PMID: 29963966

59. Chen ZJ, Mas P. Interactive roles of chromatin regulation and circadian clock function in plants. Genome Biol. 2019; 20: 62. https://doi.org/10.1186/s13059-019-1672-9 PMID: 30902105

60. Pacheco-Bernal I, Becerril-Pérez F, Aguilar-Arnal L. Circadian rhythms in the three-dimensional genome: implications of chromatin interactions for cyclic transcription. Clin Epigenetics. 2019; 11: 79. https://doi.org/10.1186/s13148-019-0677-2 PMID: 31092281

61. Tao W, Chen S, Shi G, Guo J, Xu Y, Liu C. SWItch/sucrose nonfermentable (SWI/SNF) complex subunit BAF60a integrates hepatic circadian clock and energy metabolism. Hepatology. 2011; 54: 1410–1420. https://doi.org/10.1002/hep.24514 PMID: 21725993

62. Kuintzle RC, Chow ES, Westby TN, Gvakharia BO, Giebultowicz JM, Hendrix DA. Circadian deep sequencing reveals stress-response genes that adopt robust rhythmic expression during aging. Nat Commun. 2017; 8: 14529. https://doi.org/10.1038/ncomms14529 PMID: 28221375

63. Luo W, Chen W-F, Yue Z, Chen D, Sowcik M, Sehgal A, et al. Old flies have a robust central oscillator but weaker behavioral rhythms that can be improved by genetic and environmental manipulations. Aging Cell. 2012; 11: 428–438. https://doi.org/10.1111/j.1474-9726.2012.00800.x PMID: 22268765

64. Umezaki Y, Yoshii T, Kawaguchi T, Helfrich-Förster C, Tomioka K. Pigment-Dispersing Factor Is Involved in Age-Dependent Rhythm Changes in *Drosophila melanogaster*. J Biol Rhythms. 2012; 27: 423–432. https://doi.org/10.1177/0748730412462206 PMID: 23223368

65. Kim JY, Kwak PB, Weitz CJ. Specificity in Circadian Clock Feedback from Targeted Reconstitution of the NuRD Corepressor. Mol Cell. 2014; 56: 738–748. https://doi.org/10.1016/j.molcel.2014.10.017 PMID: 25453762

66. Cheng Y, Hardin PE. *Drosophila* Photoreceptors Contain an Autonomous Circadian Oscillator That Can Function without *period* mRNA Cycling. J Neurosci. 1998; 18: 741–750. https://doi.org/10.1523/JNEUROSCI.18-02-00741.1998 PMID: 9425016

67. Damulewicz M, Loboda A, Bukowska-Strakova K, Jozkowicz A, Dulak J, Pyza E. Clock and clock-controlled genes are differently expressed in the retina, lamina and in selected cells of the visual system of *Drosophila melanogaster*. Front Cell Neurosci. 2015; 9. Available: https://www.frontiersin.org/articles/10.3389/fncel.2015.00353

68. Ma D, Przybylski D, Abruzzi KC, Schlichting M, Li Q, Long X, et al. A transcriptomic taxonomy of *Drosophila* circadian neurons around the clock. eLife. 2021; 10: e63056. https://doi.org/10.7554/eLife.63056 PMID: 33438579

69. You S, Yu AM, Roberts MA, Joseph IJ, Jackson FR. Circadian regulation of the *Drosophila* astrocyte transcriptome. PLoS Genet. 2021; 17: e1009790. https://doi.org/10.1371/journal.pgen.1009790 PMID: 34543266

70. Akten B, Jauch E, Genova GK, Kim EY, Edery I, Raabe T, et al. A role for CK2 in the *Drosophila* circadian oscillator. Nat Neurosci. 2003; 6: 251–257. https://doi.org/10.1038/nn1007 PMID: 12563262

71. Lin J-M, Kilman VL, Keegan K, Paddock B, Emery-Le M, Rosbash M, et al. A role for casein kinase 2α in the *Drosophila* circadian clock. Nature. 2002; 420: 816–820. https://doi.org/10.1038/nature01235 PMID: 12447397

72. Lin J-M, Schroeder A, Allada R. In Vivo Circadian Function of Casein Kinase 2 Phosphorylation Sites in *Drosophila* PERIOD. J Neurosci. 2005; 25: 11175–11183. https://doi.org/10.1523/JNEUROSCI.2159-05.2005 PMID: 16319317

73. Meissner R-A, Kilman VL, Lin J-M, Allada R. TIMELESS Is an Important Mediator of CK2 Effects on Circadian Clock Function In Vivo. J Neurosci. 2008; 28: 9732–9740. https://doi.org/10.1523/JNEUROSCI.0840-08.2008 PMID: 18815259

74. Padilla-Benavides T, Nasipak BT, Paskavitz AL, Haokip DT, Schnabl JM, Nickerson JA, et al. Casein kinase 2-mediated phosphorylation of Brahma-related gene 1 controls myoblast proliferation and contributes to SWI/SNF complex composition. J Biol Chem. 2017; 292: 18592–18607. https://doi.org/10.1074/jbc.M117.799676 PMID: 28939766

75. Padilla-Benavides T, Haokip DT, Yoon Y, Reyes-Gutierrez P, Rivera-Pérez JA, Imbalzano AN. CK2-Dependent Phosphorylation of the Brg1 Chromatin Remodeling Enzyme Occurs during Mitosis. Int J Mol Sci. 2020; 21: E923. https://doi.org/10.3390/ijms21030923 PMID: 32019271

76. Dhalluin C, Carlson JE, Zeng L, He C, Aggarwal AK, Zhou M-M, et al. Structure and ligand of a histone acetyltransferase bromodomain. Nature. 1999; 399: 491–496. https://doi.org/10.1038/20974 PMID: 10365964

77. Haynes SR, Dollard C, Winston F, Beck S, Trowsdale J, Dawid IB. The bromodomain: a conserved sequence found in human, *Drosophila* and yeast proteins. Nucleic Acids Res. 1992; 20: 2603. https://doi.org/10.1093/nar/20.10.2603 PMID: 1350857

78. Owen DJ, Ornaghi P, Yang JC, Lowe N, Evans PR, Ballario P, et al. The structural basis for the recognition of acetylated histone H4 by the bromodomain of histone acetyltransferase gcn5p. EMBO J. 2000; 19: 6141–6149. https://doi.org/10.1093/emboj/19.22.6141 PMID: 11080160

79. Tamkun JW, Deuring R, Scott MP, Kissinger M, Pattatucci AM, Kaufman TC, et al. brahma: A regulator of *Drosophila* homeotic genes structurally related to the yeast transcriptional activator SNF2SWI2. Cell. 1992; 68: 561–572. https://doi.org/10.1016/0092-8674(92)90191-E PMID: 1346755

80. Doi M, Hirayama J, Sassone-Corsi P. Circadian Regulator CLOCK Is a Histone Acetyltransferase. Cell. 2006; 125: 497–508. https://doi.org/10.1016/j.cell.2006.03.033 PMID: 16678094

81. Nakahata Y, Kaluzova M, Grimaldi B, Sahar S, Hirayama J, Chen D, et al. The NAD+-Dependent Deacetylase SIRT1 Modulates CLOCK-Mediated Chromatin Remodeling and Circadian Control. Cell. 2008; 134: 329–340. https://doi.org/10.1016/j.cell.2008.07.002 PMID: 18662547

82. Hung H-C, Maurer C, Kay SA, Weber F. Circadian Transcription Depends on Limiting Amounts of the Transcription Co-activator *nejire*/CBP *. J Biol Chem. 2007; 282: 31349–31357. https://doi.org/10.1074/jbc.M702319200 PMID: 17635913

83. Lim C, Lee J, Choi C, Kim J, Doh E, Choe J. Functional role of CREB-binding protein in the circadian clock system of *Drosophila melanogaster*. Mol Cell Biol. 2007; 27: 4876–4890. https://doi.org/10.1128/MCB.02155-06 PMID: 17452464

84. Mohrmann L, Langenberg K, Krijgsveld J, Kal AJ, Heck AJR, Verrijzer CP. Differential Targeting of Two Distinct SWI/SNF-Related *Drosophila* Chromatin-Remodeling Complexes. Mol Cell Biol. 2004; 24: 3077–3088.

85. Liu Z, Tabuloc CA, Xue Y, Cai Y, Mcintire P, Niu Y, et al. Splice variants of DOMINO control *Drosophila* circadian behavior and pacemaker neuron maintenance. PLOS Genet. 2019; 15: e1008474. https://doi.org/10.1371/journal.pgen.1008474 PMID: 31658266

86. Torres ES, Deal RB. The histone variant H2A.Z and chromatin remodeler BRAHMA act coordinately and antagonistically to regulate transcription and nucleosome dynamics in *Arabidopsis*. Plant J. 2019; 99: 144–162. https://doi.org/10.1111/tpj.14281 PMID: 30742338

87. Price JL, Dembinska ME, Young MW, Rosbash M. Suppression of PERIOD protein abundance and circadian cycling by the *Drosophila* clock mutation *timeless*. EMBO J. 1995; 14: 4044–4049.

88. Saez L, Derasmo M, Meyer P, Stieglitz J, Young MW. A key temporal delay in the circadian cycle of *Drosophila* is mediated by a nuclear localization signal in the timeless protein. Genetics. 2011; 188: 591–600. https://doi.org/10.1534/genetics.111.127225 PMID: 21515571

89. Vosshall LB, Price JL, Sehgal A, Saez L, Young MW. Block in nuclear localization of period protein by a second clock mutation, *timeless*. Science. 1994; 263: 1606–1609. https://doi.org/10.1126/science.8128247 PMID: 8128247

90. Hara T, Koh K, Combs DJ, Sehgal A. Post-Translational Regulation and Nuclear Entry of TIMELESS and PERIOD Are Affected in New *timeless* Mutant. J Neurosci. 2011; 31: 9982–9990. https://doi.org/10.1523/JNEUROSCI.0993-11.2011 PMID: 21734289

91. Fang Y, Sathyanarayanan S, Sehgal A. Post-translational regulation of the *Drosophila* circadian clock requires protein phosphatase 1 (PP1). Genes Dev. 2007; 21: 1506–1518. https://doi.org/10.1101/gad.1541607 PMID: 17575052

92. Kula-Eversole E, Lee DH, Samba I, Yildirim E, Levine DC, Hong H-K, et al. Phosphatase of Regenerating Liver-1 Selectively Times Circadian Behavior in Darkness via Function in PDF Neurons and

Dephosphorylation of TIMELESS. Curr Biol. 2021; 31: 138–149.e5. https://doi.org/10.1016/j.cub.2020.10.013 PMID: 33157022

93. Sathyanarayanan S, Zheng X, Xiao R, Sehgal A. Posttranslational Regulation of *Drosophila* PERIOD Protein by Protein Phosphatase 2A. Cell. 2004; 116: 603–615. https://doi.org/10.1016/S0092-8674(04)00128-X PMID: 14980226

94. Sharma T, Robinson DCL, Witwicka H, Dilworth FJ, Imbalzano AN. The Bromodomains of the mammalian SWI/SNF (mSWI/SNF) ATPases Brahma (BRM) and Brahma Related Gene 1 (BRG1) promote chromatin interaction and are critical for skeletal muscle differentiation. Nucleic Acids Res. 2021; 49: 8060–8077. https://doi.org/10.1093/nar/gkab617 PMID: 34289068

95. Foteinou PT, Venkataraman A, Francey LJ, Anafi RC, Hogenesch JB, Doyle FJ. Computational and experimental insights into the circadian effects of SIRT1. Proc Natl Acad Sci. 2018; 115: 11643–11648. https://doi.org/10.1073/pnas.1803410115 PMID: 30348778

96. Wang G, Fu Y, Hu F, Lan J, Xu F, Yang X, et al. Loss of BRG1 induces CRC cell senescence by regulating p53/p21 pathway. Cell Death Dis. 2017; 8: e2607–e2607. https://doi.org/10.1038/cddis.2017.1 PMID: 28182012

97. Foley LE, Ling J, Joshi R, Evantal N, Kadener S, Emery P. *Drosophila* PSI controls circadian period and the phase of circadian behavior under temperature cycle via *tim* splicing. Ramaswami M, Calabrese RL, editors. eLife. 2019; 8: e50063. https://doi.org/10.7554/eLife.50063 PMID: 31702555

98. Martin Anduaga A, Evantal N, Patop IL, Bartok O, Weiss R, Kadener S. Thermosensitive alternative splicing senses and mediates temperature adaptation in *Drosophila*. Ramaswami M, Calabrese RL, editors. eLife. 2019; 8: e44642. https://doi.org/10.7554/eLife.44642 PMID: 31702556

99. Gaillard H, Aguilera A. Transcription as a Threat to Genome Integrity. Annu Rev Biochem. 2016; 85: 291–317. https://doi.org/10.1146/annurev-biochem-060815-014908 PMID: 27023844

100. Lans H, Hoeijmakers JHJ, Vermeulen W, Marteijn JA. The DNA damage response to transcription stress. Nat Rev Mol Cell Biol. 2019; 20: 766–784. https://doi.org/10.1038/s41580-019-0169-4 PMID: 31558824

101. Lamm N, Rogers S, Cesare AJ. Chromatin mobility and relocation in DNA repair. Trends Cell Biol. 2021; 31: 843–855. https://doi.org/10.1016/j.tcb.2021.06.002 PMID: 34183232

102. Xiao Y, Yuan Y, Jimenez M, Soni N, Yadlapalli S. Clock proteins regulate spatiotemporal organization of clock genes to control circadian rhythms. Proc Natl Acad Sci. 2021; 118: e2019756118. https://doi.org/10.1073/pnas.2019756118 PMID: 34234015

103. Brand AH, Perrimon N. Targeted gene expression as a means of altering cell fates and generating dominant phenotypes. Dev Camb Engl. 1993; 118: 401–415. https://doi.org/10.1242/dev.118.2.401 PMID: 8223268

104. Blau J, Young MW. Cycling *vrille* Expression Is Required for a Functional *Drosophila* Clock. Cell. 1999; 99: 661–671. https://doi.org/10.1016/S0092-8674(00)81554-8 PMID: 10612401

105. Chiu JC, Ko HW, Edery I. NEMO/NLK Phosphorylates PERIOD to Initiate a Time-Delay Phosphorylation Circuit that Sets Circadian Clock Speed. Cell. 2011; 145: 357–370. https://doi.org/10.1016/j.cell.2011.04.002 PMID: 21514639

106. Taylor P, Hardin PE. Rhythmic E-Box Binding by CLK-CYC Controls Daily Cycles in per and tim Transcription and Chromatin Modifications. Mol Cell Biol. 2008; 28: 4642–4652. https://doi.org/10.1128/MCB.01612-07 PMID: 18474612

107. Majercak J, Chen W-F, Edery I. Splicing of the period Gene 3′-Terminal Intron Is Regulated by Light, Circadian Clock Factors, and Phospholipase C. Mol Cell Biol. 2004; 24: 3359–3372. https://doi.org/10.1128/MCB.24.8.3359-3372.2004 PMID: 15060157

108. Thaben PF, Westermark PO. Detecting Rhythms in Time Series with RAIN. J Biol Rhythms. 2014; 29: 391–400. https://doi.org/10.1177/0748730414553029 PMID: 25326247

109. Thaben PF, Westermark PO. Differential rhythmicity: detecting altered rhythmicity in biological data. Bioinformatics. 2016; 32: 2800–2808. https://doi.org/10.1093/bioinformatics/btw309 PMID: 27207944

110. Parsons R, Parsons R, Garner N, Oster H, Rawashdeh O. CircaCompare: a method to estimate and statistically support differences in mesor, amplitude and phase, between circadian rhythms. Bioinforma Oxf Engl. 2020; 36: 1208–1212. https://doi.org/10.1093/bioinformatics/btz730 PMID: 31588519

CLOCK and TIMELESS regulate rhythmic occupancy of the BRAHMA chromatin-remodeling protein at clock gene promoters

Christine A. Tabuloc, Yao D. Cai, Rosanna S. Kwok, Elizabeth C. Chan, Sergio Hidalgo, and Joanna C. Chiu

Supporting information:

Supplemental Figs. 1 to 4 and Supplemental Table 1

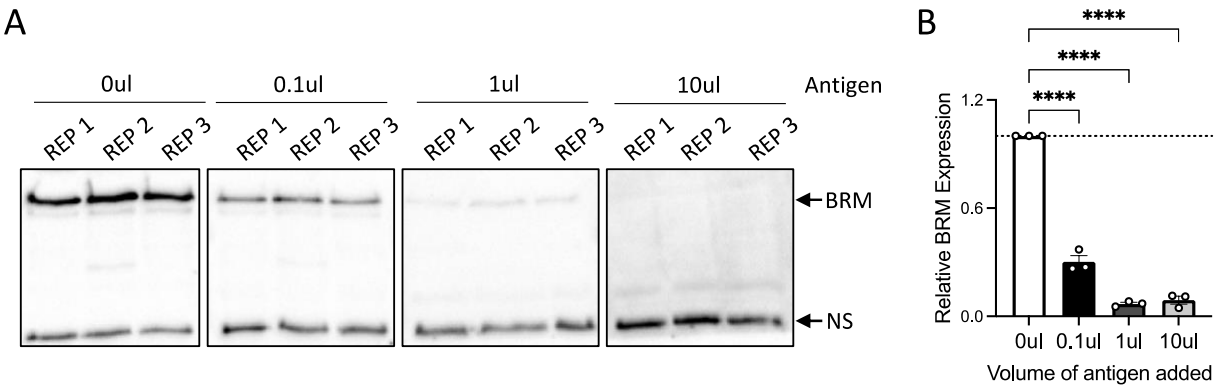

S1 Fig: Pre-adsorption of BRM polyclonal antibody with BRM antigen supports the specificity of the BRM antibody signal. (A) The BRM antibody was incubated with a dilution series of the BRM antigen (0.1ul, 1ul, and 10ul at 1ug/ul) prior to detecting BRM in protein lysate extracted from w^{1118} flies collected at ZT16. The non-specific band is denoted as NS. (B) BRM signal was normalized to the NS signal (n=3). Each data point represents a biological replicate. Error bars represent ±SEM. Asterisks denote significant p-values: ****p<0.0001.

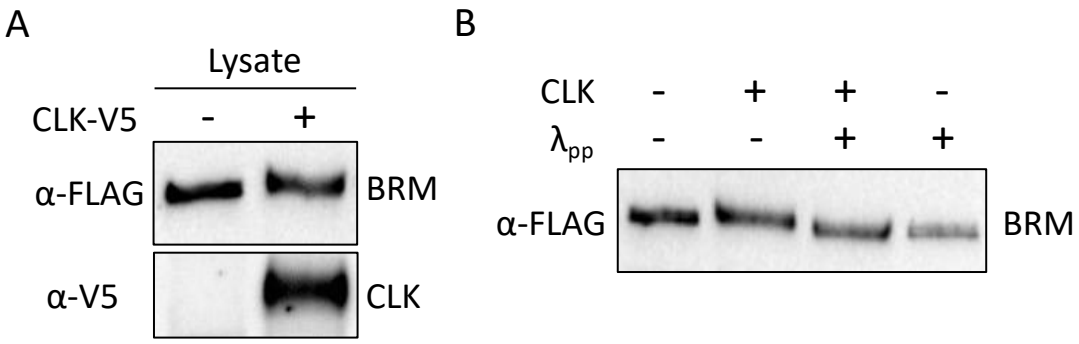

S2 Fig: Lambda phosphatase treatment reveals BRM is phosphorylated when expressed with CLK. (A) BRM (top panel) and CLK (bottom panel) expression prior to lambda phosphatase (λpp) treatment in protein lysate from S2 cells expressing either BRM alone or BRM co-expressed with CLK. (B) BRM protein after treatment with λpp.

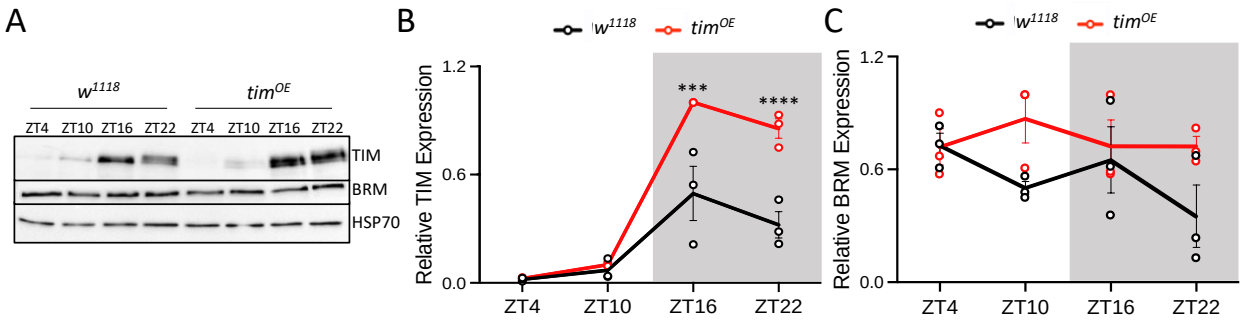

S3 Fig: Protein expression in *tim*^{OE} flies. (A) TIM (top panel) and BRM (middle panel) protein in *w*^{1118} and *w*^{1118}*;ptim(WT)* fly heads collected at the indicated time-points on LD3. *w*^{1118}*;ptim(WT)* flies are denoted as *tim*^{OE} flies**.** HSP70 (bottom panel) was used as a loading control. (B-C) Normalized (B) TIM and (C) BRM expression in *w*^{1118} (black) and *tim*^{OE} (red) flies (n=3). Each data point represents a biological replicate. Error bars represent ±SEM. The grey background denotes the dark phase of the LD cycle.

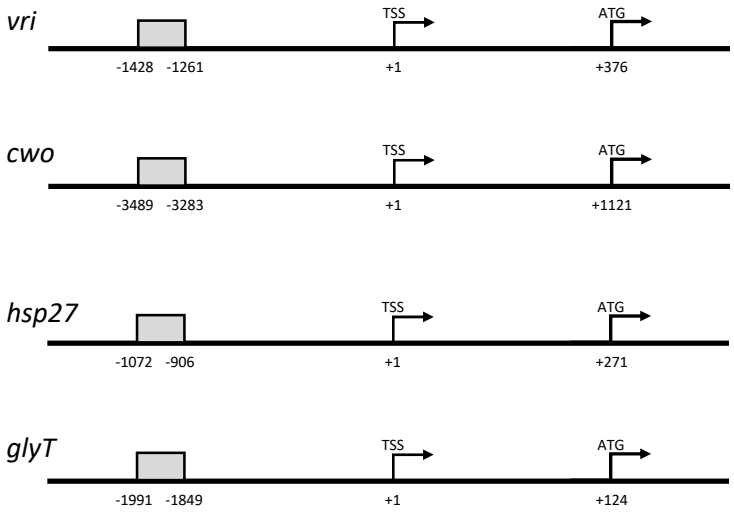

S4 Fig: Primer locations. Schematic of region amplified by primers (grey) used in ChIP to assess BRM occupancy at the promoters of *vri, cwo, hsp27,* and *glyT.* Positions are relative to the transcription start site (TSS). Locations of other ChIP primers are shown in Kwok et al. 2015.

S1 Table: Sequences for primers used for generation of BRM antigen, Chromatin Immunoprecipitation-qPCR, and steady-state mRNA analysis.

Purpose	Primer Name	5'-Sequence-3'	Reference
Antigen generation	*brm* (3961) Forward	GTG TGG ATC CGA TGA GTC CGA GCT ACC CGA CTG G	This study
	brm (4518) Reverse	GTG TGC GGC CGC CTA AGA CGC CTC TTC GTT GTA GAT CTG	This study
Chromatin Immunoprecipitation	*per* CRS Forward	TGC CAG TGC CAG TGC GAG TTC G	Kwok et al. 2015 [1]
	per CRS Reverse	TGC CTG GTG GGC GGC TGG	Kwok et al. 2015 [1]
Chromatin Immunoprecipitation	*tim E-box 1* Forward	ACG TTG TGA TTA CAC GTG AGC CG	Kwok et al. 2015 [1]
	tim E-box 1 Reverse	TAC ACA CAC TGA CCG AAA CAC CC	Kwok et al. 2015 [1]
Chromatin Immunoprecipitation	*vri* (-1428) Forward	AAC CAG ACA GTT TGG TGG CTG GG	This study
	vri (-1261) Reverse	CAG TGC TAG CTA ACT ATT TGA ACT CGT C	This study
Chromatin Immunoprecipitation	*cwo* (-3283) Forward	TTC TCC GGC AGT TGC ACC G	This study
	cwo (-3489) Reverse	TTA CTC ATG TGC CAC ATT CTC G	This study
Chromatin Immunoprecipitation	FBgn0003638 Forward	ACT GCG TAT TCA GGA TAC ATG CC	Kwok et al. 2015 [1]
	FBgn0003638 Reverse	TGT CCA CTT TAA TTG ATT GCG TGG	Kwok et al. 2015 [1]
Chromatin Immunoprecipitation	*hsp27* (-1027) Forward	TGA ATG TAA GGA ACT TCA GTC AAG G	This study
	hsp27 (-906) Reverse	TGC TAT AAG GAC GTA CAT AAC GTA C	This study
Chromatin Immunoprecipitation	*glyT* (-1991) Forward	TGA GCA GCG ATC GAC GCT GAC G	This study
	glyT (-1849) Reverse	TCG GTG CTG CAA AGC GCC GTT C	This study
mRNA analysis	*brm b3* qPCR Forward	AGC CAG GTA CAA GCT GAA C	Kwok et al. 2015 [1]
	brm b3 qPCR Reverse	TGA TCA TTT CGT CAT CGG	Kwok et al. 2015 [1]
mRNA analysis	*cbp20* qPCR Forward	GTC TGA TTC GTG TGG ACT GG	Majercak et al. 2004 [2]
	cbp20 qPCR Reverse	CAA CAG TTT GCC ATA ACC CC	Majercak et al. 2004 [2]
mRNA analysis	*per* qPCR Forward	GAC CGA ATC CCT GCT CAA	Kwok et al. 2015 [1]
	per qPCR Reverse	GTG TCA TTG GCG GAC TTC	Kwok et al. 2015 [1]

Chapter 2: Transcriptome analysis of *Drosophila suzukii* reveals molecular mechanisms conferring pyrethroid and spinosad resistance

Christine A. Tabuloc[1], Curtis R. Carlson[1], Fatemeh Ganjisaffar[1], Hongtao Zhang[2], Cindy C. Truong[1], Ching-Hsuan Chen[1], Kyle M. Lewald[1], Sergio Hidalgo[1], Frank G. Zalom[1], and Joanna C. Chiu[1]*

[1]Department of Entomology and Nematology, College of Agricultural and Environmental Sciences, University of California Davis, CA, USA

[2] Department of Plant Biology, College of Biological Sciences, University of California Davis, CA, USA

Author contributions: J.C.C., C.A.T., and F.Z. designed research; F.G. collected field samples; C.A.T., C.C.T., and F.G. performed bioassays, and C.A.T. and F.G. performed accompanying statistical analyses; C.A.T. and C.C.T. performed RNA extraction, and C.A.T. prepared Illumina sequencing libraries; C.A.T. and J.C.C. analyzed RNA-Seq data with the help of C.R.C., K.M.L., H.Z., and S.H.; C.A.T. and C.C. designed primers; C.A.T., F.G., F.Z., and J.C.C. contributed to critical interpretation of the data; C.A.T. and J.C.C wrote the paper with the input of all authors.

Transcriptome analysis of *Drosophila suzukii* reveals molecular mechanisms conferring pyrethroid and spinosad resistance

Christine A. Tabuloc[1], Curtis R. Carlson[1], Fatemeh Ganjisaffar[1], Hongtao Zhang[2], Cindy C. Truong[1], Ching-Hsuan Chen[1], Kyle M. Lewald[1], Sergio Hidalgo[1], Frank G. Zalom[1], and Joanna C. Chiu[1]*

[1] Department of Entomology and Nematology, College of Agricultural and Environmental Sciences, University of California Davis, CA, USA

[2] Department of Plant Biology, College of Biological Sciences, University of California Davis, CA, USA

***Corresponding author**: Joanna C. Chiu, email: jcchiu@ucdavis.edu, Phone no: (530) 752-1839

Keywords: spotted wing *Drosophila*, insecticide resistance, zeta-cypermethrin, metabolic resistance, penetration resistance, splicing, Entrust, Mustang Maxx

Author contributions

JCC, CAT, and FZ designed research; FG collected field samples; CAT, CCT, and FG performed bioassays, and CAT and FG performed accompanying statistical analyses; CAT and CCT performed RNA extraction, and CAT prepared Illumina sequencing libraries; CAT and JCC analyzed RNA-Seq data with the help of CRC, KML, HZ, and SH; CAT and CC designed primers; CAT, FG, FZ, and JCC contributed to critical interpretation of the data; CAT and JCC wrote the paper with the input of all authors.

Key message

- This is the first study to characterize molecular mechanisms of insecticide resistance in field-collected *Drosophila suzukii*.
- We identified genes that can serve as biomarkers to detect insecticide resistance in field populations of *D. suzukii*. We designed and validated qPCR-based molecular diagnostics for these biomarkers.
- Using RNA sequencing, we identified evidence of metabolic resistance in pyrethroid-resistant *D. suzukii* as well as evidence of metabolic and penetration resistance in spinosad-resistant *D. suzukii*.
- Long-read sequencing suggests that *D. suzukii* that are resistant to pyrethroid and spinosad insecticides exhibit changes in transcriptome-wide alternative splicing. This could represent an additional mechanism that underlies resistance.

Abstract

Drosophila suzukii, also known as spotted wing *Drosophila* (SWD), is an invasive agricultural pest that is a threat to berry production due to a serrated ovipositor on female flies that enable them to lay eggs in soft-skinned, ripening fruits. Currently, growers rely heavily on the use of insecticides to manage *D. suzukii*. Over the past six years, insecticide resistance has been detected in *D. suzukii* in California, but the molecular mechanism underlying this adaptation is unknown. Therefore, we sought to identify the molecular mechanism conferring insecticide resistance in these pests. We generated isogenic lines from field-collected resistant populations and sequenced the transcriptomes of two pyrethroid- and two spinosad-resistant lines. In both pyrethroid-resistant isogenic lines and one spinosad-resistant line, we identified overexpression of metabolic genes that have been previously implicated in insecticide resistance in other insect pests. In the other spinosad-resistant line, we observed an overexpression of cuticular genes that have been linked to insecticide resistance. Additionally, we observed decreased expression of the pyrethroid target gene, *paralytic*, in both pyrethroid-resistant lines. Our findings enabled the development of molecular diagnostics that can be used to monitor resistance development in the field, specifically by monitoring overexpression of specific target genes. Finally, long-read sequencing reveals transcriptome-wide changes in the expression of different splice variant isoforms, suggesting that alternative splicing can be an additional mechanism enabling insecticide resistance. This study is the first to characterize the molecular mechanisms of insecticide resistance in field-collected *D. suzukii* and provides insights into how current management practices can be improved.

Introduction

Drosophila suzukii (Matsumura), also known as spotted wing *Drosophila* (SWD), is an invasive, agricultural pest originally from Southeast Asia and was first detected in the continental United States in 2008 (Bolda et al., 2010; Chiu et al., 2013). Since then, *D. suzukii* has been detected across North America (Hauser, 2011; Walsh et al., 2011), Europe (Cini et al., 2014; Rota-Stabelli et al., 2020), South America (Andreazza et al., 2017; Deprá et al., 2014), and Africa (Hassani et al., 2020). Female *D. suzukii* flies have a serrated ovipositor that enables them to lay eggs in soft-skinned, ripening fruit such as strawberries and caneberries (Walsh et al., 2011; Walton et al., 2016). The ability of *D. suzukii* to infest ripening fruit as opposed to over-ripened fruit, like other *Drosophila* species, poses a unique threat to both fresh and processed berry production. In fact, in the first year after its detection, *D. suzukii* caused considerable damage to raspberries, blackberries, blueberries, and cherries leading Bolda et al. (2010) to estimate the annual potential economic impact of this pest in the Pacific Coast region to be US$421.5 million.

Current *D. suzukii* management strategies consist of intensive spray programs (Bruck et al., 2011; Van Timmeren & Isaacs, 2013) of several insecticides including pyrethroids and spinosads (Diepenbrock et al., 2016; Knight et al., 2016; Van Timmeren et al., 2019). Pyrethroid insecticides target the insect nervous system by binding to the active site of a voltage-gated sodium channel (VGSC), *paralytic* (*para*), causing overstimulation of the nervous system that results in excessive twitching and eventually death (Lund & Narahashi, 1982). Spinosad insecticides, on the other hand, target the insect nervous system by binding to an allosteric site on the alpha 6 subunit of the nicotinic acetylcholine receptor (*nAChRα6*), resulting in overexcitation of motor neurons causing paralysis and eventually death (Salgado, 1998; Salgado et al., 1998). Due to repeated insecticide exposure, the short generation time, and high fecundity of *D. suzukii*, this pest has great potential for developing insecticide resistance (Asplen et al., 2015). To date, there are three reports in California, U.S. that have documented the detection of spinosad-

(Ganjisaffar, Gress, et al., 2022; Gress & Zalom, 2019) and pyrethroid-resistance (Ganjisaffar, Demkovich, et al., 2022) in *D. suzukii*, but the exact mechanisms driving these adaptations have yet to be described.

Thus far, common molecular mechanisms conferring insecticide resistance characterized in other insect pests include penetration resistance, metabolic resistance, and target-site resistance. Penetration resistance occurs when there is an overexpression of cuticular genes such as *cuticle protein (Cpr) 30*, resulting in a less penetrable insect integument and therefore reduced dermal entry of the insecticide (Balabanidou et al., 2018). Metabolic resistance is defined by an upregulation of metabolic enzymes that detoxify the insecticide prior to its binding to the target protein (Li et al., 2007). The classes of metabolic genes implicated in insecticide resistance include *cytochrome P450s* (*cyp*) (Liu et al., 2015), *glutathione S-transferases* (*gst*) (Pavlidi et al., 2018), *esterases* (Montella et al., 2012), and *heat shock proteins* (*hsp*) (Silva et al., 2012). Finally, target-site resistance occurs when a mutation within the target protein prevents the docking of the insecticide to its binding site (Dong et al., 2014; Grauso et al., 2002). It is currently unknown whether any of these mechanisms underlie resistance observed in *D. suzukii*. Therefore, there is a need for identifying the possible molecular mechanisms conferring insecticide resistance in this pest as this will enable the development of molecular diagnostics to monitor insecticide resistance development in the field as well as provide insights into how growers can improve their *D. suzukii* management programs.

Here, we generated isogenic lines from field-collected *D. suzukii* populations determined to be resistant to either pyrethroids (specifically zeta-cypermethrin) or spinosads. We then sequenced the transcriptomes of two zeta-cypermethrin-resistant and two spinosad-resistant isogenic lines and compared them to respective susceptible lines to investigate the molecular mechanisms driving insecticide resistance in these flies. We observed that *D. suzukii* flies resistant to zeta-cypermethrin exhibit increased expression of metabolic enzymes, indicative of metabolic resistance, as well as decreased expression of *para*. In one spinosad-resistant line, we observed evidence of metabolic resistance.

However, we observed increased expression of cuticular genes in a second spinosad-resistant line, suggesting that penetration resistance is at play. Leveraging our results, we developed a quantitative polymerase chain reaction (qPCR)-based assay to diagnose overexpression of specific target genes, which could reflect metabolic or penetration resistance. Finally, we also observed that many genes within the spliceosome pathway are differentially expressed in resistant isogenic lines. Therefore, we performed long-read sequencing to assess the expression of full-length transcripts and observed global changes in alternative splicing (AS) between resistant and susceptible *D. suzukii* lines. Our results suggest that transcriptome-wide changes in AS may represent an additional mechanism conferring insecticide resistance in *D. suzukii*. Taken together, our findings provide molecular diagnostics that can be leveraged in efficient resistance development monitoring prior to conducting conventional insecticide bioassays, which are much more laborious. Our study also provides insights into how growers can adjust *D. suzukii* management protocols to counter insecticide resistance development.

Materials And Methods

Field *D. suzukii* populations and development of isogenic lines

To assess resistance to zeta-cypermethrin (Mustang Maxx 0.8 EC, FMC Corporation, Philadelphia, PA), isogenic lines were established from *D. suzukii* adults reared from fruits collected in October 2019 from a strawberry field in Monterey County, CA. Sixty fruits were collected and transported to the laboratory of Dr. Frank Zalom at the University of California, Davis. Twenty of the fruits were transferred to a plastic container containing a layer of cotton topped with sand as a substrate for pupation, for a total of three containers. The containers were maintained at 23 ± 1°C, 55-65% relative humidity (RH), and a 14-hour light:10-hour dark photoperiod in a walk-in growth chamber (Percival Scientific Inc., Perry, IA) and checked daily until fly emergence. Emerged *D. suzukii* flies were separated from non-target species and reared in bottles containing Bloomington standard *Drosophila*

cornmeal diet (https://bdsc.indiana.edu/information/recipes/bloomfood.html).

To assess resistance to spinosad (Entrust 22.5% spinosad, a mixture of spinosyn A & D, Corteva Agriscience, Indianapolis, IN), isogenic lines were established from *D. suzukii* adults collected from a caneberry field in Santa Cruz County, CA in November 2019. Adult flies were live-captured using McPhail traps (Great Lakes IPM, Inc., Vestaburg, MI) baited with approximately 20 ml of a yeast (7 g)-sugar (113 g)-water (355 ml) solution. Traps were collected the next day and returned to the laboratory. Flies were anesthetized using CO_2 to facilitate the removal of any non-target species (approximately twenty females and twenty males per bottle) and transferred into diet bottles (described above). Field-collected *D. suzukii* were assessed for resistance, as described below in the "Bioassays" section. Each isogenic line was established from a single mated, non-insecticide-treated female from a resistant population. Crossing of siblings was repeated for eight generations for each isogenic line. A total of eight isogenic lines were established for each site, for a total of sixteen lines. Bioassays were performed once isogenic lines were established to identify resistant and susceptible isogenic lines.

Field-collected populations used for quantitative PCR (qPCR) assays were reared from fruits collected from two California open strawberry fields in Santa Cruz County in September 2022. A hundred ripe fruits were collected from each field and placed in plastic containers and transported to the laboratory. Fruits were transferred to new plastic containers containing a layer of cotton topped with sand. For each site, five containers of twenty fruits were prepared and placed at 23±1°C, 55-65% RH, 14-hour light: 10-hour dark photoperiod and checked daily until fly emergence. Emerged flies were aspirated into diet bottles. Twenty female and twenty male *D. suzukii* adults were then moved to new diet bottles for propagation to increase total available flies, and the progeny (F1) from each site were used in bioassays.

Insecticide bioassays

Bioassays were performed using a glass vial residue bioassay (Van Timmeren et al., 2018, 2019). Briefly, the interior of 20-ml glass scintillation vials (Fisher Scientific, Pittsburgh, PA) were coated with insecticide solution at each concentration indicated below. Excess insecticide was removed, and treated vials and caps were placed upright in a fume hood to dry overnight. Five male and five female adults (3-5 days after emergence) from each isogenic line were transferred into each treated vial. The vials were then maintained at 23±1°C, 55-65% RH, 14-hour light: 10-hour dark photoperiod for the duration of the experiment.

Susceptibility of the established isogenic lines to zeta-cypermethrin (Mustang Maxx 0.8 EC, FMC Corporation, Philadelphia, PA) was assessed at the discriminating dose (which is eight times the concentration required to kill 90% of the tested population) of 6.89 mg liter^{-1} (Disi & Sial, 2021; Ganjisaffar, Demkovich, et al., 2022). Based on mortality at this concentration, two resistant lines and one susceptible line were selected per site for dose-response bioassays. Various concentrations of 1-18 mg liter^{-1} zeta-cypermethrin (0ppm, 1ppm, 2ppm, 4ppm, 6.89ppm, 10ppm, 12ppm, 15ppm, and 18ppm) were tested for the resistant isogenic lines. For the susceptible isogenic line, six concentrations of 0.2-10 mg liter^{-1} zeta-cypermethrin (0ppm, 0.2ppm, 0.5ppm, 1ppm, 2ppm, 4ppm, 6.89ppm) were tested. Mortality was recorded after six hours, and the number of dead flies was recorded.

The susceptibility of isogenic lines to spinosad (Entrust 22.5% spinosad, a mixture of spinosyn A & D, Corteva Agriscience, Indianapolis, IN) was assessed at the discriminating dose of 928 mg liter^{-1} (Ganjisaffar, Gress, et al., 2022; Gress & Zalom, 2019). The insecticide was diluted in Induce (Helena Chemical Company, Memphis, TN) – deionized water solution at a rate of 1266 µl Induce per liter of deionized water. Induce is a non-ionic surfactant used to help spread the solution uniformly and increase adherence to the vial surfaces. Two resistant lines and one susceptible isogenic line were selected for dose-response bioassays. Several concentrations of 100-10,000 mg liter^{-1} spinosad (100ppm, 300ppm, 928ppm, 3000ppm, 6000ppm, 8000ppm, and 10,000ppm) were tested for the

resistant isogenic lines while six concentrations of 30-3,000 mg liter^{-1} spinosad (30ppm, 65ppm, 100ppm, 300ppm, 928ppm, and 3000ppm) were tested for the susceptible isogenic line. Eight replicates were tested per concentration, and mortality of flies was recorded after eight hours of spinosad exposure.

Moribund and dead individuals were combined and considered as dead. Moribund flies are defined as those showing clear signs of toxicity (i.e. slow uneven movements, leg twitching, and inability to hold on to the bioassay vial). Despite being alive, these flies would not recover from the insecticide. Mortality data from dose-response bioassays were fitted to a two-parameter log-logistic model with a lower limit of 0 and an upper limit of 1 using the 'drc' package (Ritz et al., 2015) in R 4.2.1 (R Core Team, 2022). The function 'ED' was used to calculate estimated effective doses (LC50 values). Pairwise z-tests were conducted with the 'compParm' function to compare LC50 values between different isogenic lines to further analyze susceptibility. All models included insecticide concentration (mg liter^{-1}) and isogenic line as predictor variables, while the response variable was the proportion of dead flies. Proportions were weighted by total sample size in each vial. As a control, we included 2 isogenic lines established from flies collected in an untreated orchard located in Winters in Solano County, CA (Gress & Zalom, 2019), referred as Wolfskill populations. Differences of mortality between isogenic lines and the Wolfskill control were assessed by one-way ANOVA followed by Tukey's multiple comparison test using GraphPad Prism Version 9.3.1 (GraphPad Software, La Jolla, California, USA).

RNA extraction, library preparation, and high throughput sequencing

Female *D. suzukii* flies were entrained at 25°C in 12-hour light:12-hour dark cycles for two full days. On the third day, flies were collected on dry ice sixteen hours after lights-on. This time point was selected because *D. suzukii* was previously observed to exhibit a low level of *cytochrome P450* expression at this time (Hamby et al., 2013). This means any overexpression may be more easily

observed. Fly bodies were separated from heads using frozen metal sieves (Newark Wire Cloth Company, Clifton, New Jersey). Eight to ten female bodies were homogenized using a motor and pestle in 300 μL TRI reagent (Sigma, St. Louis, MO). 60 μL of 100% chloroform (Sigma) was added and incubated at room temperature for 10 minutes. The upper aqueous layer was recovered after spinning down and transferred to a new microcentrifuge tube. RNA was precipitated with an equal volume of 100% isopropanol at −20°C overnight. After spinning down, the RNA pellet was washed with 70% ethanol once and allowed to air dry. The pellet was then resuspended in 20 μL 1X Turbo DNA-free kit buffer (Thermo Fisher Scientific, Waltham, MA) and treated with Turbo DNase per manufacturer's instructions. RNA quality was assessed with both the Agilent 2100 Bioanalyzer system (Agilent Technologies, Santa Clara, CA) and the Qubit RNA IQ kit (Invitrogen, Waltham, MA) on the Qubit 4 Fluorometer (Invitrogen). RNA purity was measured with the Nanodrop 1000 (Thermo Fisher Scientific).

Illumina short-read sequencing libraries were prepared with 1 μg of high-quality RNA and the TruSeq Stranded mRNA Library Prep Kit (Illumina, San Diego, CA) according to manufacturer's protocol. A total of twenty-four libraries were prepared: three biological replicates of two zeta-cypermethrin-resistant lines, two zeta-cypermethrin-susceptible lines, two spinosad-resistant lines, and two spinosad-susceptible lines. Library insert size and quality was measured with the Agilent 2100 Bioanalyzer System. Library concentration was measured with the Qubit 4 Fluorometer. All libraries generated from zeta-cypermethrin-resistant and susceptible SWD lines were pooled together, and all libraries generated from spinosad-resistant and susceptible SWD lines were pooled together, such that there were twelve libraries per pool. Pooled samples were sent to Novogene (Sacramento, CA) for sequencing on the HiSeq X Ten platform (Illumina) using PE150. For PacBio Iso-Seq, high-quality RNA was sent to the DNA Technologies and Expression Analysis Core Laboratory at UC Davis for library preparation and sequencing. Two 8M SMRT cells were sequenced on a PacBio Sequel system (PacBio, Menlo Park, CA).

Differential expression gene analysis

Differential gene expression analysis was performed using sequencing reads derived from llumina short-read sequencing. First, rRNA reads were removed using SortMeRNA v2.1 (Kopylova et al., 2012). Adapters (ILLUMINACLIP parameters 2:30:10) and low-quality ends (LEADING: 10, TRAILING:10, MINLEN:36) were trimmed using Trimmomatic v0.35 (Bolger et al., 2014). Cleaned reads were aligned to the NCBI *Drosophila suzukii* Annotation Release 102 based on the LBDM_Dsuz_2.1.pri assembly (accession no. GCF_013340165.1) (Paris et al., 2020) using STAR v2.7.9a (Dobin et al., 2013). Count data from STAR (--quantMode GeneCounts) served as input in the DESeq2 package (Love et al., 2014) in R to perform differential expression analysis on each resistant line vs all susceptible samples. Each resistant line was compared to susceptible samples separately as each line might exhibit resistance due to different mechanisms. Genes with fold change differences between resistant vs susceptible populations with a Benjamini-Hochberg adjusted p-value < 0.05 were considered differentially expressed. Expression levels of genes were also measured as fragments per kilobase of exon per million mapped (FPKM) values calculated with Stringtie v2.0.4 (Pertea et al., 2015). The consistency between biological replicates was calculated with Pearson's correlation coefficient, which was determined with the 'stats' package in R version 4.2.1. Expression differences of key genes between the resistant and susceptible populations were calculated with two-way ANOVA followed by two-stage linear set-up procedure of Benjamini, Krieger, and Yekutieli on GraphPad Prism.

Weighted Gene Co-expression Network Analysis

Gene expression (in FPKM) served as input for Weighted Gene Co-expression Network Analysis (WGCNA). Genes with an expression value of zero for more than six samples were excluded from analysis. To explore the modules most correlated with insecticide resistance, a correlation analysis using resistance status was performed with the WGCNA package (Version 1.72.1) (Langfelder & Horvath,

2008) on R. Modules with a p-value < 0.05 were considered significant. Functional enrichment analysis (described below) was performed on the module with the highest correlation with resistance.

Functional enrichment analysis

Genes were functionally annotated using BLAST against the NCBI *Drosophila melanogaster* Annotation r6.32 based on the Release 6 plus ISO1 mitochondrial genome assembly (accession no. GCA_000001215.4) (dos Santos et al., 2015). Gene Ontology (GO) enrichment of genes were performed using ShinyGO 0.76.3 (Ge et al., 2020). GO terms and pathways were considered enriched if the false discovery rate (FDR) < 0.05.

Variant calling

To identify allelic changes between the resistant and susceptible populations in the target genes *paralytic* and *nicotinic acetylcholine receptor subunit alpha 7*, variants were called using Freebayes v1.3.5 (Garrison & Marth, 2012). Differences between allelic counts between the resistant and susceptible groups were compared using Fisher's Exact Test on R v4.2.1.

Transcriptome annotation and alternative splicing analysis

Both 8M SMRT Cells of Iso-Seq data were pooled together and run through the isoseq3 pipeline (https://github.com/PacificBiosciences/IsoSeq, v. 3.8.0) to generate full-length non-chimeric (FLNC) isoform sequences. PolyA and concatemer sequences were removed from PacBio sequencing reads using 'isoseq refine.' To maximize detection of rare isoforms, both high-quality and low-quality FLNC isoform sequences were concatenated and mapped to the *D. suzukii* reference genome (accession no. GCF_013340165.1) (Paris et al., 2020) using minimap2 (H. Li, 2018) (v. 2.24-r1122; -ax splice -uf --secondary=no -C5). Mapped FLNC isoforms were then filtered and collapsed using cDNA_Cupcake

(https://github.com/Magdoll/cDNA_Cupcake, collapse_isoforms_by_sam.py), retaining nonredundant isoforms. Nonredundant isoforms were classified against the reference genome and transcriptome using SQANTI3 QC v. 5.1 (Tardaguila et al., 2018). All short-read RNA-Seq data were used as evidence in SQANTI3 QC to validate isoforms. Isoforms flagged as artifacts by SQANTI3 QC were filtered using the SQANTI3 "rules" filter, retaining all full-splice matching isoforms not flagged as an intrapriming artifact and all non-full-splice matching isoforms not flagged as an intrapriming artifact, having a reverse-transcriptase-switching junction, and/or non-canonical splice junctions without short-read support. After filtering, SQANTI3 rescue was run to recover discarded reference transcripts that have long-read support, resulting in a final long-read supported transcriptome. This long-read transcriptome was then merged with the reference transcriptome to create a final, nonredundant expanded transcriptome. Splice junction and exon counts were then generated using Quality of RNA-Seq Tool-Set (QoRTs) (Hartley & Mullikin, 2015). Differential usage of exons and splice junctions was determined with JunctionSeq (Hartley & Mullikin, 2016). Features with FDR < 0.05 were considered differentially expressed/utilized. In line-to-line comparisons (**Fig 9J-K**), the number of differentially spliced genes was divided by the total number of genes sequenced in each condition. This value was normalized to the susceptible-to-susceptible comparison. The proportion of differentially spliced genes in each comparison was compared to the susceptible-to-susceptible comparison using Fisher's Exact Test on R v4.2.1. Functional enrichment was performed as described above in the "Functional enrichment analysis" section. GO and KEGG terms in a resistant-to-susceptible comparison that overlaps with terms in the susceptible-to-susceptible comparison were removed such that only unique terms remained (**Tables 2-3**).

Quantitative polymerase chain reaction (qPCR) for gene expression analysis

Total RNA extraction from F3 progeny of the 2022 collection (see "Field populations and development of isogenic lines") was performed as described above (see "RNA extraction, library

preparation, and high throughput sequencing"). cDNA synthesis was performed with the SuperScript IV Reverse Transcriptase kit (ThermoFisher Scientific) according to the manufacturer's instructions, using 4ug of RNA as input. cDNA was then diluted ten-fold with nuclease-free water. qPCR was performed using Sso Advanced SYBR green supermix (Bio-Rad, Hercules, CA) in a CFX384 (Bio-Rad). Primer sequences are listed in **Suppl. Table 1**. Cycling conditions were 95°C for 30 seconds followed by forty cycles of 95°C for 5 seconds and an annealing/extension phase at 60°C for 30 seconds. The reaction was concluded with a melt curve analysis from 65°C to 95°C in 0.5°C increments at 5 seconds per step. Three technical replicates were performed per biological replicate for a total of five biological replicates. Isogenic lines served as the susceptible and resistant controls. Resistant control lines were selected based off whether the line overexpressed the gene of interest in the differential gene expression analysis. Data were analyzed using the standard ΔΔCt method (Livak & Schmittgen, 2001), and target gene mRNA expression levels were normalized to the reference gene, *ribosomal protein L32* (*rpL32*) (Ponton et al., 2011). Finally, relative expression was calculated by dividing the expression level for each sample by the average expression of the susceptible control for all biological replicates such that the expression of the susceptible line would be one. To compare the expression levels of each sample to the susceptible control, a one sample t and Wilcoxon test were performed on GraphPad Prism. Additionally, gene expression levels of the resistant control line were compared to the expression level of the 2022 populations using one-way ANOVA followed by Holm-Sidak's multiple comparisons test on GraphPad Prism.

Results

Development and identification of insecticide-resistant *Drosophila suzukii* isogenic lines

We first generated multiple isogenic lines derived from a single *Drosophila suzukii* population, such that we can attribute observed gene expression differences between susceptible vs resistant

isogenic lines to causal genetic determinants with higher confidence. This is more appropriate than comparing resistant and susceptible flies collected from geographically separated locations given they are likely to be more genetically different, resulting in gene expression differences unrelated to insecticide resistance. Isogenic lines were developed from *D. suzukii* populations collected from either a strawberry or a caneberry field in 2019 that exhibit insecticide control failure based on reports by growers. To develop insecticide-susceptible vs resistant isogenic lines, bioassays were performed on lines generated from a zeta-cypermethrin-resistant population (herein referred to as "S" for strawberry) and a spinosad-resistant population (herein referred to as "C" for caneberry), using isogenic lines developed from a susceptible population collected from an untreated orchard as control (herein referred to as Wolfskill) (Gress & Zalom, 2019) (**Fig. 1A-B; Suppl. Table 2-3**). Lines S1, S3, and S4 had decreased mortality compared to Wolfskill when treated with zeta-cypermethrin (n=8) (**Fig. 1A; Suppl. Table 2**), while lines C3, C4, and C6 exhibited lower mortality when treated with spinosad (**Fig. 1B; Suppl. Table 3**). We opted to use two lines with the lowest rates of mortality per resistant population for further analyses (**Fig. 1A-B**).

We next determined the effective dose required to kill half of the tested population (LC50) of four resistant lines, two from each population (**Fig. 1C-1D**). The LC50 of the zeta-cypermethrin-resistant lines (S3, S4) were about three times greater than the susceptible line S8 derived from the same population (**Fig. 1C; Table 1; Suppl. Table 4**). The LC50 of the spinosad-resistant lines (C3, C4) were at least five times higher than the susceptible line C5 derived from the same population (**Fig. 1D; Table 1; Suppl. Table 4**). Therefore, we concluded that lines S3 and S4 are resistant to zeta-cypermethrin, and lines C3 and C4 are resistant to spinosad.

Overexpression of metabolic genes suggests metabolic resistance in zeta-cypermethrin-resistant *Drosophila suzukii*

We performed short-read RNA sequencing (RNA-Seq) to identify the molecular mechanisms underlying zeta-cypermethrin resistance in *D. suzukii*. We sequenced two zeta-cypermethrin-resistant lines (S3 and S4) and two susceptible lines derived from the same population as controls (S7 and S8). Triplicates were analyzed for each line, and Pearson's correlation confirmed that the biological replicates are highly correlated with one another (**Suppl. Fig. 1**).

Next, to identify whether gene expression changes underlie insecticide resistance, we identified differentially expressed genes (DEG) between the resistant and susceptible lines. We observed a total of 2,120 downregulated genes, 1,708 upregulated genes, and 8,723 genes that are not differentially expressed between line S3 and the susceptible lines (**Fig. 2A; Suppl. Table 5**). For line S4, we identified 3,686 downregulated genes, 4,240 upregulated genes, and 6,323 genes that are not differentially expressed (**Fig. 2B; Suppl. Table 6**). Amongst the upregulated genes, there are some belonging to classes of metabolic enzymes known to confer insecticide resistance. For instance, we observed that at least one of the two resistant lines we sequenced exhibit a significant increase in the expression of *Cytochrome P450* (*Cyp*) *6a20* and *Cyp4d14*, the carboxylesterase, *Cricklet*, *heat shock proteins* (*Hsp*) *60B* and *Hsp70Aa*, and *glutathione-s-transferase* (*Gst*) *E3* (**Fig. 2C; Suppl. Table 7)**. Our results suggest that zeta-cypermethrin resistance we observed in field-collected *D. suzukii* in California may be attributed to metabolic resistance. Furthermore, many of the genes downregulated in the resistant lines are genes related to cellular signaling, such as nicotinic acetylcholine receptors, acetylcholine transporters, and voltage-gated sodium channel (VGSC) subunits; notably, the VGSC *paralytic* (*para*), the target protein of zeta-cypermethrin, is among them (**Fig. 2A-B, insert)**.

We then performed functional enrichment analyses to identify which pathways these DEGs are involved in (**Fig. 2D-E; Suppl. Tables 8-9**). The downregulated genes in line S3 were enriched in several pathways involved in neuronal signaling while the upregulated genes were enriched in pathways involved in RNA processing, protein expression, and metabolism (**Fig. 2D; Suppl. Table 8**). For line S4,

the downregulated genes were enriched in pathways involving neuronal signaling and metabolism while the upregulated genes are enriched in pathways involved in protein degradation and the cell cycle (**Fig. 2E; Suppl. Table 9**).

Next, we performed Weighted Gene Co-expression Network Analysis (WGCNA), an unsupervised analysis pipeline that clusters genes into modules based on their expression profile across samples (Langfelder & Horvath, 2008), to identify genes highly correlated with resistance (**Fig. 3-4; Suppl. Table 10-11**). For line S3, genes were clustered into 35 different colored modules with the turquoise module being most correlated with resistance ($R^2 = 0.89$) (**Fig. 3A; Suppl. Table 10**). Out of the 2,908 genes in turquoise, we identified several metabolic genes within the class of cytochrome P450s, heat shock proteins, GSTs, and esterases (**Fig. 3B**). Functional analysis revealed that the genes in turquoise are enriched in pathways involved in metabolism, RNA processing, and protein expression (**Fig. 3C; Suppl. Table 11)**. For line S4, genes were clustered into 27 modules, with turquoise being most correlated with resistance ($R^2 = 0.92$) (**Fig. 4A**). Of the 4,449 genes within turquoise, several of these genes are metabolic genes known to confer insecticide resistance in other species (**Fig. 4B; Suppl. Table 12**). The pathways most enriched with genes in turquoise are those involved in RNA processing, cell cycle, cell differentiation, and protein and gene expression (**Fig. 4C; Suppl. Table 13**). Taken together, our results of the DEG analysis and WGCNA suggest that an upregulation of metabolic gene expression may confer zeta-cypermethrin resistance in field-collected *D. suzukii* in California, U.S.

Overexpression of cuticular and metabolic genes suggests penetration and metabolic resistance in spinosad-resistant SWD

We sequenced the transcriptomes of two spinosad-resistant lines (C3, C4) and two susceptible lines (C2, C5) derived from the same population to determine the molecular mechanisms conferring

spinosad-resistance. Pearson's correlation coefficients revealed a strong correlation between biological replicates, confirming that the triplicates are consistent (**Suppl. Fig. 2**).

Next, we assessed the differences in gene expression between each resistant line vs. both susceptible lines. For line C3, we observed a total of 852 DEGs, with 492 genes downregulated in the resistant line and 360 genes that were upregulated, and 11,756 genes that were not differentially expressed (**Fig. 5A; Suppl. Table 14**). In line C4, 4,233 genes were differentially expressed, with 2,132 genes upregulated in the resistant line and 2,201 genes that were downregulated, while 8,166 genes were not differentially expressed (**Fig. 5B; Suppl. Table 15**). We identified that amongst the genes upregulated in line C3 are several genes expressed within the insect integument, including *Tweedle* (*Twdl*) *F*, *TwdlG*, and *TwdlV* as well as *Cpr35B* and *Cpr66D* (Willis, 2010), while several genes upregulated in line C4 are metabolic genes, including *cyp4d8, cyp6d4, hsp68,* and *gstS1* (**Fig. 5C; Suppl. Table 16**). This suggests that penetration resistance may confer spinosad resistance in line C3 while metabolic resistance may confer resistance in line C4. This also suggests that alleles resulting in either metabolic resistance or penetration resistance are present in the field-collected spinosad-resistant *D. suzukii* population.

Furthermore, we performed functional enrichment analyses and observed that genes downregulated in line C3 are enriched in metabolic pathways, including the metabolism of xenobiotics by the *cyp* pathway, while upregulated genes are enriched in pathways related to the insect cuticle and RNA processing (**Fig. 5D; Suppl. Table 17**). In line C4 on the other hand, genes downregulated in the resistant lines are enriched in pathways pertaining to cell cycle, DNA replication and repair, and cell division while upregulated genes are enriched in metabolism and neuronal signaling pathways (**Fig. 5E; Suppl. Table 18**).

We next performed WGCNA to identify genes strongly correlated with spinosad resistance (**Fig. 6-7**). In line C3, genes were clustered into 47 different modules, with dark turquoise being most

correlated with resistance (R^2 = 0.83) (**Fig. 6A; Suppl. Table 19**). Of the 79 genes within dark turquoise, only 66 genes were functionally annotated and have a *D. melanogaster* homolog (**Fig. 6B**). Since there are few genes within this module, the genes were not enriched in any pathways, however, there are a few genes in dark turquoise that are involved in chromatin organization, such as *histone H2A* (Llorens-Giralt et al., 2021), *modifier of mdg4* (Dorn & Krauss, 2003), and *histone methyl transferase 4-20* (Schotta et al., 2004), as well as genes involved in hypoxia response (*ecdysone induced protein 93F* (Lee et al., 2008) and CG2918 (Gaudet et al., 2011)) and negative regulation of cell growth (*La-related protein4B* (Funakoshi et al., 2018) and *Forkhead box subunit O* (Jünger et al., 2003)). On the other hand, genes in line C4 were clustered into 42 colored modules, with green most correlated with resistance (R^2 = 0.96) (**Fig. 7A; Suppl. Table 20**). There are 371 genes in green and of those, only 3 genes, *cyp6d4, cyp305A1,* and *GstO1,* belong to metabolic enzymes involved in insecticide detoxification (Li et al., 2007) (**Fig. 7B**). Genes in the green module are enriched in pathways involving neuronal organization and signaling as well as metabolism (**Fig. 7C**). Therefore, the genes most correlated with resistance in line C3 are genes that have not been previously implicated in conferring insecticide resistance in other insect species, whereas in line C4, of the genes most correlated with resistance, 3 are within classes of metabolic enzymes known to promote insecticide resistance.

New field-collected *Drosophila suzukii* populations in 2022 show evidence of increased metabolic resistance as compared to flies collected in 2019

Now that we have identified genes of interest that may confer insecticide resistance in isogenic lines of *D. suzukii*, we were interested in determining whether any of these genes are also differentially expressed in resistant *D. suzukii* recently collected from the field. We assessed the resistance status of the F1 of *D. suzukii* collected in 2022 from two different strawberry fields using bioassays (**Fig. 8A**). The mortality of both populations was significantly lower than 100%, the mortality observed in the Wolfskill

and susceptible isogenic lines (**Fig. 1A-B**), suggesting that these populations are resistant to both zeta-cypermethrin and spinosad (zeta-cypermethrin: Population #1: t=23.88, df=9, p<0.0001; Population #2: t=20.82, df=9, p<0.0001) (spinosad: Population #1: t=6.736, df=9, p<0.0001; Population #2: t=6.708, df=9, p<0.0001).

Next, leveraging the results of our RNA-Seq experiment, we designed primers to amplify five genes that were upregulated in at least one resistant *D. suzukii* isogenic line (**Fig. 8B-F**). Specifically, we detected *cyp6a8*, *cyp4d14*, and *cyp6w1* to evaluate metabolic resistance (**Fig. 8B-D**) and *twdlG* and *twdlF* to evaluate penetration resistance (**Fig. 8E-F**). We observed that both populations show increased expression of *cyp6a8* (Population #1: t=6.084, df=4, p=0.0037; Population #2: t=3.780, df=4, p=0.0194; **Fig. 8B**), *cyp4d14* (Population #1: t=8.787, df=4, p=0.0009; Population #2: t=3.288, df=4, p=0.0303; **Fig. 8C**), and *cyp6w1* (Population #1: t=4.650, df=4, p=0.0097; Population #2: t=7.576, df=4, p=0.0016; **Fig. 8D**) as compared to the susceptible controls. More so, the expression of all 3 *cyp* genes was significantly higher in Population #1 as compared to the resistant isogenic lines developed from 2019 field-collected populations (**Fig. 8B**: Population #1: t=7.767, df=16, p<0.0001; Population #2: t=1.109, df=16, p=0.4872; **Fig. 8C**: Population #1: t=4.106, df=16, p=0.0033; Population #2: t=0.5145, df=16, p=0.6139; **Fig. 8D**: Population #1: t=6.117, df=16, p<0.0001; Population #2: t=0.2613, df=16, p=0.8949). In fact, the expression of *cyp6a8* was 17.3-fold higher in Population #1 as compared to the isogenic resistant line (**Fig. 8B**). Additionally, *cyp4d14* was 1.8-fold higher (**Fig. 8C**) while *cyp6w1* was 15.2-fold higher in Population #1 than in the resistant control (**Fig. 8D**).

We next assessed whether either of these lines exhibit penetration resistance by detecting cuticular genes *twdlG* (**Fig. 8E**) and *twdlF* **(Fig. 8F**). We observed a significant difference in expression of *twdlG* in only Population #1 (**Fig. 8E**: Population #1: t=2.870, df=4, p=0.0455; Population #2: t=1.595, df=4, p=0.1859) and no significant difference of *twdlF* in either of the 2022 populations (**Fig. 8F**: Population #1: t=2.235, df=4, p=0.0891; Population #2: t=1.787, df=4, p=0.1485). Finally, we also

detected *ecdysone receptor* (ecR) as a negative control (**Fig. 8G**) because it is not differentially expressed in any of the isogenic resistant lines (**Suppl. Tables 5-6, 14-15**). There was no significant difference in *ecR* in either of the 2022 populations compared to the susceptible controls (S3: t=0.8163, df=4, p=0.4602; G3: t=1.723, df=4, p=0.1601; Population #1: t=1.552, df=4, p=0.1957; Population #2: t=1.537, df=4, p=0.1992). Together, these results suggest that metabolic resistance confers insecticide resistance in these populations rather than penetration resistance. Additionally, it shows that this approach is a feasible and more efficient approach of monitoring potential insecticide resistance in field-collected samples as compared to performing bioassays to assess resistance.

Sequence analysis reveals no mutations in *paralytic* or *nAChRα7* that may contribute to insecticide resistance

To investigate whether mutations within the target protein of each insecticide confer resistance, we compared the RNA sequences between the resistant and susceptible populations of *D. suzukii* and assessed changes in allelic frequency (**Suppl. Fig. 3A-C**). Within the target gene of zeta-cypermethrin, the VGSC *para*, we identified a significant difference in allelic frequency in line S3 at base pair (bp) position 3658093, which is located within an intron in the gene body, and one difference in allelic frequency at bp position 3655811, which is located in an intron within the gene body, in line S4 (**Suppl. Fig. 3B-C**; 3658093: S3 p= 0.005171, S4 p=0.6199; 3655811: S3 p=0.4725, S4 p= 0.001131). Although we did not identify a mutation within the protein-coding region of *para*, we did observe that *para* is downregulated in zeta-cypermethrin-resistant SWD (**Fig. 2A-B**). Therefore, it is possible that reduced expression of the target protein, rather than a site-specific mutation, contributes to resistance in these flies.

We then analyzed the spinosad target protein *nAChRα7,* the *D. suzukii* homolog of *D. melanogaster nAChRα6* inferred by sequence similarity. We identified three bp positions within the 5’

untranslated region (UTR) that exhibit a significant change in allelic frequency in line C3 and no changes in line C4 (**Suppl. Fig. 3D-G**; 6579905: C3 p=0.0101, C4 p=0.06667; 6580106: C3 p=0.01515, C4 p=0.2424; 6580194: C3 p=0.04762, C4 p=1). Therefore, because we did not identify a mutation within the protein-coding region of the gene or any differential expression of *nAChRα7* (**Suppl. Table 14-15**) in the resistant lines, we suspect that target-site resistance is not an underlying mechanism for spinosad resistance in these lines. However, we cannot rule out that the allelic frequency changes we observed in the 5' UTR do not affect *NACHRα7* protein levels given that the 5'UTR is important for translation initiation [reviewed in (Leppek et al., 2018)].

Global changes in alternative splicing may confer insecticide resistance

Based on our RNA-Seq analyses, we observed that genes differentially expressed in the isogenic resistant lines are enriched in splicing pathways (**Fig. 2D, 3C, 4C and Suppl. Tables 8-9, 11-13, and 18**). Therefore, we hypothesized that the resistant isogenic lines may undergo differential splicing events. More so, it has been shown in other insect species that differential expression of various isoforms of *nAChRα6* confers insecticide resistance (Berger et al., 2016; Ureña et al., 2019). We leveraged PacBio long-read sequencing to examine whether the resistant isogenic lines exhibit changes in alternative splicing (AS) as compared to the susceptible isogenic lines developed from the same *D. suzukii* field-collected population from 2019 (**Fig. 9; Suppl. Table 22**). We characterized alternative splicing events into five categories: exon skipping (ES), exon inclusion (EI), intron retention (IR), and alternative splice sites (Alt. ss) (**Fig 9A**). In line S3, we identified a total of 307 AS events with 137 ES events, 113 EI events, 52 IR events, and 5 Alt. ss events (**Fig. 9B**). In total, 116 genes were differentially spliced in the S3 resistant line, with many of the genes experiencing differential expression of exons (**Fig. 9C**). Similarly, line S4 exhibited a total of 227 AS events (48 ES events, 90 EI events, 54 IR events, and 7 Alt. ss events; **Fig. 9D**) occurring in 73 genes with majority of these genes experiencing EI events (**Fig. 9E**). In the

spinosad-resistant isogenic lines, we observed 184 AS events (74 ES events, 28 EI events, 25 IR events, and 11 Alt. ss events) in line C3 (**Fig. 9F**) and 232 AS events (60 ES events, 73 EI events, 43 IR events, and 9 Alt. ss events) in line C4 (**Fig. 9H**). The majority of the AS events in line C3 are ES events while in line C4, ES and EI events are occurring at similar frequencies. These events occurred in a total of 57 genes in line C3 (**Fig. 9G**) and 90 genes in line C4 (**Fig. 9I**). Finally, 27 genes were differentially spliced exclusively in zeta-cypermethrin-resistant *D. suzukii*, 41 genes were differentially spliced exclusively in spinosad-resistant lines, and 2 genes (*Minerva* and *Gasz*) were differentially spliced in both zeta-cypermethrin- and spinosad-resistant *D. suzukii*.

To test the hypothesis that changes in AS can result in insecticide resistance, pairwise comparisons were performed between each of the 4 isogenic lines (**Fig. 9J-K; Suppl. Table 23**). We reason that if splicing is a mechanism of resistance, we should see a difference in how many genes are differentially spliced in the resistant to susceptible comparisons as opposed to the susceptible-to-susceptible comparisons. We observed that resistant line S4 has fewer differentially spliced genes when compared to susceptible line S8 ($p=0.0118$) but not susceptible line S7 ($p=0.6039$) (**Fig. 9K**). The number of differentially spliced genes in resistant line S3 did not differ from the susceptible lines (S3 vs S7 $p= 0.5133$; S3 vs S8 $p=0.334$). In the spinosad-resistant lines, the number of differentially spliced genes in lines C3 (C3 vs C2 $p=0.395$; C3 vs C5 $p=0.3485$) and C4 does not differ from the number of differentially spliced genes in the susceptible-to-susceptible comparison (C4 vs C2 $p=0.4369$; C4 v C5 $p=0.2855$) (**Fig 9K**). However, it is possible that the classes of genes that are differentially spliced have a greater effect on resistance than the total number of spliced genes. We performed functional enrichment analyses to determine whether the differentially spliced genes in the resistant lines are enriched in pathways different than the differentially spliced genes in the susceptible lines (**Tables 2-3; Suppl. Table 24**). In the zeta-cypermethrin susceptible lines (S7 and S8), pathways involving photoreceptor development and meiosis are enriched in the differentially spliced genes (**Table 2**). In resistant line S3, differentially spliced

genes are enriched in apoptosis and cell development (S3 vs S7) as well as muscle maintenance and cell signaling (S3 vs S8). Differentially spliced genes in resistant line S4 are in pathways involving DNA replication (S4 vs S7) and metabolism (S4 vs S7 and S8) as well as cell development and hypoxia (S4 vs S8). In the lines susceptible to spinosad (C2 and C5), the differentially spliced genes are in pathways involved in RNA degradation as well as amino acid and carbon metabolism (**Table 3**). In resistant line C3, differentially spliced genes are enriched in response to DDT, another type of insecticide (Beard, 2006) (C3 vs C2). Differentially spliced genes in resistant line C4 are in pathways involving response to DDT and melanosomes (C4 vs C2) as well as metabolism and germ cell development (C4 vs C5). Together, this suggests that different classes of genes are differentially spliced in the resistant lines as compared to the susceptible lines; this difference, rather than changes in the number of alternatively-spliced genes, may contribute to insecticide resistance.

Discussion

Insecticide resistance in the invasive agricultural pest *D. suzukii* has been detected in California over the past several years, but the molecular mechanisms driving these changes have yet to be identified (Ganjisaffar, Demkovich, et al., 2022; Ganjisaffar, Gress, et al., 2022; Gress & Zalom, 2019). Therefore, we developed isogenic lines from field-collected populations of *D. suzukii* resistant to either zeta-cypermethrin or spinosad to identify the molecular mechanisms underlying insecticide resistance. We sequenced the transcriptome of these lines and found evidence of metabolic resistance in zeta-cypermethrin-resistant *D. suzukii* while lines resistant to spinosad display evidence of penetration resistance and metabolic resistance (**Fig. 10A**). Specifically, we observed an upregulation of genes encoding metabolic detoxification enzymes in zeta-cypermethrin-resistant *D. suzukii*. Interestingly, we also observed decreased expression of the target gene *paralytic*. This does not constitute conventional

target-site resistance as resistant lines do not have a mutation in the target protein, but rather, an overall decrease in the target gene could in turn render the insecticide less effective.

In *D. suzukii* resistant to spinosad, on the other hand, we identified an upregulation of several genes expressed in the insect cuticle such as *tweedle* genes and *cuticle proteins* as well as an upregulation of metabolic genes. Finally, using long-read sequencing, we observed changes in AS between resistant and susceptible *D. suzukii*. Taken together, our findings provide evidence that the concerted effects of multiple molecular mechanisms confer insecticide resistance in *D. suzukii*.

We leveraged our findings to design molecular diagnostics that could identify insecticide resistance in the field. Thus far, insecticide resistance in *D. suzukii* has only been detected in California (Ganjisaffar, Demkovich, et al., 2022; Ganjisaffar, Gress, et al., 2022; Gress & Zalom, 2019). Therefore, our diagnostic can be used to monitor insecticide resistance development in California and in locations where resistance has yet to be detected. Utilizing a few differentially expressed genes we identified between the resistant and susceptible populations as diagnostics, such as *cytochrome P450* (*cyp*) and *tweedle* genes, we designed qPCR-based assays to monitor resistance development. A benefit to using molecular diagnostics to detect resistance as opposed to insecticide bioassays is that they require few individuals (as little as 5 flies) as input whereas bioassays require at least fifty flies. A similar molecular diagnostic detecting *cyp* expression to identify metabolic resistance has been previously developed and validated in mosquitoes (Mavridis et al., 2019). More so, beyond just validating our diagnostic, we observed significantly higher levels of *cyp* expression in a 2022 field-collected population (**Fig. 8**), suggesting that resistance has increased since the 2019 collection. This observation is consistent with the general trend of increased spinosad resistance in *D. suzukii* from 2018 to 2020 (Ganjisaffar, Gress, et al., 2022).

Our study also provides insights into the possibility of cross-resistance. Currently, in order to delay the development of resistance, there are restrictions on how many applications of a single type of

insecticide are permitted in a site (Tait et al., 2021). As a result, organic berry growers alternate usage between pyrethroids and spinosads (Farnsworth et al., 2017; Goodhue et al., 2011; Van Timmeren & Isaacs, 2013). Therefore, it is important to understand whether the mechanisms conferring resistance to one insecticide enables the insect to be resistant to other classes of insecticides as well. For instance, because the spinosad-resistant line C3 has increased expression of cuticular genes (**Fig. 5C**) suggesting a less penetrable cuticle, it is likely that the integument is less penetrable to other insecticides as well. Furthermore, zeta-cypermethrin-resistant *D. suzukii* and spinosad-resistant line C4 express high levels of many metabolic enzymes implicated in metabolic resistance (**Fig. 2C and 5C**). There are studies in house flies and onion thrips that attribute spinosad resistance to an upregulation in *cyp* expression (Højland et al., 2014; Rosen et al., 2021). Notably, our 2022 collections of *D. suzukii* exhibit resistance to both zeta-cypermethrin and spinosad and appear to be resistant through an upregulation of metabolic genes (**Fig. 8A**). Thus, our results suggest a high likelihood for cross-resistance. Additional experiments will need to be performed to assess for cross-resistance.

In addition to identifying penetration and metabolic resistance in insecticide-resistant *D. suzukii*, all of which have been previously studied in several other insect pest species [reviewed in (Siddiqui et al., 2023)], we hypothesize that changes in alternative splicing also confer insecticide resistance. Splicing is a biological process that produces proteins with diverse structures and functions encoded by a singular gene [reviewed in (Wright et al., 2022)]. Splicing has been shown to change in response to environmental stressors such as unfavorable temperatures [reviewed in (Shiina & Shimizu, 2020); thus, it is possible that regulation of alternative splicing could change in insect populations as an additional mechanism that enables for insecticide resistance. In fact, one study in spider mites demonstrated that an alternative isoform of a metabolic enzyme, the carboxyl/choline esterase gene *CCE04*, is associated with increased resistance to the pesticide, spirodiclofen (Wei et al., 2020). Furthermore, different isoforms of the spinosad target protein, nAChRα6, have been shown to confer insecticide resistance in

other insect species (Berger et al., 2016; Ureña et al., 2019). In line with these findings, we identified genes within the splicing pathway to be differentially expressed in the resistant lines (**Fig. 2D, 3C, 4C and Suppl. Tables 8-9, 11-13, and 18**)**.** Previously, it was difficult to measure the expression of each gene isoform using short-read transcriptome sequencing because one could not definitively identify which sequencing read belonged to which isoform. However, with the advent of long-read sequencing, it is now possible to determine the abundance of each gene isoform and more accurately assess alternative splicing. We leveraged long-read sequencing and identified global changes in alternative splicing between the resistant and susceptible populations (**Fig. 9 and Suppl. Table 22**). Overall, our observations support the notion that one way in which insects can be resistant is to produce various isoforms of genes that produce the resistant phenotype.

One drawback to long-read sequencing is the low sequencing depth as compared to short-read sequencing methods (Kanwar et al., 2021). As a result, we could not assess the expression of various isoforms of lowly expressed genes such as insecticide target proteins and other metabolic genes. However, our results suggest that changes in splicing patterns are not exclusive to genes involved in insecticide resistance. Rather, we hypothesize that it is a transcriptome-wide phenomenon in response to stressors, e.g. insecticide applications, from which one consequence is resistance. Supporting this, a study in cichlids proposed that alternative splicing may have played a role in producing diverse jaw structures between different species of cichlids as a form of adaptive evolution (Singh et al., 2017). Therefore, splicing is likely a mechanism by which organisms respond and adapt to environmental stress to promote survival.

However, it is unclear based on the data whether splicing is a cause or consequence of resistance. We reason that there are 3 possibilities in which changes in splicing are related to the resistance phenotype (**Fig. 10B**). First, changes in alternative splicing may enable for resistance mechanisms including penetration resistance, metabolic resistance, and target site resistance. It is

reasonable to assume that for this to be the case, all lines that share the same resistance mechanism will also display changes in alternative splicing. We see that all 4 resistance lines, which either show evidence of metabolic resistance or penetration resistance, show differences in splicing, providing evidence for the first possibility. The second possibility is that the changes in gene expression that enable for penetration resistance and/or metabolic resistance result in changes in spliceosome expression and/or function. For this scenario to be true, we would expect to see changes in the expression of spliceosome components. In line S3, we observe an enrichment of spliceosome factors amongst the upregulated genes (**Suppl. Table 8**). In both resistant lines S3 and S4, amongst the downregulated genes, there is an enrichment for the splicing selectivity pathway (**Suppl. Tables 8-9**), suggesting that global changes in splicing are occurring in these lines given that there is decreased regulation on splicing selectivity. This may be why there are more pathways enriched in the differentially spliced genes of the resistant lines than the pathways that are enriched the susceptible lines (**Table 2**). Thus, we cannot rule out the second scenario. In resistant line C4, we observed an enrichment of the spliceosome pathway amongst the downregulated genes (**Suppl. Table 18**), thus decreased expression of the spliceosome will result in differential expression or various gene isoforms. Interestingly though, we did not observe any spliceosome expression differences in resistant line C3 (**Suppl. Table 17**). Rather, only lines exhibiting evidence of metabolic resistance express differences in spliceosome expression. This may be why we see fewer changes in functional enrichment pathways in resistant line C3 as the pathways enriched in the susceptible lines (**Table 3**), providing further support for scenarios 1 and 2. It is also possible that these changes in spliceosome expression produce variants of *para* that are less stable, resulting in decreased expression of the *para* gene (**Fig. 2A-B**). Finally, the third possibility is that global changes in alternative splicing occur in response to environmental stress that, by chance, produces isoforms that enable for insecticide resistance. In this case, we would expect no correlation between the types of insecticide resistance mechanisms and changes in global alternative splicing. Therefore, this

study provides stronger support for 1) changes in splicing enable for metabolic and penetration resistance and 2) changes in splicing are an outcome of resistance mechanisms. Further experiments will need to be conducted to elucidate whether splicing is a cause or consequence of resistance.

Finally, we anticipate the ability to leverage our results to adjust current *D. suzukii* management practices. For instance, we identified an upregulation of metabolic enzymes in *D. suzukii* resistant to zeta-cypermethrin (**Fig. 2 and Fig. 5C**). Presumably, this upregulation will increase detoxification, rendering the insecticide less effective. To combat this effect, synergists can be applied in conjunction with insecticides. Synergists are metabolic enzyme inhibitors, so when used in conjunction with insecticides, they can increase their efficacy (Snoeck et al., 2017). An alternative approach would be for growers to adopt an integrated pest management (IPM) strategy to control *D. suzukii*. IPM promotes increased control of a pest by adopting a combination of different strategies including biological, cultural, and chemical control (Deguine et al., 2021). It is possible that alternating between the use of insecticides will alleviate the pressure driving insecticide resistance such that it is selected out of the population. Based on our data, it is likely that there is a high fitness cost associated with insecticide resistance. For example, in zeta-cypermethrin-resistant flies, we observed differential expression of many genes involved in neuronal system development and signaling (**Fig 2C**), suggesting that neuronal processing is affected, compromising a wide range of behaviors such as mating and feeding (Lenschow & Lima, 2020; Miroschnikow et al., 2020). In the case of spinosad-resistant flies, we observed that many of the downregulated genes are enriched with metabolic pathways, suggesting that spinosad-resistant flies have energy usage deficiencies. Therefore, it is possible that in the absence of selective pressure caused by spraying insecticides, in combination with the fast generation time of *D. suzukii* and their short lifespans (Tait et al., 2021), alternating between spray programs and other forms of control can be more effective at controlling *D. suzukii* infestations in the field. In fact, a previous study (Ganjisaffar, Gress, et al., 2022) has demonstrated that resistance increases throughout the growing season, likely due to

increased uses of insecticide application. Therefore, it is possible that a short-term halt in spraying of insecticides of a specific chemistry for a few generations would increase susceptibility again given the selective pressure is removed. Experiments are currently in progress to assess how long resistance persists in a population after spraying has ceased. Further, to combat penetration resistance, insecticides can be administered in bait traps as opposed to spraying such that the insecticide enters the flies through the digestive system rather than through the insect cuticle.

In conclusion, our study characterizes the mechanisms of insecticide resistance in *D. suzukii*. We provide evidence of metabolic and penetration resistance. Furthermore, we identified changes in alternative splicing as a possible mechanism of insecticide resistance. Finally, we developed and validated molecular diagnostics that can monitor resistance in field populations of *D. suzukii*. Finally, our study provides insights into the possibility of cross-resistance and generates information that can be used to improve *D. suzukii* management programs.

Acknowledgements

We thank all lab members of the Chiu laboratory for their feedback and suggestions. This project is supported by NIFA SCRI2020-51181-3214 and the CDFA Specialty Crop Block Grant 21SCBPCA1002 awarded to JCC.

Declaration of Interests

The authors declare no competing interests.

Data Availability Statement

Raw Illumina reads have been deposited to the NCBI Sequence Read Archive (SRA) and can be found under BioProject accession number PRJNA983428. Supplementary Tables S5-24 contain the lists of differentially expressed genes, the results of the functional enrichment analyses, WGCNA, and splice junction analyses have been uploaded to Dryad (https://doi.org/10.25338/B8PH17). All data discussed in the paper have been made available to readers.

References

Andreazza, F., Bernardi, D., Dos Santos, R. S. S., Garcia, F. R. M., Oliveira, E. E., Botton, M., & Nava, D. E. (2017). *Drosophila suzukii* in Southern Neotropical Region: Current Status and Future Perspectives. *Neotropical Entomology*, *46*(6), 591–605. https://doi.org/10.1007/s13744-017-0554-7

Asplen, M. K., Anfora, G., Biondi, A., Choi, D.-S., Chu, D., Daane, K. M., Gibert, P., Gutierrez, A. P., Hoelmer, K. A., Hutchison, W. D., Isaacs, R., Jiang, Z.-L., Kárpáti, Z., Kimura, M. T., Pascual, M., Philips, C. R., Plantamp, C., Ponti, L., Vétek, G., … Desneux, N. (2015). Invasion biology of spotted wing *Drosophila* (*Drosophila suzukii*): A global perspective and future priorities. *Journal of Pest Science*, *88*(3), 469–494. https://doi.org/10.1007/s10340-015-0681-z

Balabanidou, V., Grigoraki, L., & Vontas, J. (2018). Insect cuticle: A critical determinant of insecticide resistance. *Current Opinion in Insect Science*, *27*, 68–74. https://doi.org/10.1016/j.cois.2018.03.001

Beard, J. (2006). DDT and human health. *Science of The Total Environment*, *355*(1), 78–89. https://doi.org/10.1016/j.scitotenv.2005.02.022

Berger, M., Puinean, A. M., Randall, E., Zimmer, C. T., Silva, W. M., Bielza, P., Field, L. M., Hughes, D., Mellor, I., Hassani-Pak, K., Siqueira, H. A. A., Williamson, M. S., & Bass, C. (2016). Insecticide

resistance mediated by an exon skipping event. *Molecular Ecology*, *25*(22), 5692–5704. https://doi.org/10.1111/mec.13882

Bolda, M. P., Goodhue, R. E., & Zalom, F. G. (2010). Spotted Wing *Drosophila*: Potential Economic Impact of a Newly Established Pest. *Agricultural and Resource Economics Update*, *13*(3), 5–8.

Bolger, A. M., Lohse, M., & Usadel, B. (2014). Trimmomatic: A flexible trimmer for Illumina sequence data. *Bioinformatics*, *30*(15), 2114–2120. https://doi.org/10.1093/bioinformatics/btu170

Bruck, D. J., Bolda, M., Tanigoshi, L., Klick, J., Kleiber, J., DeFrancesco, J., Gerdeman, B., & Spitler, H. (2011). Laboratory and field comparisons of insecticides to reduce infestation of *Drosophila suzukii* in berry crops. *Pest Management Science*, *67*(11), 1375–1385. https://doi.org/10.1002/ps.2242

Chiu, J. C., Jiang, X., Zhao, L., Hamm, C. A., Cridland, J. M., Saelao, P., Hamby, K. A., Lee, E. K., Kwok, R. S., Zhang, G., Zalom, F. G., Walton, V. M., & Begun, D. J. (2013). Genome of *Drosophila suzukii*, the Spotted Wing *Drosophila*. *G3: Genes|Genomes|Genetics*, *3*(12), 2257–2271. https://doi.org/10.1534/g3.113.008185

Cini, A., Anfora, G., Escudero-Colomar, L. A., Grassi, A., Santosuosso, U., Seljak, G., & Papini, A. (2014). Tracking the invasion of the alien fruit pest *Drosophila suzukii* in Europe. *Journal of Pest Science*, *87*(4), 559–566. https://doi.org/10.1007/s10340-014-0617-z

Deguine, J.-P., Aubertot, J.-N., Flor, R. J., Lescourret, F., Wyckhuys, K. A. G., & Ratnadass, A. (2021). Integrated pest management: Good intentions, hard realities. A review. *Agronomy for Sustainable Development*, *41*(3), 38. https://doi.org/10.1007/s13593-021-00689-w

Deprá, M., Poppe, J. L., Schmitz, H. J., De Toni, D. C., & Valente, V. L. S. (2014). The first records of the invasive pest *Drosophila suzukii* in the South American continent. *Journal of Pest Science*, *87*(3), 379–383. https://doi.org/10.1007/s10340-014-0591-5

Diepenbrock, L. M., Rosensteel, D. O., Hardin, J. A., Sial, A. A., & Burrack, H. J. (2016). Season-long programs for control of *Drosophila suzukii* in southeastern U.S. blueberries. *Crop Protection*, *81*, 76–84. https://doi.org/10.1016/j.cropro.2015.12.012

Disi, J. O., & Sial, A. A. (2021). Laboratory Selection and Assessment of Resistance Risk in *Drosophila suzukii* (Diptera: Drosophilidae) to Spinosad and Malathion. *Insects*, *12*(9), 794. https://doi.org/10.3390/insects12090794

Dobin, A., Davis, C. A., Schlesinger, F., Drenkow, J., Zaleski, C., Jha, S., Batut, P., Chaisson, M., & Gingeras, T. R. (2013). STAR: Ultrafast universal RNA-seq aligner. *Bioinformatics*, *29*(1), 15–21. https://doi.org/10.1093/bioinformatics/bts635

Dong, K., Du, Y., Rinkevich, F., Nomura, Y., Xu, P., Wang, L., Silver, K., & Zhorov, B. S. (2014). Molecular biology of insect sodium channels and pyrethroid resistance. *Insect Biochemistry and Molecular Biology*, *50*, 1–17. https://doi.org/10.1016/j.ibmb.2014.03.012

Dorn, R., & Krauss, V. (2003). The *modifier of mdg4* locus in *Drosophila*: Functional complexity is resolved by trans splicing. *Genetica*, *117*(2–3), 165–177. https://doi.org/10.1023/a:1022983810016

dos Santos, G., Schroeder, A. J., Goodman, J. L., Strelets, V. B., Crosby, M. A., Thurmond, J., Emmert, D. B., & Gelbart, W. M. (2015). FlyBase: Introduction of the *Drosophila melanogaster* Release 6 reference genome assembly and large-scale migration of genome annotations. *Nucleic Acids Research*, *43*(Database issue), D690–D697. https://doi.org/10.1093/nar/gku1099

Farnsworth, D., Hamby, K. A., Bolda, M., Goodhue, R. E., Williams, J. C., & Zalom, F. G. (2017). Economic analysis of revenue losses and control costs associated with the spotted wing *Drosophila*, *Drosophila suzukii* (Matsumura), in the California raspberry industry. *Pest Management Science*, *73*(6), 1083–1090. https://doi.org/10.1002/ps.4497

Funakoshi, M., Tsuda, M., Muramatsu, K., Hatsuda, H., Morishita, S., & Aigaki, T. (2018). Overexpression of Larp4B downregulates dMyc and reduces cell and organ sizes in *Drosophila*. *Biochemical and Biophysical Research Communications*, *497*(2), 762–768. https://doi.org/10.1016/j.bbrc.2018.02.148

Ganjisaffar, F., Demkovich, M. R., Chiu, J. C., & Zalom, F. G. (2022). Characterization of Field-Derived *Drosophila suzukii* (Diptera: Drosophilidae) Resistance to Pyrethroids in California Berry Production. *Journal of Economic Entomology*, *115*(5), 1676–1684. https://doi.org/10.1093/jee/toac118

Ganjisaffar, F., Gress, B. E., Demkovich, M. R., Nicola, N. L., Chiu, J. C., & Zalom, F. G. (2022). Spatio-temporal Variation of Spinosad Susceptibility in *Drosophila suzukii* (Diptera: Drosophilidae), a Three-year Study in California's Monterey Bay Region. *Journal of Economic Entomology*, *115*(4), 972–980. https://doi.org/10.1093/jee/toac011

Garrison, E., & Marth, G. (2012). *Haplotype-based variant detection from short-read sequencing* (arXiv:1207.3907). arXiv. https://doi.org/10.48550/arXiv.1207.3907

Gaudet, P., Livstone, M. S., Lewis, S. E., & Thomas, P. D. (2011). Phylogenetic-based propagation of functional annotations within the Gene Ontology consortium. *Briefings in Bioinformatics*, *12*(5), 449–462. https://doi.org/10.1093/bib/bbr042

Ge, S. X., Jung, D., & Yao, R. (2020). ShinyGO: A graphical gene-set enrichment tool for animals and plants. *Bioinformatics*, *36*(8), 2628–2629. https://doi.org/10.1093/bioinformatics/btz931

Goodhue, R. E., Bolda, M., Farnsworth, D., Williams, J. C., & Zalom, F. G. (2011). Spotted wing *Drosophila* infestation of California strawberries and raspberries: Economic analysis of potential revenue losses and control costs. *Pest Management Science*, *67*(11), 1396–1402. https://doi.org/10.1002/ps.2259

Grauso, M., Reenan, R. A., Culetto, E., & Sattelle, D. B. (2002). Novel putative nicotinic acetylcholine receptor subunit genes, *Dα5*, *Dα6* and *Dα7*, in *Drosophila melanogaster* identify a new and highly conserved target of adenosine deaminase acting on RNA-mediated A-to-I pre-mRNA editing. *Genetics*, *160*(4), 1519–1533.

Gress, B. E., & Zalom, F. G. (2019). Identification and risk assessment of spinosad resistance in a California population of *Drosophila suzukii*. *Pest Management Science*, *75*(5), 1270–1276. https://doi.org/10.1002/ps.5240

Hamby, K. A., Kwok, R. S., Zalom, F. G., & Chiu, J. C. (2013). Integrating Circadian Activity and Gene Expression Profiles to Predict Chronotoxicity of *Drosophila suzukii* Response to Insecticides. *PLOS ONE*, *8*(7), e68472. https://doi.org/10.1371/journal.pone.0068472

Hartley, S. W., & Mullikin, J. C. (2015). QoRTs: A comprehensive toolset for quality control and data processing of RNA-Seq experiments. *BMC Bioinformatics*, *16*(1), 224. https://doi.org/10.1186/s12859-015-0670-5

Hartley, S. W., & Mullikin, J. C. (2016). Detection and visualization of differential splicing in RNA-Seq data with JunctionSeq. *Nucleic Acids Research*, *44*(15), e127. https://doi.org/10.1093/nar/gkw501

Hassani, I. M., Behrman, E. L., Prigent, S. R., Gidaszewski, N., Ravaomanarivo, L. H. R., Suwalski, A., Debat, V., David, J. R., & Yassin, A. (2020). First occurrence of the pest *Drosophila suzukii* (Diptera: Drosophilidae) in the Comoros Archipelago (Western Indian Ocean). *African Entomology*, *28*(1), 78–83. https://doi.org/10.4001/003.028.0078

Hauser, M. (2011). A historic account of the invasion of *Drosophila suzukii* (Matsumura) (Diptera: Drosophilidae) in the continental United States, with remarks on their identification. *Pest Management Science*, *67*(11), 1352–1357. https://doi.org/10.1002/ps.2265

Højland, D. H., Jensen, K.-M. V., & Kristensen, M. (2014). Expression of xenobiotic metabolizing cytochrome P450 genes in a spinosad-resistant *Musca domestica* L. strain. *PloS One*, *9*(8), e103689. https://doi.org/10.1371/journal.pone.0103689

Jünger, M. A., Rintelen, F., Stocker, H., Wasserman, J. D., Végh, M., Radimerski, T., Greenberg, M. E., & Hafen, E. (2003). The *Drosophila* Forkhead transcription factor FOXO mediates the reduction in cell number associated with reduced insulin signaling. *Journal of Biology*, *2*(3), 20. https://doi.org/10.1186/1475-4924-2-20

Kanwar, N., Blanco, C., Chen, I. A., & Seelig, B. (2021). PacBio sequencing output increased through uniform and directional fivefold concatenation. *Scientific Reports*, *11*(1), Article 1. https://doi.org/10.1038/s41598-021-96829-z

Knight, A. L., Basoalto, E., Yee, W., Hilton, R., & Kurtzman, C. P. (2016). Adding yeasts with sugar to increase the number of effective insecticide classes to manage *Drosophila suzukii* (Matsumura) (Diptera: Drosophilidae) in cherry. *Pest Management Science*, *72*(8), 1482–1490. https://doi.org/10.1002/ps.4171

Kopylova, E., Noé, L., & Touzet, H. (2012). SortMeRNA: Fast and accurate filtering of ribosomal RNAs in metatranscriptomic data. *Bioinformatics*, *28*(24), 3211–3217. https://doi.org/10.1093/bioinformatics/bts611

Langfelder, P., & Horvath, S. (2008). WGCNA: An R package for weighted correlation network analysis. *BMC Bioinformatics*, *9*(1), 559. https://doi.org/10.1186/1471-2105-9-559

Lee, S.-J., Feldman, R., & O'Farrell, P. H. (2008). An RNA Interference Screen Identifies a Novel Regulator of Target of Rapamycin That Mediates Hypoxia Suppression of Translation in *Drosophila* S2 Cells. *Molecular Biology of the Cell*, *19*(10), 4051–4061. https://doi.org/10.1091/mbc.e08-03-0265

Lenschow, C., & Lima, S. Q. (2020). In the mood for sex: Neural circuits for reproduction. *Current Opinion in Neurobiology*, *60*, 155–168. https://doi.org/10.1016/j.conb.2019.12.001

Leppek, K., Das, R., & Barna, M. (2018). Functional 5′ UTR mRNA structures in eukaryotic translation regulation and how to find them. *Nature Reviews Molecular Cell Biology*, *19*(3), Article 3. https://doi.org/10.1038/nrm.2017.103

Li, H. (2018). Minimap2: Pairwise alignment for nucleotide sequences. *Bioinformatics*, *34*(18), 3094–3100. https://doi.org/10.1093/bioinformatics/bty191

Li, X., Schuler, M. A., & Berenbaum, M. R. (2007). Molecular Mechanisms of Metabolic Resistance to Synthetic and Natural Xenobiotics. *Annual Review of Entomology*, *52*(1), 231–253. https://doi.org/10.1146/annurev.ento.51.110104.151104

Liu, N., Li, M., Gong, Y., Liu, F., & Li, T. (2015). Cytochrome P450s – Their expression, regulation, and role in insecticide resistance. *Pesticide Biochemistry and Physiology*, *120*, 77–81. https://doi.org/10.1016/j.pestbp.2015.01.006

Livak, K. J., & Schmittgen, T. D. (2001). Analysis of Relative Gene Expression Data Using Real-Time Quantitative PCR and the $2^{-\Delta\Delta CT}$ Method. *Methods*, *25*(4), 402–408. https://doi.org/10.1006/meth.2001.1262

Llorens-Giralt, P., Camilleri-Robles, C., Corominas, M., & Climent-Cantó, P. (2021). Chromatin Organization and Function in *Drosophila*. *Cells*, *10*(9), 2362. https://doi.org/10.3390/cells10092362

Love, M. I., Huber, W., & Anders, S. (2014). Moderated estimation of fold change and dispersion for RNA-seq data with DESeq2. *Genome Biology*, *15*(12), 550. https://doi.org/10.1186/s13059-014-0550-8

Lund, A. E., & Narahashi, T. (1982). Dose-dependent interaction of the pyrethroid isomers with sodium channels of squid axon membranes. *Neurotoxicology*, *3*(1), 11–24.

Mavridis, K., Wipf, N., Medves, S., Erquiaga, I., Müller, P., & Vontas, J. (2019). Rapid multiplex gene expression assays for monitoring metabolic resistance in the major malaria vector *Anopheles gambiae*. *Parasites & Vectors*, *12*(1), 9. https://doi.org/10.1186/s13071-018-3253-2

Miroschnikow, A., Schlegel, P., & Pankratz, M. J. (2020). Making Feeding Decisions in the *Drosophila* Nervous System. *Current Biology*, *30*(14), R831–R840. https://doi.org/10.1016/j.cub.2020.06.036

Montella, I. R., Schama, R., & Valle, D. (2012). The classification of esterases: An important gene family involved in insecticide resistance - A review. *Memórias Do Instituto Oswaldo Cruz*, *107*, 437–449. https://doi.org/10.1590/S0074-02762012000400001

Paris, M., Boyer, R., Jaenichen, R., Wolf, J., Karageorgi, M., Green, J., Cagnon, M., Parinello, H., Estoup, A., Gautier, M., Gompel, N., & Prud'homme, B. (2020). Near-chromosome level genome assembly of the fruit pest *Drosophila suzukii* using long-read sequencing. *Scientific Reports*, *10*(1), Article 1. https://doi.org/10.1038/s41598-020-67373-z

Pavlidi, N., Vontas, J., & Van Leeuwen, T. (2018). The role of glutathione S-transferases (GSTs) in insecticide resistance in crop pests and disease vectors. *Current Opinion in Insect Science*, *27*, 97–102. https://doi.org/10.1016/j.cois.2018.04.007

Pertea, M., Pertea, G. M., Antonescu, C. M., Chang, T.-C., Mendell, J. T., & Salzberg, S. L. (2015). StringTie enables improved reconstruction of a transcriptome from RNA-seq reads. *Nature Biotechnology*, *33*(3), 290–295. https://doi.org/10.1038/nbt.3122

Ponton, F., Chapuis, M.-P., Pernice, M., Sword, G. A., & Simpson, S. J. (2011). Evaluation of potential reference genes for reverse transcription-qPCR studies of physiological responses in *Drosophila melanogaster*. *Journal of Insect Physiology*, *57*(6), 840–850. https://doi.org/10.1016/j.jinsphys.2011.03.014

R Core Team. (2022). R: A Language and Environment for Statistical Computing. R Foundation for Statistical Computing. https://www.R-project.org/

Ritz, C., Baty, F., Streibig, J. C., & Gerhard, D. (2015). Dose-Response Analysis Using R. *PLOS ONE*, *10*(12), e0146021. https://doi.org/10.1371/journal.pone.0146021

Rosen, R., Lebedev, G., Kontsedalov, S., Ben-Yakir, D., & Ghanim, M. (2021). A De Novo Transcriptomics Approach Reveals Genes Involved in *Thrips Tabaci* Resistance to Spinosad. *Insects*, *12*(1), Article 1. https://doi.org/10.3390/insects12010067

Rota-Stabelli, O., Ometto, L., Tait, G., Ghirotto, S., Kaur, R., Drago, F., González, J., Walton, V. M., Anfora, G., & Rossi-Stacconi, M. V. (2020). Distinct genotypes and phenotypes in European and American strains of *Drosophila suzukii*: Implications for biology and management of an invasive organism. *Journal of Pest Science*, *93*(1), 77–89. https://doi.org/10.1007/s10340-019-01172-y

Salgado, V. L. (1998). Studies on the Mode of Action of Spinosad: Insect Symptoms and Physiological Correlates. *Pesticide Biochemistry and Physiology*, *60*(2), 91–102. https://doi.org/10.1006/pest.1998.2332

Salgado, V. L., Sheets, J. J., Watson, G. B., & Schmidt, A. L. (1998). Studies on the Mode of Action of Spinosad: The Internal Effective Concentration and the Concentration Dependence of Neural Excitation. *Pesticide Biochemistry and Physiology*, *60*(2), 103–110. https://doi.org/10.1006/pest.1998.2333

Schotta, G., Lachner, M., Sarma, K., Ebert, A., Sengupta, R., Reuter, G., Reinberg, D., & Jenuwein, T. (2004). A silencing pathway to induce H3-K9 and H4-K20 trimethylation at constitutive heterochromatin. *Genes & Development*, *18*(11), 1251–1262. https://doi.org/10.1101/gad.300704

Shiina, T., & Shimizu, Y. (2020). Temperature-Dependent Alternative Splicing of Precursor mRNAs and Its Biological Significance: A Review Focused on Post-Transcriptional Regulation of a Cold Shock

Protein Gene in Hibernating Mammals. *International Journal of Molecular Sciences*, *21*(20), 7599. https://doi.org/10.3390/ijms21207599

Siddiqui, J. A., Fan, R., Naz, H., Bamisile, B. S., Hafeez, M., Ghani, M. I., Wei, Y., Xu, Y., & Chen, X. (2023). Insights into insecticide-resistance mechanisms in invasive species: Challenges and control strategies. *Frontiers in Physiology*, *13*. https://www.frontiersin.org/articles/10.3389/fphys.2022.1112278

Silva, A. X., Jander, G., Samaniego, H., Ramsey, J. S., & Figueroa, C. C. (2012). Insecticide Resistance Mechanisms in the Green Peach Aphid *Myzus persicae* (Hemiptera: Aphididae) I: A Transcriptomic Survey. *PLOS ONE*, *7*(6), e36366. https://doi.org/10.1371/journal.pone.0036366

Singh, P., Börger, C., More, H., & Sturmbauer, C. (2017). The Role of Alternative Splicing and Differential Gene Expression in Cichlid Adaptive Radiation. *Genome Biology and Evolution*, *9*(10), 2764–2781. https://doi.org/10.1093/gbe/evx204

Snoeck, S., Greenhalgh, R., Tirry, L., Clark, R. M., Van Leeuwen, T., & Dermauw, W. (2017). The effect of insecticide synergist treatment on genome-wide gene expression in a polyphagous pest. *Scientific Reports*, *7*(1), 13440. https://doi.org/10.1038/s41598-017-13397-x

Tait, G., Mermer, S., Stockton, D., Lee, J., Avosani, S., Abrieux, A., Anfora, G., Beers, E., Biondi, A., Burrack, H., Cha, D., Chiu, J. C., Choi, M.-Y., Cloonan, K., Crava, C. M., Daane, K. M., Dalton, D. T., Diepenbrock, L., Fanning, P., … Walton, V. M. (2021). *Drosophila suzukii* (Diptera: Drosophilidae): A Decade of Research Towards a Sustainable Integrated Pest Management Program. *Journal of Economic Entomology*, *114*(5), 1950–1974. https://doi.org/10.1093/jee/toab158

Tardaguila, M., de la Fuente, L., Marti, C., Pereira, C., Pardo-Palacios, F. J., del Risco, H., Ferrell, M., Mellado, M., Macchietto, M., Verheggen, K., Edelmann, M., Ezkurdia, I., Vazquez, J., Tress, M., Mortazavi, A., Martens, L., Rodriguez-Navarro, S., Moreno-Manzano, V., & Conesa, A. (2018). SQANTI: Extensive characterization of long-read transcript sequences for quality control in full-

length transcriptome identification and quantification. *Genome Research*, *28*(3), 396–411. https://doi.org/10.1101/gr.222976.117

Ureña, E., Guillem-Amat, A., Couso-Ferrer, F., Beroiz, B., Perera, N., López-Errasquín, E., Castañera, P., Ortego, F., & Hernández-Crespo, P. (2019). Multiple mutations in the nicotinic acetylcholine receptor *Cc*α*6* gene associated with resistance to spinosad in medfly. *Scientific Reports*, *9*(1), Article 1. https://doi.org/10.1038/s41598-019-38681-w

Van Timmeren, S., & Isaacs, R. (2013). Control of spotted wing *Drosophila*, *Drosophila suzukii*, by specific insecticides and by conventional and organic crop protection programs. *Crop Protection*, *54*, 126–133. https://doi.org/10.1016/j.cropro.2013.08.003

Van Timmeren, S., Mota-Sanchez, D., Wise, J. C., & Isaacs, R. (2018). Baseline susceptibility of spotted wing *Drosophila* (*Drosophila suzukii*) to four key insecticide classes. *Pest Management Science*, *74*(1), 78–87. https://doi.org/10.1002/ps.4702

Van Timmeren, S., Sial, A. A., Lanka, S. K., Spaulding, N. R., & Isaacs, R. (2019). Development of a rapid assessment method for detecting insecticide resistance in spotted wing *Drosophila* (*Drosophila suzukii* Matsumura). *Pest Management Science*, *75*(7), 1782–1793. https://doi.org/10.1002/ps.5341

Walsh, D. B., Bolda, M. P., Goodhue, R. E., Dreves, A. J., Lee, J., Bruck, D. J., Walton, V. M., O'Neal, S. D., & Zalom, F. G. (2011). *Drosophila suzukii* (Diptera: Drosophilidae): Invasive Pest of Ripening Soft Fruit Expanding its Geographic Range and Damage Potential. *Journal of Integrated Pest Management*, *2*(1), G1–G7. https://doi.org/10.1603/IPM10010

Walton, V. M., Burrack, H. J., Dalton, D. T., Isaacs, R., Wiman, N., & Ioriatti, C. (2016). Past, present and future of *Drosophila suzukii:* distribution, impact and management in United States berry fruits. *Acta Horticulturae*, *1117*, 87–94. https://doi.org/10.17660/ActaHortic.2016.1117.16

Wei, P., Demaeght, P., De Schutter, K., Grigoraki, L., Labropoulou, V., Riga, M., Vontas, J., Nauen, R., Dermauw, W., & Van Leeuwen, T. (2020). Overexpression of an alternative allele of carboxyl/choline esterase 4 (CCE04) of *Tetranychus urticae* is associated with high levels of resistance to the keto-enol acaricide spirodiclofen. *Pest Management Science*, *76*(3), 1142–1153. https://doi.org/10.1002/ps.5627

Willis, J. H. (2010). Structural cuticular proteins from arthropods: Annotation, nomenclature, and sequence characteristics in the genomics era. *Insect Biochemistry and Molecular Biology*, *40*(3), 189–204. https://doi.org/10.1016/j.ibmb.2010.02.001

Wright, C. J., Smith, C. W. J., & Jiggins, C. D. (2022). Alternative splicing as a source of phenotypic diversity. *Nature Reviews Genetics*, *23*(11), Article 11. https://doi.org/10.1038/s41576-022-00514-4

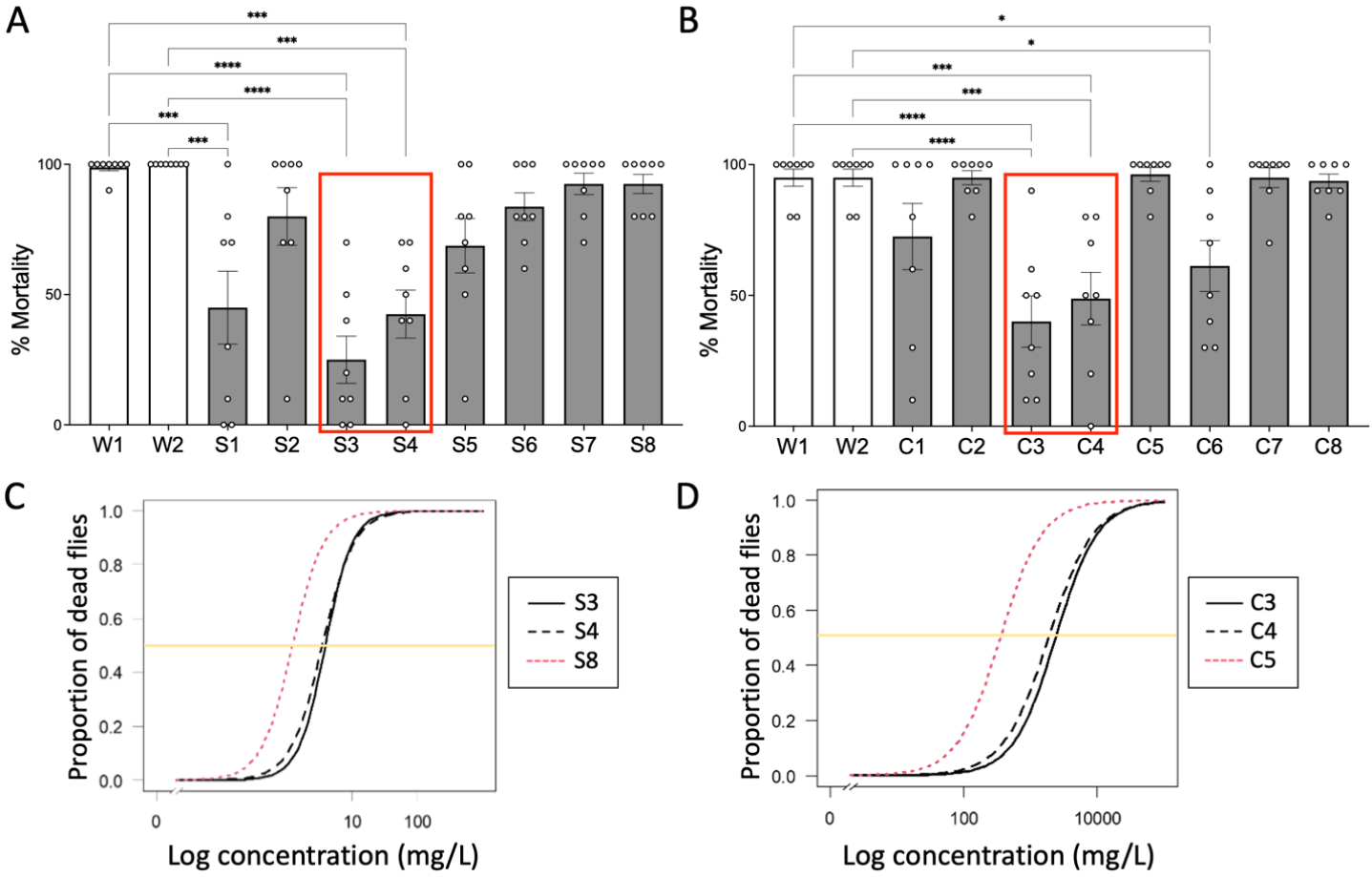

Fig. 1: Identification of insecticide-resistant isogenic *Drosophila suzukii* lines. (A-B) Bioassays to identify isogenic lines resistant to (A) zeta-cypermethrin (Mustang® Maxx) or (B) spinosad (Entrust). Eight isogenic lines were tested (indicated as S# and C#). Two isogenic lines from an untreated orchard (Wolfskill, W#) served as the susceptible control. Each point represents a biological replicate of 5 males and 5 females (n=8), and error bars indicate ± SEM. Resistant lines used for subsequent experiments are indicated by the red box. Asterisks denote significant p-values as determined by one-way ANOVA followed by Tukey's multiple comparison test: * $p<0.05$, *** $p<0.001$, and **** $p<0.0001$. Non-significant comparisons are omitted. (C) Dose-response relationship between zeta-cypermethrin-resistant isogenic lines (S3 and S4, black) vs a susceptible sibling line (S8, red) (n=8 biological replicates of 5 males and 5 females). (D) Dose-response relationship between spinosad-resistant isogenic lines (C3

and C4, black) vs a susceptible sibling line (C5, red) (n=8). The lethal concentration required to kill 50% of the population (LC_{50}) is indicated by the yellow line.

Table 1: Susceptibility of *Drosophila suzukii* isogenic lines to zeta-cypermethrin and spinosad

Insecticide	Isogenic line	LC_{50} (mg/L) ± SE
Zeta-cypermethrin	S3	3.9 ± 0.2
	S4	3.5 ± 0.2
	S8	1.2 ± 0.1
Spinosad	C3	2378.5 ± 210.8
	C4	1868.7 ± 177.2
	C5	351.8 ± 35.0

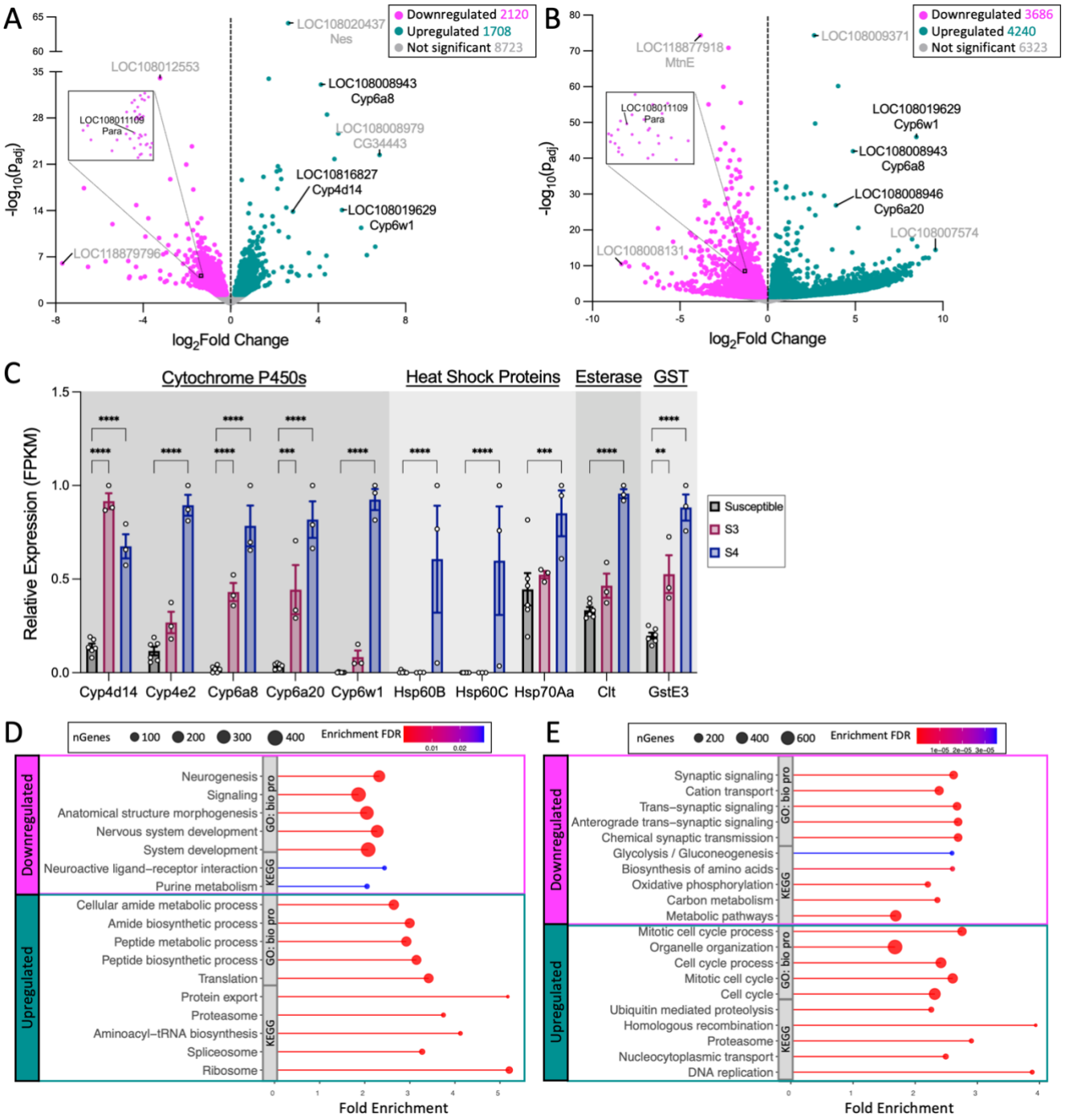

Fig. 2: Zeta-cypermethrin-resistant lines exhibit increased expression of genes involved in metabolic resistance. (A) Volcano plot of genes displaying fold change gene expression differences between the resistant S3 line vs 2 susceptible lines (S7 and S8). Genes upregulated in the resistant populations (green) are to the right of the dotted line while genes downregulated in the resistant populations (pink) lie to the left of the dotted line. Genes that exhibit no significant difference (NS) in expression between

the two populations are in grey. Highly significant differences are located higher up on the y-axis (where p_{adj} is the adjusted p-value corrected with Benjamin-Hochberg). Labeled points signify genes that satisfy at least one of the following criteria: (1) have the largest fold change difference between the two groups, (2) have the lowest p_{adj}, and (3) are genes known to be involved in insecticide resistance. Labels contain the *D. suzukii* gene symbol (LOC#########) and the corresponding *D. melanogaster* gene symbol homolog. Genes known to be involved in conferring resistance are labeled in black while genes in grey are not known to be directly involved in conferring resistance. The black box denotes the region containing *para*, zoomed-in in the insert. (B) Volcano plot of genes displaying fold change gene expression differences between the resistant S4 line vs 2 susceptible lines (S7 and S8). (C) Relative expression (FPKM) of *cytochrome P450* genes (*Cyp*), *heat shock proteins* (*Hsp*), the carboxylesterase *Cricklet* (*Clt*), and *glutathione-s-transferase E3* (*GstE3*) in the susceptible (S7 and S8: black) vs resistant (S3: magenta; S4: blue) groups. Each point denotes a biological replicate (n=3 replicates of 8-10 females per line). Asterisks denote significant p-values as determined by 2-way ANOVA: ** p<0.01, ***p<0.001, and **** p<0.0001. (D-E) Top 5 enrichment pathways within the Kyoto Encyclopedia of Genes and Genomes (KEGG) and Gene Ontology (GO) Biological Processes (bio proc) categories for genes up- or down-regulated in line (D) S3 and (E) S4. The x-axis is Fold Enrichment, which is defined as the percentage of differentially expressed genes that belong to each pathway. Point size represents the number of genes (nGenes) within the category while color denotes the false discovery rate (FDR) correction of enrichment p-values.

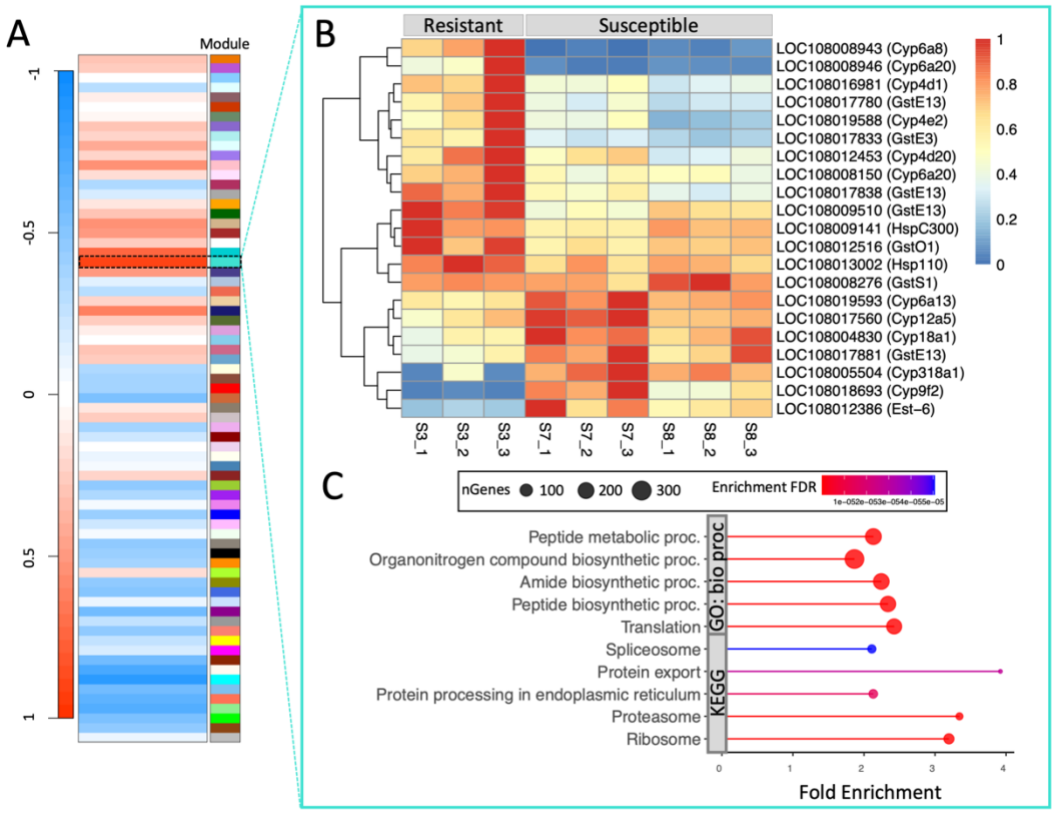

Fig. 3: Genes involved in metabolic resistance are highly correlated with zeta-cypermethrin resistance in *Drosophila suzukii* line S3. (A) Heat map of gene clusters determined by Weighted Gene Correlation Network Analysis (WGCNA). Modules that are positively correlated with resistance are red while those that are negatively correlated are blue. (B) Heat map showing the expression of metabolic genes (in FPKM) within the turquoise module. Labels contain the *D. suzukii* gene symbol (LOC#########) and the corresponding *D. melanogaster* gene symbol. Red indicates high expression while blue indicates low expression. Line S3 is resistant while lines S7 and S8 are susceptible. The number following the underscore indicates different biological replicates. (C) Top 5 enrichment pathways within the Kyoto Encyclopedia of Genes and Genomes (KEGG) and Gene Ontology (GO) Biological Processes (bio proc) categories for genes within the turquoise module. The x-axis is Fold Enrichment, which is defined as the percentage of differentially expressed genes that belong to each pathway. Point size represents the

number of genes (nGenes) within the category while color denotes the false discovery rate (FDR) correction of enrichment p-values.

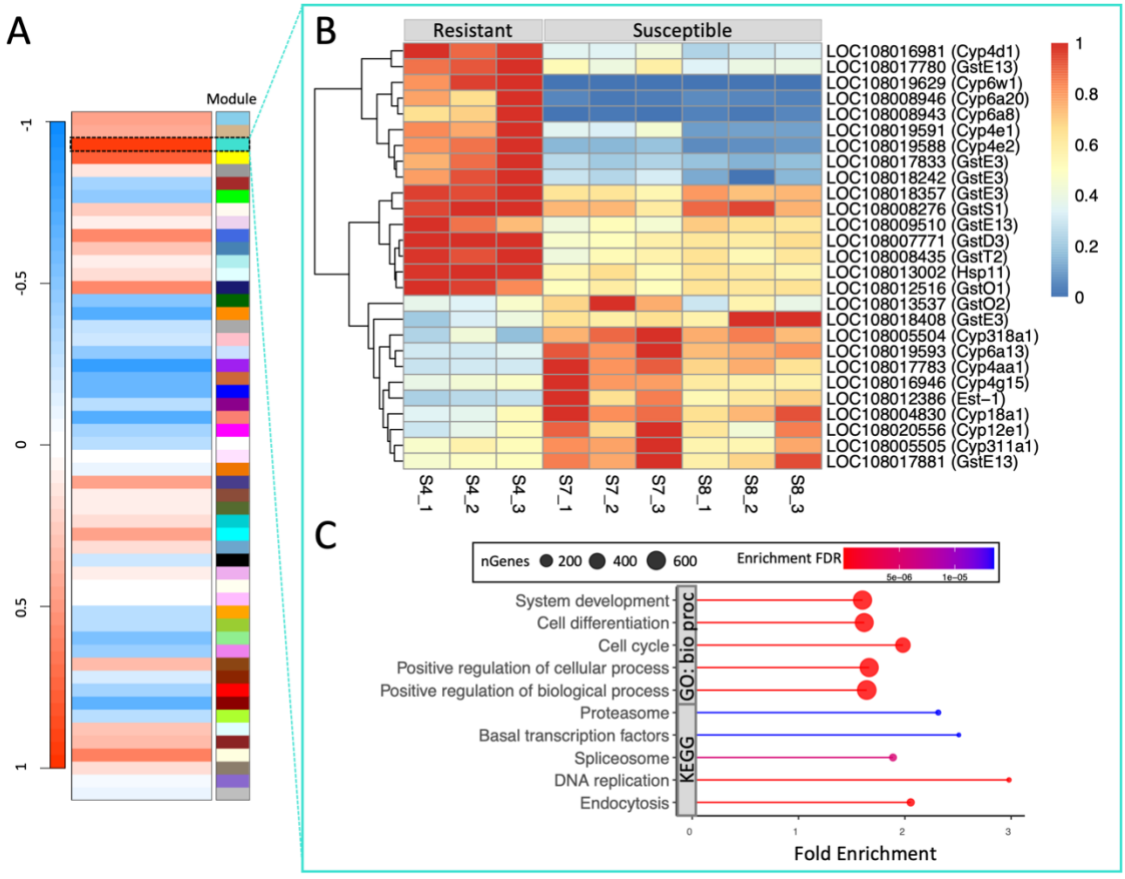

Fig. 4: Genes involved in metabolic resistance are highly correlated with zeta-cypermethrin resistance in *Drosophila suzukii* line S4. (A) Heat map of gene clusters determined by Weighted Gene Correlation Network Analysis (WGCNA). Modules that are positively correlated with resistance are red while those that are negatively correlated are blue. (B) Heat map showing the expression of metabolic genes (in FPKM) within the turquoise module. Labels contain the *D. suzukii* gene symbol (LOC#########) and the corresponding *D. melanogaster* gene symbol. Red indicates high expression while blue indicates low expression. Line S4 is resistant while lines S7 and S8 are susceptible. The number following the underscore indicates different biological replicates. (C) Top 5 enrichment pathways within the Kyoto Encyclopedia of Genes and Genomes (KEGG) and Gene Ontology (GO) Biological Processes (bio proc) categories for genes within the turquoise module. The x-axis is Fold Enrichment, which is defined as the

percentage of differentially expressed genes that belong to each pathway. Point size represents the number of genes (nGenes) within the category while color denotes the false discovery rate (FDR) correction of enrichment p-values.

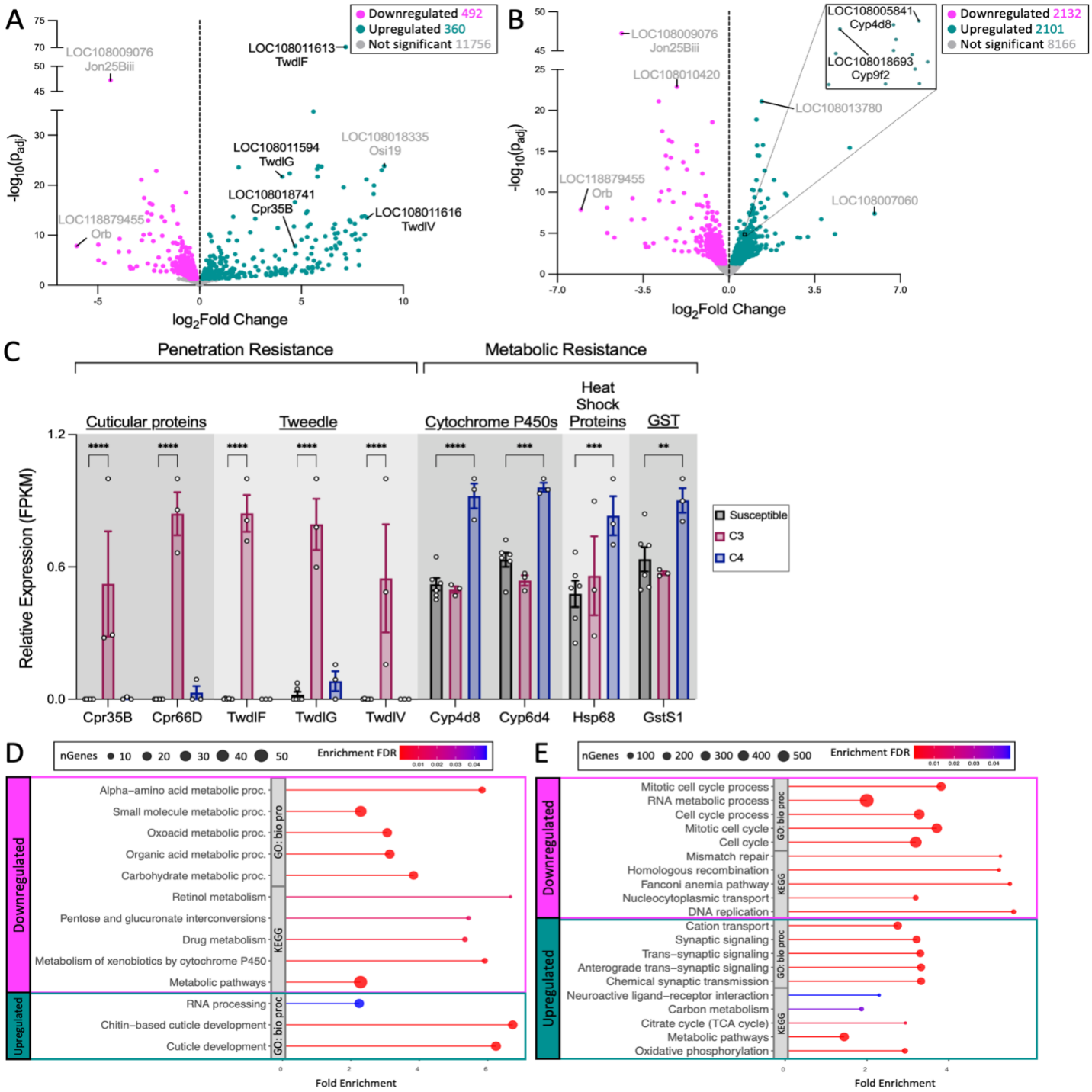

Fig. 5: Spinosad-resistant lines exhibit either increased expression of genes associated with penetration resistance or metabolic resistance. (A) Volcano plot of genes displaying fold change gene expression differences between the resistant C3 line vs 2 susceptible lines (C2 and C5). Genes upregulated in the resistant populations (green) are to the right of the dotted line while genes

downregulated in the resistant populations (pink) lie to the left of the dotted line. Genes that exhibit no significant difference (NS) in gene expression between the two populations are in grey. Highly significant differences are located higher up on the y-axis where p_{adj} is the adjusted p-value corrected with Benjamin-Hochberg. Labelled points signify genes that satisfy at least one of the following criteria: (1) have the largest fold change difference between the two groups, (2) have the lowest p_{adj}, and (3) are genes known to be involved in insecticide resistance. Labels contain the *D. suzukii* gene symbol (LOC#########) and the corresponding *D. melanogaster* gene symbol. Genes known to be involved in conferring resistance are labeled in black while genes labeled in grey are not known to be directly involved in conferring resistance. (B) Volcano plot of genes displaying fold change gene expression differences between the resistant C4 line vs 2 susceptible lines (C2 and C5). The black box denotes the region zoomed-in in the insert. (C) Relative expression (FPKM) of metabolic and cuticular genes (*twdl*: *tweedle*; *cpr*: *cuticular protein*) in the susceptible (C2 and C5: black) and resistant (C3: magenta; C4: blue) groups. Each point denotes a biological replicate (n=3 replicates of 8-10 females per line). Asterisks denote significant p-values as determined by 2-way ANOVA: **p<0.01, ***p<0.001, and ****p<0.0001. (D-E) Top 5 enrichment pathways within the Kyoto Encyclopedia of Genes and Genomes (KEGG) and Gene Ontology (GO) Biological Processes (bio proc) categories for genes up- or down-regulated in lines (D) C3 and (E) C4. The x-axis is Fold Enrichment, which is defined as the percentage of differentially expressed genes that belong to each pathway. Point size represents the number of genes (nGenes) within the category while color denotes the false discovery rate (FDR) correction of enrichment p-values.

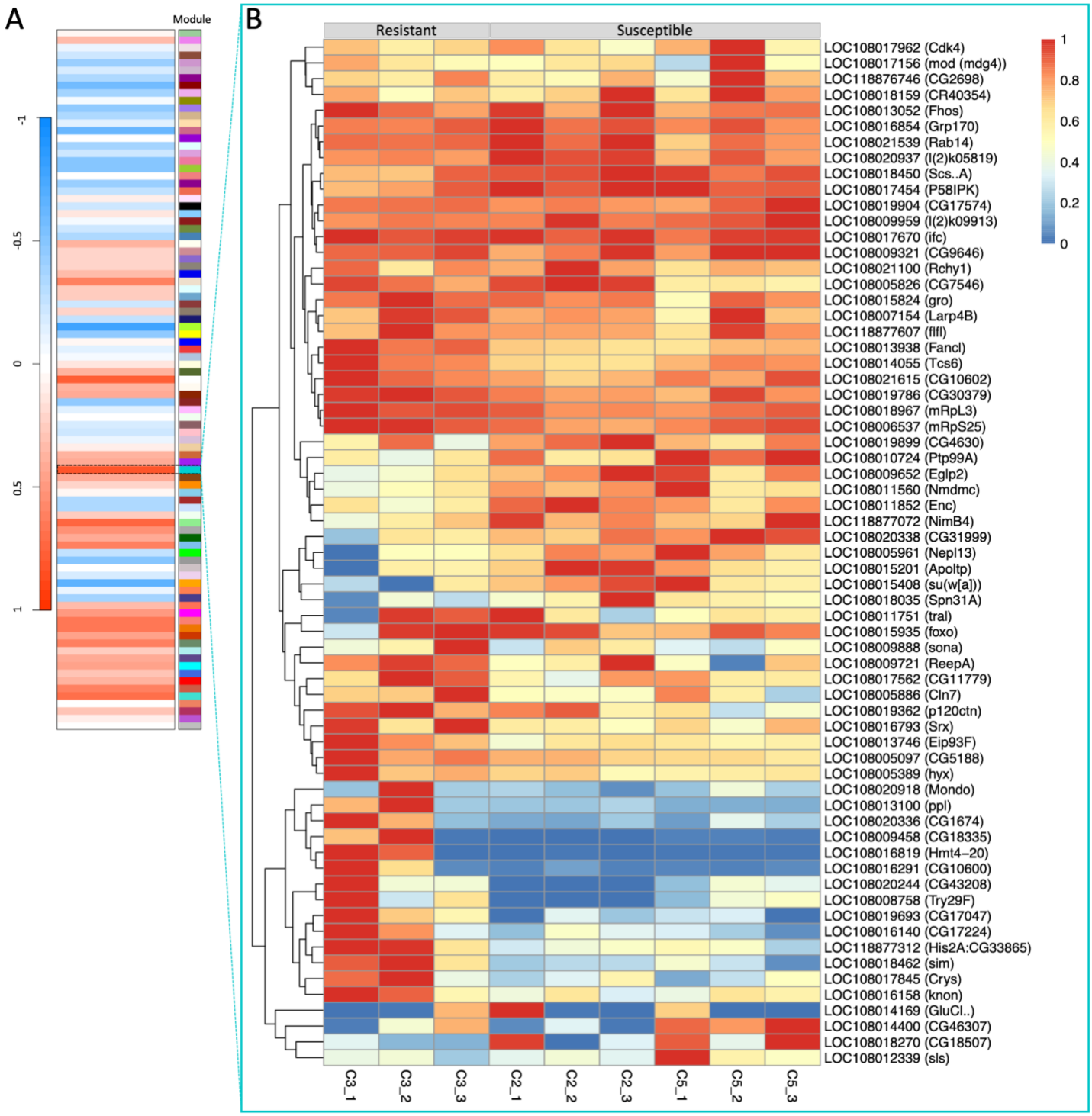

Fig. 6: Genes highly correlated with spinosad resistance in *Drosophila suzukii* line C3. (A) Heat map of gene clusters determined by Weighted Gene Correlation Network Analysis (WGCNA). Modules that are positively correlated with resistance are red while those that are negatively correlated are blue. (B) Heat

map showing the expression of all genes (in FPKM) within the dark turquoise module. Labels contain the *D. suzukii* gene symbol (LOC#########) and the corresponding *D. melanogaster* gene symbol. Red indicates high expression while blue indicates low expression. Line C3 is resistant while lines C2 and C5 are susceptible. The number following the underscore indicates different biological replicates.

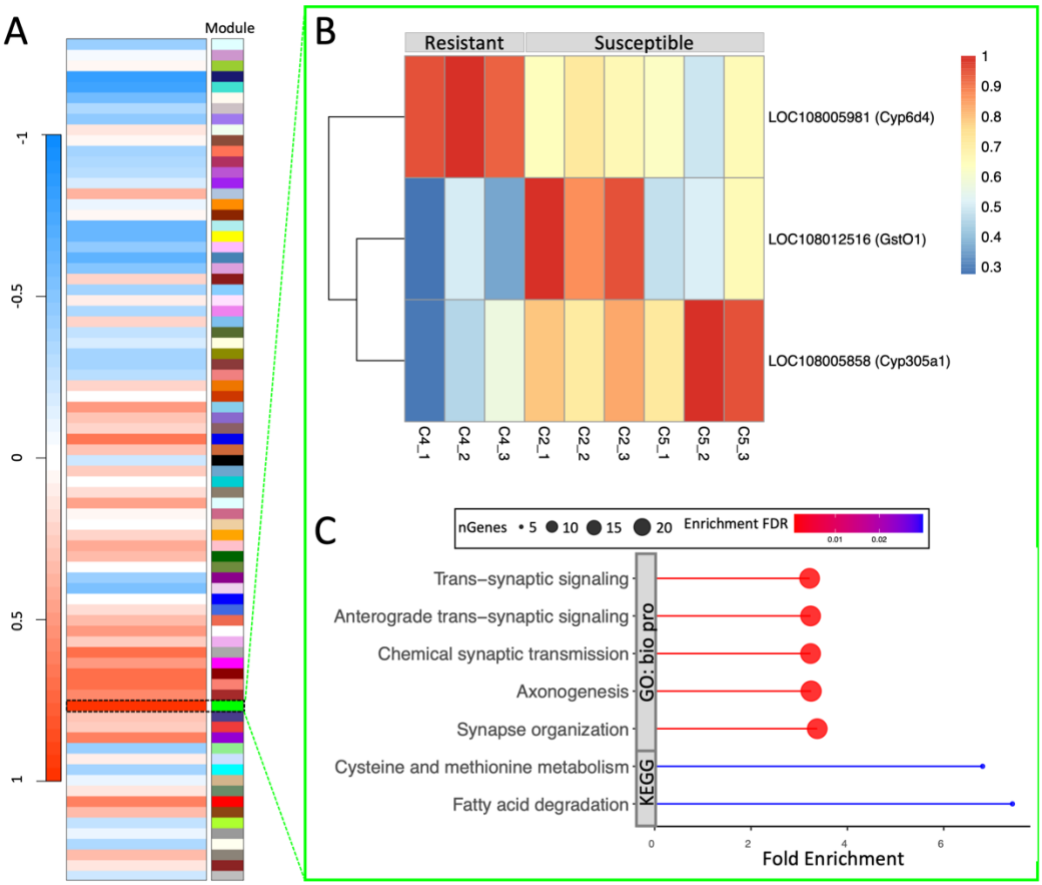

Fig. 7: Genes highly correlated with spinosad resistance in *Drosophila suzukii* line C4 include metabolic genes. (A) Heat map of gene clusters determined by Weighted Gene Correlation Network Analysis (WGCNA). Modules that are positively correlated with resistance are red while those that are negatively correlated are blue. (B) Heat map showing the expression of metabolic genes (in FPKM) within the green module. Labels contain the *D. suzukii* gene symbol (LOC##########) and the corresponding *D. melanogaster* gene symbol. Red indicates high expression while blue indicates low expression. Line C4 is resistant while lines C2 and C5 are susceptible. The number following the underscore indicates different biological replicates. (C) Enriched pathways within the Kyoto Encyclopedia of Genes and Genomes (KEGG) category and the top 5 pathways within Gene Ontology (GO) Biological Processes (bio proc) category for genes within the green module. The x-axis is Fold Enrichment, which is defined as the percentage of differentially expressed genes that belong to each pathway. Point size represents the

number of genes (nGenes) within the category while color denotes the false discovery rate (FDR) correction of enrichment p-values.

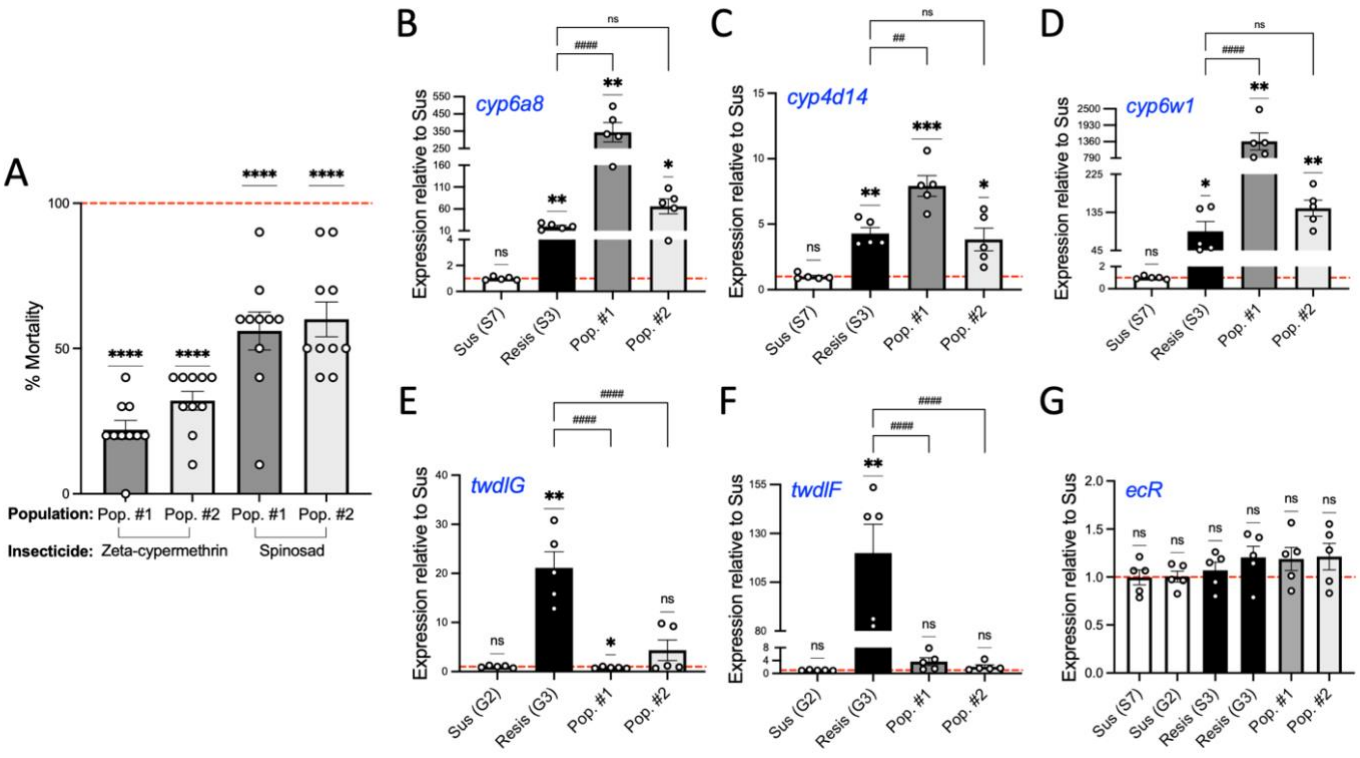

Fig. 8: New field-collected *Drosophila suzukii* populations show increased expression of metabolic genes. (A) Bioassay to assess mortality of 2022 field-collected *D. suzukii* populations (Pop. #1 and #2) when exposed to zeta-cypermethrin and spinosad. Each point represents a biological replicate of 5 males and 5 females (n=10), and error bars indicate ±SEM. Asterisks denote significant p-values as determined by one-sample t and Wilcoxon Test compared to a hypothetical mean of 100 (denoted by the dashed red line): **** p<0.0001. (B-G) Gene expression of (B-D) *cytochrome P450* (*cyp*) genes, (E-F) *tweedle* (*twdl*) genes, and (G) *ecdysone receptor* (*ecR*) in susceptible (S7 and G2) and resistant (S3 and G3) isogenic lines (from 2019 collections) as well as 2022 field-collected populations (n=5 biological replicates of 8-10 females). Asterisks denote significant p-values as determined by one sample T and Wilcoxon Test compared to the average gene expression of the susceptible line (denoted by the red dashed line): **p<0.01 and **** p<0.0001. The hash marks denote significant p-values as determined by One-way ANOVA followed by Holm-Sidak's multiple comparisons test to assess expression differences between the 2022 populations and the resistant line. Non-significant comparisons are denoted as "ns".

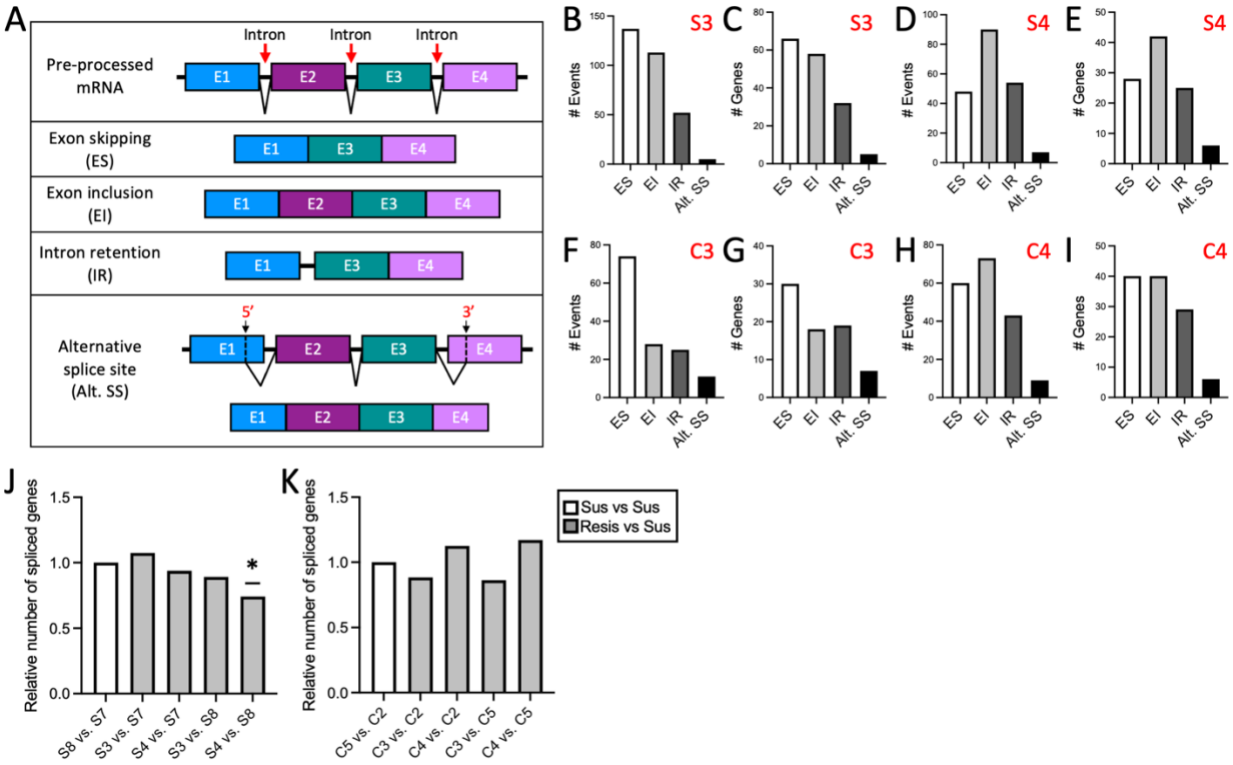

Fig. 9: Insecticide-resistant and susceptible *Drosophila suzukii* exhibit differences in alternative splicing. (A) Schematic of the various types of alternative splicing (AS) events that can occur. "E" represents exons. (B, D, F, H) Number of AS events that occur in (B, D) zeta-cypermethrin-resistant lines and (F, H) spinosad-resistant lines. (C, E, G, I) Number of genes in each AS category in (C, E) zeta-cypermethrin-resistant lines and (G, I) and spinosad-resistant lines. (J-K) Pairwise comparisons of differentially spliced genes in (J) zeta-cypermethrin-resistant and -susceptible lines and (K) spinosad-resistant and -susceptible lines. Asterisks denote significance by Fisher's Exact Test; * $p<0.05$.

Table 2: Functional enrichment categories of differentially spliced genes in zeta-cypermethrin-resistant (R) vs susceptible (S) *D. suzukii* isogenic lines

S vs S	R vs S	R vs S	R vs S	R vs S
S8 vs. S7	S3 vs. S7	S4 vs. S7	S3 vs. S8	S4 vs. S8
Photoreceptor cell development	Reg. of localization	Non-homologous end-joining	Intracellular signal transduction	Other glycan degradation
Meiotic cell cycle proc.	Lipid oxidation	Starch and sucrose metabolism	Intercellular bridge organization	Organelle organization
Meiotic cell cycle	Nurse cell apoptotic proc.	Nucleotide excision repair	Striated muscle cell differentiation	Phosphorus metabolic proc.
	Lipid modification		Neg. reg. of protein-containing complex disassembly	Phosphate-containing compound metabolic proc.
	Pos. reg. of cellular amide metabolic proc.		Neg. reg. of protein depolymerization	Reg. of supramolecular fiber organization
	Reg. of axon guidance		Muscle cell differentiation	Reg. of protein-containing complex assembly
	Apoptotic proc. involved in development		Mannosylation	Reg. of cellular component biogenesis
	Reg. of intracellular mRNA localization			Reg. of protein polymerization
	Programmed cell death involved in cell development			Reg. of organelle organization
	Morphogenesis of a polarized epithelium			Cell development
				Phosphorylation
				Protein phosphorylation
				Cellular response to hypoxia
				Protein polymerization
				Cellular response to decreased oxygen levels
				Mitochondrion organization
				Sarcomere organization

Table 3: Functional enrichment categories of differentially spliced genes in spinosad-resistant (R) vs susceptible (S) *D. suzukii* isogenic lines

S vs S	R vs S	R vs S	R vs S	R vs S
C5 vs C2	C3 vs C2	C4 vs C2	C3 vs C5	C4 vs C5
RNA degradation	Response to DDT	Melanosome organization		Germ cell development
Biosynthesis of amino acids		Response to DDT		Female gamete generation
Carbon metabolism				Ovarian nurse cell to oocyte transport
				Catabolic proc.
				Cell differentiation
				Oogenesis
				Cellular developmental proc.
				Pos. reg. of transport
				Organic substance catabolic proc.
				Lipid oxidation
				Meiotic spindle organization
				Actin filament organization
				Cellular proc. involved in reproduction in multicellular organism
				Cell development
				Developmental proc. involved in reproduction
				Gamete generation

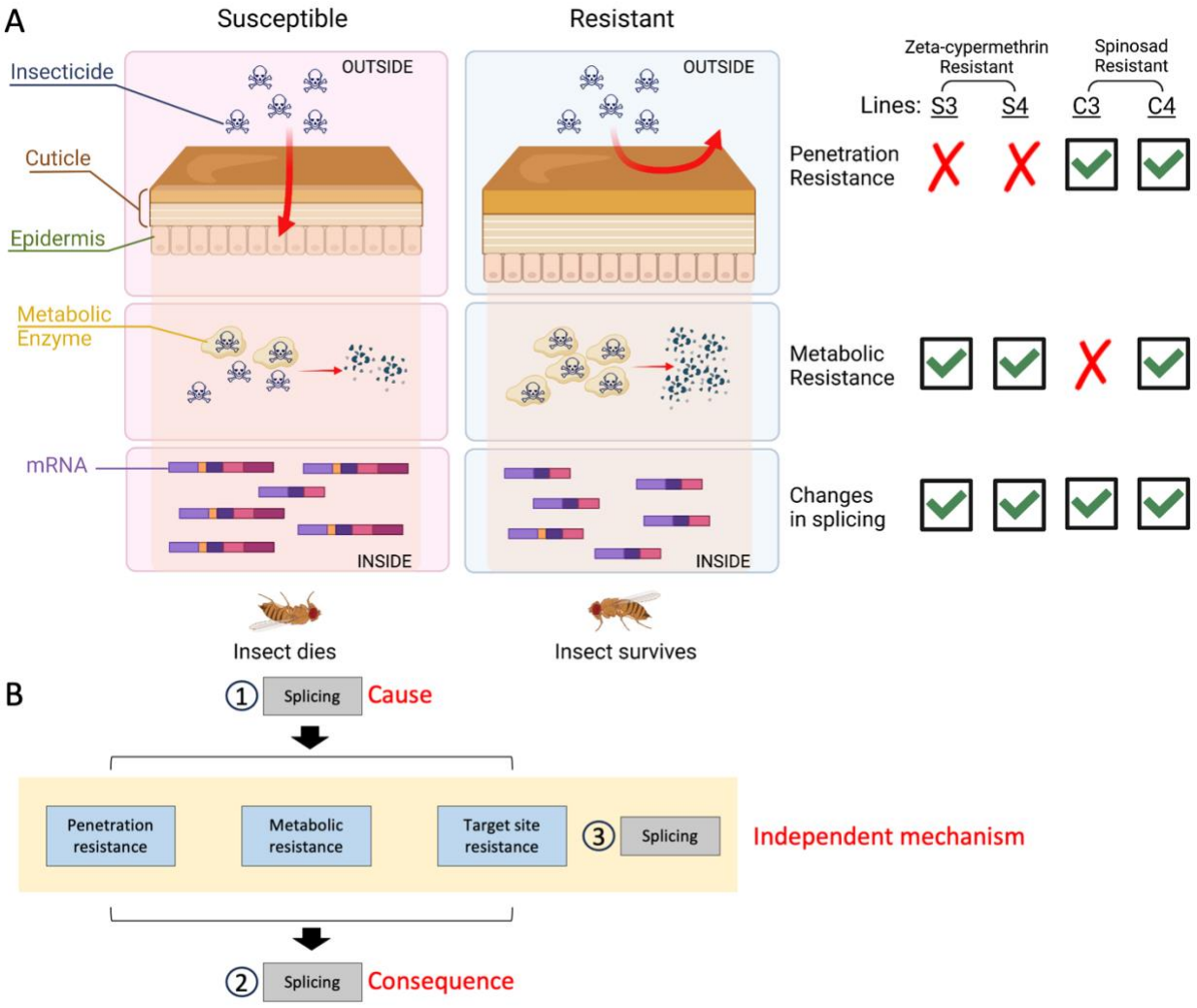

Fig. 10: Schematic representation of the molecular mechanisms conferring either zeta-cypermethrin or spinosad-resistance in *Drosophila suzukii*. (A) The cuticle of susceptible *D. suzukii* is more permeable to insecticides, enabling the insecticide to enter the insect and bind to its target protein, ultimately killing the insect. However, in the case of zeta-cypermethrin-resistant *D. suzukii*, an increased expression of metabolic enzymes results in an increased breakdown of the insecticide before it can bind to its target protein. Spinosad-resistant *D. suzukii* have increased expression of cuticular genes such that the cuticle is less penetrable by insecticides, allowing them to survive. Additionally, spinosad-resistant *D. suzukii* can also exhibit an upregulation of metabolic enzymes to increase detoxification of the

insecticide, promoting the survival of the flies. Finally, changes in transcriptome-wide alternative splicing were detected in both zeta-cypermethrin and spinosad-resistant *D. suzukii* lines. This figure was created with BioRender.com (license to lab of JCC). (B) Schematic depicting 3 possible scenarios as to how splicing and resistance can be correlated. Blue boxes represent characterized molecular mechanisms of resistance and the yellow box represents possible molecular mechanisms of resistance.

Transcriptome analysis of *Drosophila suzukii* reveals molecular mechanisms conferring pyrethroid and spinosad resistance

Christine A. Tabuloc, Curtis R. Carlson, Fatemeh Ganjisaffar, Hongtao Zhang, Cindy C. Truong, Ching-Hsuan Chen, Kyle M. Lewald, Sergio Hidalgo, Frank G. Zalom, and Joanna C. Chiu*

Supporting information:

Supplemental Figs. 1 to 3 and Supplemental Tables 1 and 4

Note that the following are provided as .xlsx files on Dryad (https://doi.org/10.25338/B8PH17)**:**

Suppl. Table 2: Statistics for zeta-cypermethrin bioassay
Suppl. Table 3: Statistics for spinosad bioassay
Suppl. Table 5: DEGs in zeta-cypermethrin-resistant *Drosophila suzukii* (line S3)
Suppl. Table 6: DEGs in zeta-cypermethrin-resistant *Drosophila suzukii* (line S4)
Suppl. Table 7: Statistics comparing the expression of metabolic genes in zeta-cypermethrin-resistant vs. susceptible *Drosophila suzukii*
Suppl. Table 8: Enrichment of DEGs in zeta-cypermethrin-resistant *Drosophila suzukii* (line S3)
Suppl. Table 9: Enrichment of DEGs in zeta-cypermethrin-resistant *Drosophila suzukii* (line S4)
Suppl. Table 10: Genes in all WGCNA modules for zeta-cypermethrin-resistant *Drosophila suzukii* line S3
Suppl. Table 11: Enrichment of the turquoise module in zeta-cypermethrin-resistant *Drosophila suzukii* line S3
Suppl. Table 12: Genes in all WGCNA modules for zeta-cypermethrin-resistant *Drosophila suzukii* line S4
Suppl. Table 13: Enrichment of the turquoise module in zeta-cypermethrin-resistant *Drosophila suzukii* line S4
Suppl. Table 14: DEGs in spinosad-resistant *Drosophila suzukii* (line C3)
Suppl. Table 15: DEGs in spinosad-resistant *Drosophila suzukii* (line C4)
Suppl. Table 16: Statistics comparing the expression of metabolic and cuticular genes in spinosad-resistant vs. susceptible *Drosophila suzukii*
Suppl. Table 17: Enrichment of DEGs in spinosasd-resistant *Drosophila suzukii* (line S3)
Suppl. Table 18: Enrichment of DEGs in spinosad-resistant *Drosophila suzukii* (line S4)
Suppl. Table 19: Genes in all WGCNA modules for spinosasd-resistant *Drosophila suzukii* line C3
Suppl. Table 20: Genes in all WGCNA modules for spinosasd-resistant *Drosophila suzukii* line C4
Suppl. Table 21: Enrichment of the green module in spinosasd-resistant *Drosophila suzukii* line C4
Suppl. Table 22: Differential usage of splice junctions, exons, and introns in insecticide-resistant *Drosophila suzukii*
Suppl. Table 23: Pairwise comparisons of differentially spliced genes
Suppl. Table 24: Enrichment of differentially spliced genes

Suppl. Table 1: Sequences for primers used in quantitative PCR

Primer Name	5'- Sequence -3'
Ds*RpL32* (137) Forward	TGC GTC GCC GCT TCA AGG GAC
Ds*RpL32* (3287) Reverse	TGC GCT TCT TGG AGC TCA CGC C
Ds*Cyp6a8* (1049) Forward	TGA GGT GGA GGA TGT CCT AGA GC
Ds*Cyp6a8* (1215) Reverse	TCG GAT GGC CGG GAA CTT CG
Ds*Cyp4d14* (1589) Forward	TCC AGG AGA TTC GAG ATG TCC TTG
Ds*Cyp4d14* (1756) Reverse	TGC CGT CTA GCA CGG TGT CC
Ds*Cyp6w1* (1290) Forward	TCC GGC GAA CCG CTG TAA CCT C
Ds*Cyp6w1* (1479) Reverse	AAC CGG ACT AGT AGC AGC CCA C
Ds*TwdlG* (822) Forward	TCG CAC CCA AGC AAC CTA GCA AG
Ds*TwdlG* (999) Reverse	TGG TGG TCC AGA ACG CCA ATT AC
Ds*TwdlF* (842) Forward	AGC GCG CCC AGC AGG AGA
Ds*TwdlF* (1033) Reverse	AGC TCT GCT GCT GAA TGC CCT G
Ds*EcR* (2010) Forward	AGT CGC ACC TCC AGG TTA CA
Ds*EcR* (2174) Reverse	CGG TTG CGT ATT GTT TTG GGT

Suppl. Table 4: Results of pairwise *z*-tests comparing LC_{50}s among resistant and susceptible *Drosophila suzukii* isogenic lines

Insecticide	Comparison	Estimate ± SE	*t* value	*p* value
Zeta-cypermethrin	S3 - S4	1.1178 ± 0.0990	1.1906	0.2338
	S3 - S8	3.1908 ± 0.2962	7.3954	< 0.0001
	S4 - S8	2.8545 ± 0.2763	6.7111	< 0.0001
Spinosad	C3 - C4	1.2728 ± 0.1652	1.6513	0.0987
	C3 - C5	6.7611 ± 0.9006	6.3966	< 0.0001
	C4 - C5	5.3119 ± 0.7301	5.9063	< 0.0001

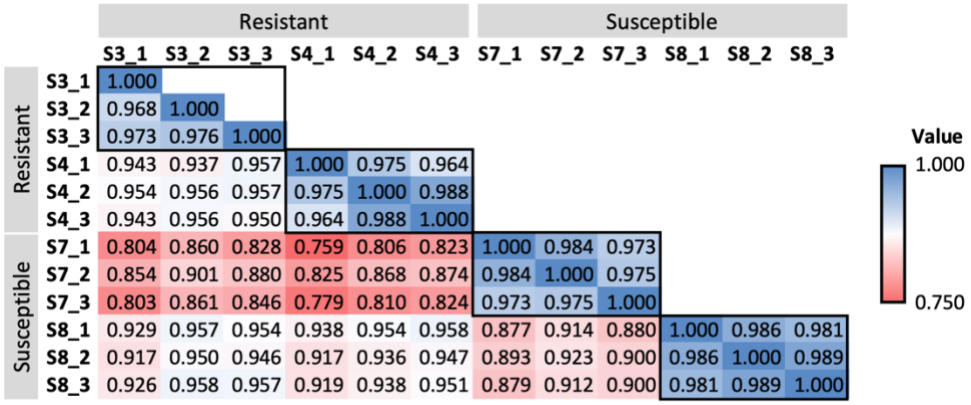

Suppl. Fig. 1: Heatmap of Pearson's correlation coefficients between zeta-cypermethrin-resistant and susceptible lines. Comparisons between lines resistant (S3, S4) or susceptible (S7, S8) to zeta-cypermethrin. The numbers following the underscore indicate biological replicates, each consisting of 8-10 female flies. Comparisons between biological replicates are indicated by black boxes. Highly correlated samples are in blue while less correlated samples are in red.

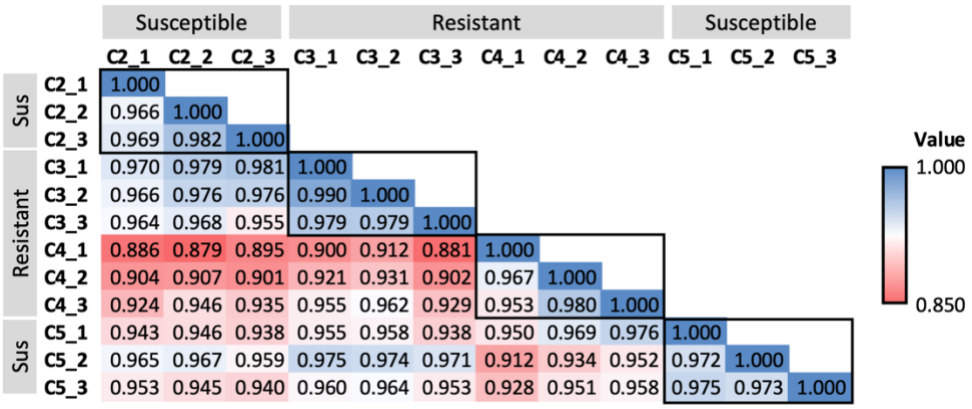

Suppl. Fig. 2: Heatmap of Pearson's correlation coefficients between spinosad-resistant and susceptible lines. Comparisons between lines resistant (C3, C4) or susceptible (C2, C5) to spinosad. The numbers following the underscore indicate biological replicates. Comparisons between biological replicates are indicated by black boxes. Highly correlated samples are in blue while less correlated samples are in red.

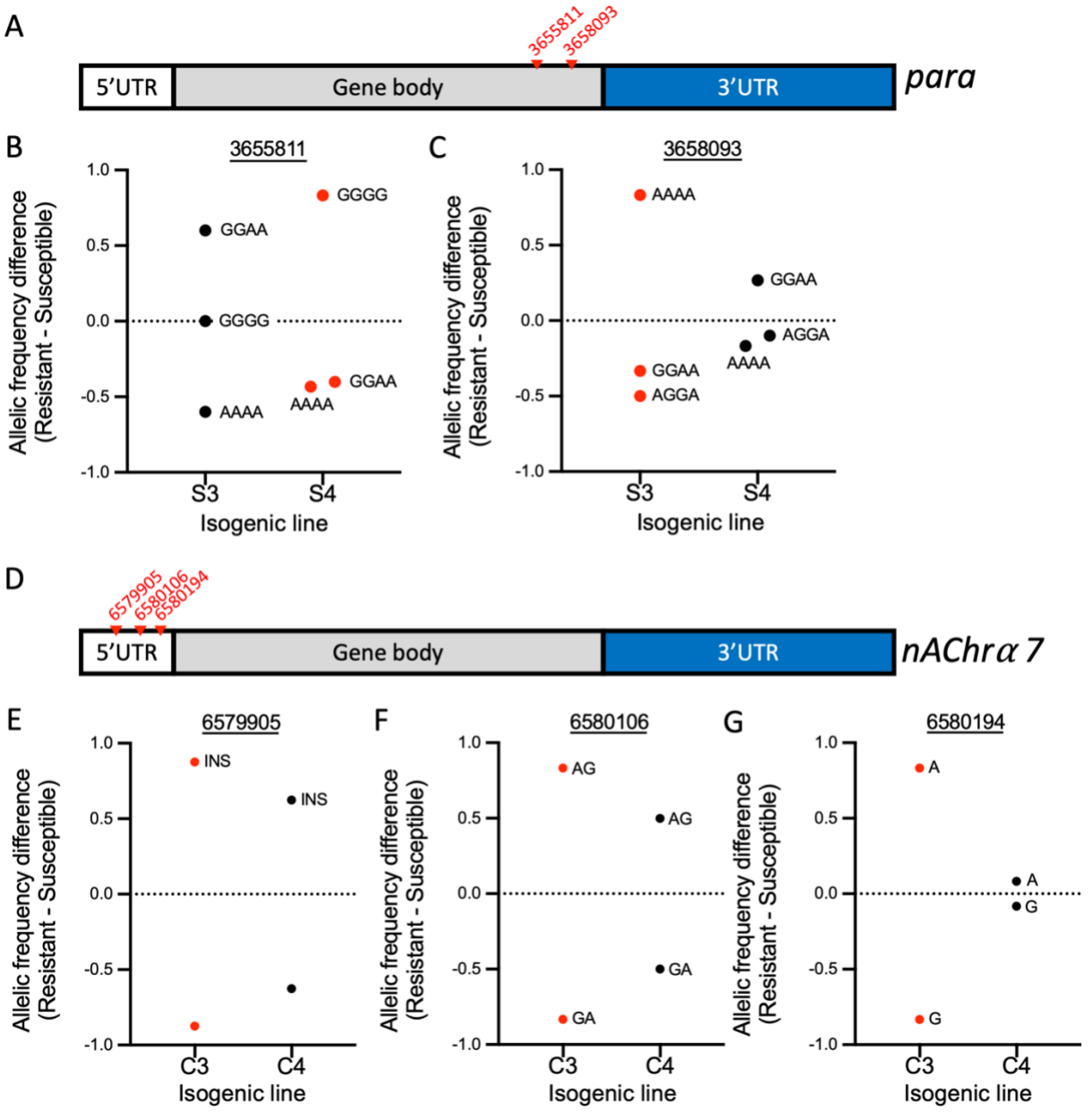

Suppl. Fig. 3: Insecticide-resistant lines exhibit allele frequency differences in the insecticide target protein. (A) Schematic of the gene, *paralytic* (*para*), the target protein of zeta-cypermethrin. Red labels indicate genomic loci shown in panels B and C. (B-C) Scatter plots of allele frequency differences on chromosome NW_023496846.1 at positions (B) 3655811 and (C) 3658093, which are both located within introns in the gene body of *para,* between each zeta-cypermethrin resistant line (S3 or S4; x-axis) vs both susceptible lines (S7 and S8). Each point is labeled with the allele variant. Red points indicate

significant allele frequency differences between at least one resistant line and both susceptible lines as determined by Fisher's Exact Test while black points indicate differences that are not significantly different between the resistant and susceptible lines. Alleles located above the dotted line are more prevalent in the resistant line while alleles that fall below the line are more prevalent in the susceptible lines. (D) Schematic of the gene, *nicotinic acetylcholine receptor alpha* 7 (*nAChrα7)*, the target of spinosad. The red labels indicate positions on chromosome NW_023496800.1 shown in panels E-G. (E-G) Scatter plots of allele frequency differences at positions (E) 6579905, (F) 6580106, and (G) 6580194, which are located within exons in the gene body of *nAchrα7,* between each spinosad-resistant line (C3 or C4) vs both susceptible lines (C2 and C5). Insertions are labeled as "INS."

Conclusion

Gene expression is the process by which genotype manifests into phenotype (Nachtomy et al., 2007). Gene expression regulation is influenced by environmental factors, both naturally occurring and human-introduced (Gibson, 2008). In this dissertation, I sought to understand how environmental factors affect gene expression regulation at the chromatin level and at the mRNA expression level. In Chapter 1, I assessed the effect of a naturally occurring factor, specifically the day-night cycle, on transcriptional regulation by the BRAHMA (BRM) chromatin remodeling complex using *D. melanogaster* as a model. In Chapter 2, I assessed whether insecticide resistance, resulting from exposure to repeated insecticide applications, resulted in changes in mRNA expression in the agricultural pest, *D. suzukii*.

Chapter 1 (Tabuloc et al., 2023) expands our current understanding of the mechanisms underlying the daily rhythmic chromatin landscape at clock gene loci. Previously, it has been shown that BRM reduces clock gene expression by condensing the chromatin at these loci and by recruiting repressors (Kwok et al., 2015). Here, I built on this model by demonstrating that BRM facilitates rhythms in nucleosome density through its rhythmic occupancy at clock genes. This daily rhythmic occupancy is regulated by two core clock proteins, CLOCK (CLK) and TIMELESS (TIM), demonstrating reciprocal regulation between BRM and the clock. Thus, our findings suggest that factors affecting clock gene expression, such as environmental (Dubruille & Emery, 2008), nutritional (Guan & Lazar, 2021), or genetic factors such as aging (Kuintzle et al., 2017; Luo et al., 2012; Umezaki et al., 2012), could disrupt the robustness of the clock and therefore can further dampen clock gene expression. Additionally, the involvement of TIM in regulating BRM occupancy and the chromatin landscape, prompts interesting questions as to whether light and temperature affect the chromatin landscape at loci rhythmically targeted by BRM. It has been reported that TIM protein abundance is regulated by light (Hunter-Ensor et al., 1996; Myers et al., 1996; Zeng et al., 1996) while temperature-dependent splicing produces

different TIM isoforms with altered properties (Abrieux et al., 2020; Foley et al., 2019; Martin Anduaga et al., 2019). Therefore, it is possible that chromatin structure changes in response to light exposure at the wrong time of day or even in different seasons. Future studies assessing BRM and histone occupancy in different environmental conditions such as varying day lengths, temperatures, or exposure to light at night can aid in understanding how environmental stimuli affect chromatin structure and consequently gene expression.

In Chapter 2, I sequenced the transcriptomes of *D. suzukii* resistant to either pyrethroid or spinosad insecticides and identified mechanisms likely conferring resistance. Leveraging my results, I produced molecular diagnostics to monitor resistance development. Furthermore, our understanding of these mechanisms will shed light on the possibility of cross-resistance as well as provide useful information growers can utilize to enhance *D. suzukii* control programs. For instance, the overexpression of cuticular genes in flies resistant to spinosad suggest a more impenetrable insect cuticle; therefore, it is possible that these flies are also resistant to other classes of insecticides. One possible solution to better control these resistant flies is for growers to administer insecticides using bait traps as opposed to spraying, circumventing the need for the insecticide penetrate the cuticle (Furnival-Adams et al., 2020). In the case of resistant *D. suzukii* overexpressing detoxification enzymes, growers can utilize synergists, or metabolic enzyme inhibitors, to increase the efficacy of the insecticides (Snoeck et al., 2017). Finally, I identified transcriptome-wide changes in splicing in resistant *D. suzukii*. Future studies can investigate which splicing events contribute to the resistant phenotype and this could pave the way to the development of new technology to prevent such splicing events from occurring to counteract resistance.

In summary, the work presented in this dissertation contributes to our overall understanding of how environmental factors can influence gene expression regulation. For instance, environmental factors can directly impact chromatin structure, but they can also affect gene expression levels. Given

that gene expression regulation can occur at multiple levels, such as transcription, splicing, and translation (Bhattacharjee et al., 2013), future investigations exploring how environmental stimuli affect these different levels can provide a more comprehensive understanding as to how interaction with the environment directly impacts organismal gene expression.

REFERENCES

Abrieux, A., Xue, Y., Cai, Y., Lewald, K. M., Nguyen, H. N., Zhang, Y., & Chiu, J. C. (2020). EYES ABSENT and TIMELESS integrate photoperiodic and temperature cues to regulate seasonal physiology in *Drosophila*. *Proceedings of the National Academy of Sciences*, *117*(26), 15293–15304. https://doi.org/10.1073/pnas.2004262117

Bhattacharjee, S., Renganaath, K., Mehrotra, R., & Mehrotra, S. (2013). Combinatorial Control of Gene Expression. *BioMed Research International*, *2013*, 407263. https://doi.org/10.1155/2013/407263

Dubruille, R., & Emery, P. (2008). A Plastic Clock: How Circadian Rhythms Respond to Environmental Cues in *Drosophila*. *Molecular Neurobiology*, *38*(2), 129–145. https://doi.org/10.1007/s12035-008-8035-y

Foley, L. E., Ling, J., Joshi, R., Evantal, N., Kadener, S., & Emery, P. (2019). *Drosophila* PSI controls circadian period and the phase of circadian behavior under temperature cycle via tim splicing. *ELife*, *8*, e50063. https://doi.org/10.7554/eLife.50063

Furnival-Adams, J. E. C., Camara, S., Rowland, M., Koffi, A. A., Ahoua Alou, L. P., Oumbouke, W. A., & N'Guessan, R. (2020). Indoor use of attractive toxic sugar bait in combination with long-lasting insecticidal net against pyrethroid-resistant *Anopheles gambiae*: An experimental hut trial in

Mbé, central Côte d'Ivoire. *Malaria Journal*, *19*(1), 11. https://doi.org/10.1186/s12936-019-3095-1

Gibson, G. (2008). The environmental contribution to gene expression profiles. *Nature Reviews Genetics*, *9*(8), Article 8. https://doi.org/10.1038/nrg2383

Guan, D., & Lazar, M. A. (2021). Interconnections between circadian clocks and metabolism. *The Journal of Clinical Investigation*, *131*(15). https://doi.org/10.1172/JCI148278

Hunter-Ensor, M., Ousley, A., & Sehgal, A. (1996). Regulation of the *Drosophila* Protein Timeless Suggests a Mechanism for Resetting the Circadian Clock by Light. *Cell*, *84*(5), 677–685. https://doi.org/10.1016/S0092-8674(00)81046-6

Kuintzle, R. C., Chow, E. S., Westby, T. N., Gvakharia, B. O., Giebultowicz, J. M., & Hendrix, D. A. (2017). Circadian deep sequencing reveals stress-response genes that adopt robust rhythmic expression during aging. *Nature Communications*, *8*, 14529. https://doi.org/10.1038/ncomms14529

Kwok, R. S., Li, Y. H., Lei, A. J., Edery, I., & Chiu, J. C. (2015). The Catalytic and Non-catalytic Functions of the Brahma Chromatin-Remodeling Protein Collaborate to Fine-Tune Circadian Transcription in *Drosophila*. *PLOS Genetics*, *11*(7), e1005307. https://doi.org/10.1371/journal.pgen.1005307

Luo, W., Chen, W.-F., Yue, Z., Chen, D., Sowcik, M., Sehgal, A., & Zheng, X. (2012). Old flies have a robust central oscillator but weaker behavioral rhythms that can be improved by genetic and environmental manipulations. *Aging Cell*, *11*(3), 428–438. https://doi.org/10.1111/j.1474-9726.2012.00800.x

Martin Anduaga, A., Evantal, N., Patop, I. L., Bartok, O., Weiss, R., & Kadener, S. (2019). Thermosensitive alternative splicing senses and mediates temperature adaptation in *Drosophila*. *ELife*, *8*, e44642. https://doi.org/10.7554/eLife.44642

Myers, M. P., Wager-Smith, K., Rothenfluh-Hilfiker, A., & Young, M. W. (1996). Light-induced degradation of TIMELESS and entrainment of the *Drosophila* circadian clock. *Science*, *271*(5256), 1736–1740. https://doi.org/10.1126/science.271.5256.1736

Nachtomy, O., Shavit, A., & Yakhini, Z. (2007). Gene expression and the concept of the phenotype. *Studies in History and Philosophy of Science Part C: Studies in History and Philosophy of Biological and Biomedical Sciences*, *38*(1), 238–254. https://doi.org/10.1016/j.shpsc.2006.12.014

Snoeck, S., Greenhalgh, R., Tirry, L., Clark, R. M., Van Leeuwen, T., & Dermauw, W. (2017). The effect of insecticide synergist treatment on genome-wide gene expression in a polyphagous pest. *Scientific Reports*, *7*(1), 13440. https://doi.org/10.1038/s41598-017-13397-x

Tabuloc, C. A., Cai, Y. D., Kwok, R. S., Chan, E. C., Hidalgo, S., & Chiu, J. C. (2023). CLOCK and TIMELESS regulate rhythmic occupancy of the BRAHMA chromatin-remodeling protein at clock gene promoters. *PLOS Genetics*, *19*(2), e1010649. https://doi.org/10.1371/journal.pgen.1010649

Umezaki, Y., Yoshii, T., Kawaguchi, T., Helfrich-Förster, C., & Tomioka, K. (2012). Pigment-Dispersing Factor Is Involved in Age-Dependent Rhythm Changes in *Drosophila melanogaster*. *Journal of Biological Rhythms*, *27*(6), 423–432. https://doi.org/10.1177/0748730412462206

Zeng, H., Qian, Z., Myers, M. P., & Rosbash, M. (1996). A light-entrainment mechanism for the *Drosophila* circadian clock. *Nature*, *380*(6570), Article 6570. https://doi.org/10.1038/380129a0